Master Thesis, Department of Geosciences

Diagenesis and reservoir quality of Upper Jurassic sandstones in the South Viking Graben

A mineralogical, petrographical and petrophysical approach

Azeem Hussain

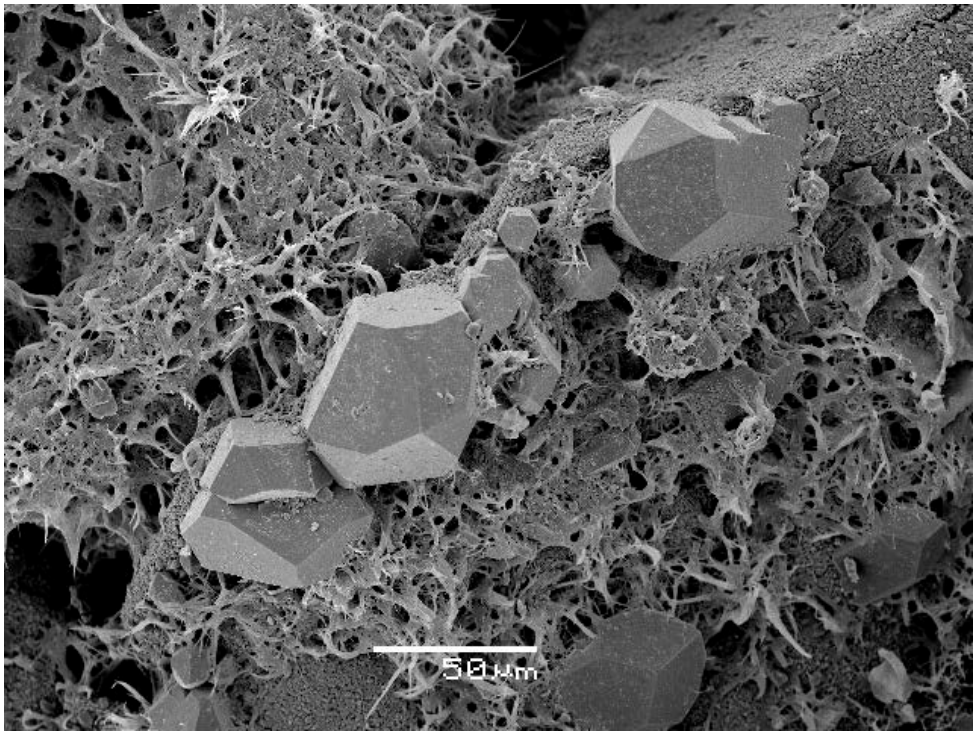

UNIVERSITY OF OSLO

FACULTY OF MATHEMATICS AND NATURAL SCIENCES

Diagenesis and reservoir quality of Upper Jurassic sandstones in the South Viking Graben

A mineralogical, petrographical and petrophysical approach

Azeem Hussain

Master Thesis in Geosciences

Discipline: Petroleum Geology and Petroleum Geophysics

Department of Geosciences

Faculty of Mathematics and Natural Sciences

University of Oslo

1st June, 2012

Tutor(s): Jens Jahren

This work is published digitally through DUO – Digitale Utgivelser ved UiO
http://www.duo.uio.no
It is also catalogued in BIBSYS (http://www.bibsys.no/english)

Acknowledgements

I am thankful to Almighty Allah whose blessings and gratitude enabled and helped me to complete this work. Special praises to Prophet Muhammad (SAW), who is the best role model for all human beings.

I would like to express great honor and respect for my supervisor Associate Professor Jens Jahren for always being supportive and thought provoking during this master's thesis and helps me in developing good understanding of reservoir geology.

Special thanks to Professor Knut Bjørlykke for constructive discussions for the understanding of sandstone diagenesis. I would like to acknowledge Berit Løken Berg and Saleh for providing technical assistance during SEM analysis and thin section preparation respectively. Special appreciation for PhD student Tom Erik Maast for encouragement, guidance and providing useful data.

Very positive discussions during every step of work with my fellow students and nice friends Danial Farwardini and Zeeshan Mohabbat will always be remembered. Special thanks to Ahmad Salman and Muhammad Jamil for helping me in review and making improvements in my work.

Endless tea and lunch breaks with my sweet friends Waqas Javed, Attiq Tanoli, Aftab Javed, Rabia Talat, Tausif Ahmad, and Muhammad Nadeem will always be remembered. I will never forget the great company of my lovely friend Mohsin Fardi Golyan during the stay at University.

Thanks and love for my parents for their patience, care and support during my whole life, I cannot pay for them. Support and love of my brothers and sisters is highly appreciated.

Azeem Hussain

1st June, 2012

University of Oslo, Norway

Abstract

The deeply buried Upper Jurassic sandstone reservoirs of the South Viking Graben are differentiated by highly variant reservoir quality. A combined petrophysical and petrographical approach is incorporated to analyze these variations. Quartz cementation developed as syntaxial overgrowth on detrital quartz grains, is the dominant porosity destroying mechanism in these reservoirs. The phenomenon of quartz cementation has proven to be precipitation rate controlled and is insensitive to pressure variations in North Sea sandstone reservoirs. Microquartz grain coatings developed as minute quartz crystals are found to be the fundamental porosity preserving mechanism in these reservoirs despite of great burial depth (>4km) and high temperature (>120^{o}C). The microquartz coatings developed at lower temperature (60-80^{o}C) thus hinders the quartz cementation.

Petrographic Upper Jurassic data evaluated during this study indicate that microquartz grain coats are common in deep marine sandstones of the Vilje sub-basin in South Viking Graben. Grain coating microquartz is generated from the dissolution of silica sponge spicules of the Rhaxella Perforata. These spicules observed in both eastern and western part of South Viking Graben indicate its occurrence in the Vilje Subbasin extensively. The porosity preserved in both Intra-Draupne Formation Sandstone and Brae Formation can be attributed to the presence of microquartz coatings that hindered the quartz overgrowth. Grain coating illite occurrence is observed only in the deep marine Kimmeridgian-Tithonian sandstones of western part of the South Viking Graben.

The authigenic clays mineral content has been evaluated both in the optical microscope and scanning electron microscopy. The deep marine Intra-Draupne Formation sandstone contains illite in abundance with detrital kaolin occurrence in traces. The Brae Formation contains both illite and kaolin as porefilling clay mineral along with partially leached feldspar grains. The occurrence of kaolin attributed to the meteoric water flushing in the Brae Formation. The lower content of illite is responsible for the better permeability of the Brae Formation because its fibrous morphology has been reported to reduce the permeability. The intergranular volume is observed to be stabilizing at 25% and the stylolization phenomenon demonstrates that dissolution at stylolites acted as source for quartz cementation, which is the mechanism behind the destruction of porosity in the Upper Jurassic sandstone reservoirs in the South Viking Graben.

Table of Contents

1. INTRODUCTION

1.1 Introduction

This master's thesis is performed as part of a collaboration project between DNO (Det Norske Oljeselskap) and University of Oslo, on reservoir quality in the Upper Jurassic sandstone reservoirs of the Gudrun and East Brae Fields in South Viking Graben.

Considerable regional variations are present in the reservoir quality of the deeply buried Upper Jurassic sandstone reservoirs in the study area. Quartz cementation and preservation of porosity are two important mechanisms during the evaluation of reservoir quality of mature sandstone prospects. For these sandstones, quartz cementation is the main porosity destroying mechanism in the deeply buried (3.5-4.5Km) sandstone reservoirs with temperature approximately greater than 80^{o}C. If quartz cementation process continues unhindered, it causes complete destruction of porosity. At greater burial depths, the grain coats (illite, chlorite, micro-quartz, detrital clay, and bitumen) are the most characteristic factor hindering the quartz cementation and hence preserve the porosity. The effect of preservation of porosity by micro-quartz grain coating was first reported by Jahren, (1993. During this analysis the amount of quartz cement is found to be the main factor controlling the reservoir quality and the micro quartz coating present hinders the quartz cementation. The prediction of development of grain coating is difficult and their distribution can be investigated petrographically from available cores.

1.2 Purpose and Methods

The purpose of this thesis project is the characterization of reservoir quality in the Upper Jurassic sandstone reservoirs of the South Viking Graben, with emphasis on the lateral equivalents Intra-Draupne Formation Sandstone and Brae Formation. The focus of this study is the understanding of the digenetic processes of mechanical and chemical compaction that affected the sandstone bodies during deep burial. The presence of anomalous high porosity is investigated in relation to the porosity preserving mechanism of grain coatings. The percentages of grain coat coverage and preserved porosity relationship has also been studied. The distribution of different authigenic clays and their source has also been discussed in relation to their influence on reservoir quality.

The following methods are integrated during this investigation

i. **Mineralogical and Petrographic Analysis**
    - Optical Microscopy
    - Scanning electron microscopy

ii. **Well Correlation and Petrophysical evaluation**

1.3 The Study Area

The study area is located in the South Viking Graben in the North Sea. The seven wells investigated during the study are from Norwegian block 15/3 and UK block 16/3B within the Vilje subbasin of the South Viking Graben.

The rifting event of Callovian-Ryazanian developed the current structural configuration of the South Viking Graben (Rattey and Hayward, 1993). The South Viking Graben structure is 20-40kms wide and 120kms long (Fraser et al., 2003). This graben can be subdivided into smaller subbasins on the basis of north westerly trending (Thornquist) transfer faults. Uplift and inversion occurred along these faults (Zanella et al., 2003). This rifting process caused the marine transgression in the South Viking Graben. Large facies variability occurs in the upper Jurassic sediments due to the deposition process which was ongoing parallel to the rifting of majority of the structures in the South Viking Graben. The Upper Jurassic sediments are highly rich in organic material which constitutes the source rocks in the area. At the same time there are several sandstone bodies deposited due to the erosion of Middle Jurassic to Devonian rocks which are exposed on the Utsira High and the East Shetland Platform by sediment gravity-flows and deposited as turbidites (Intra-Draupne Formation sandstone and Brae Formation) in deeper parts of the basin (Underhill and Partington, 1993).

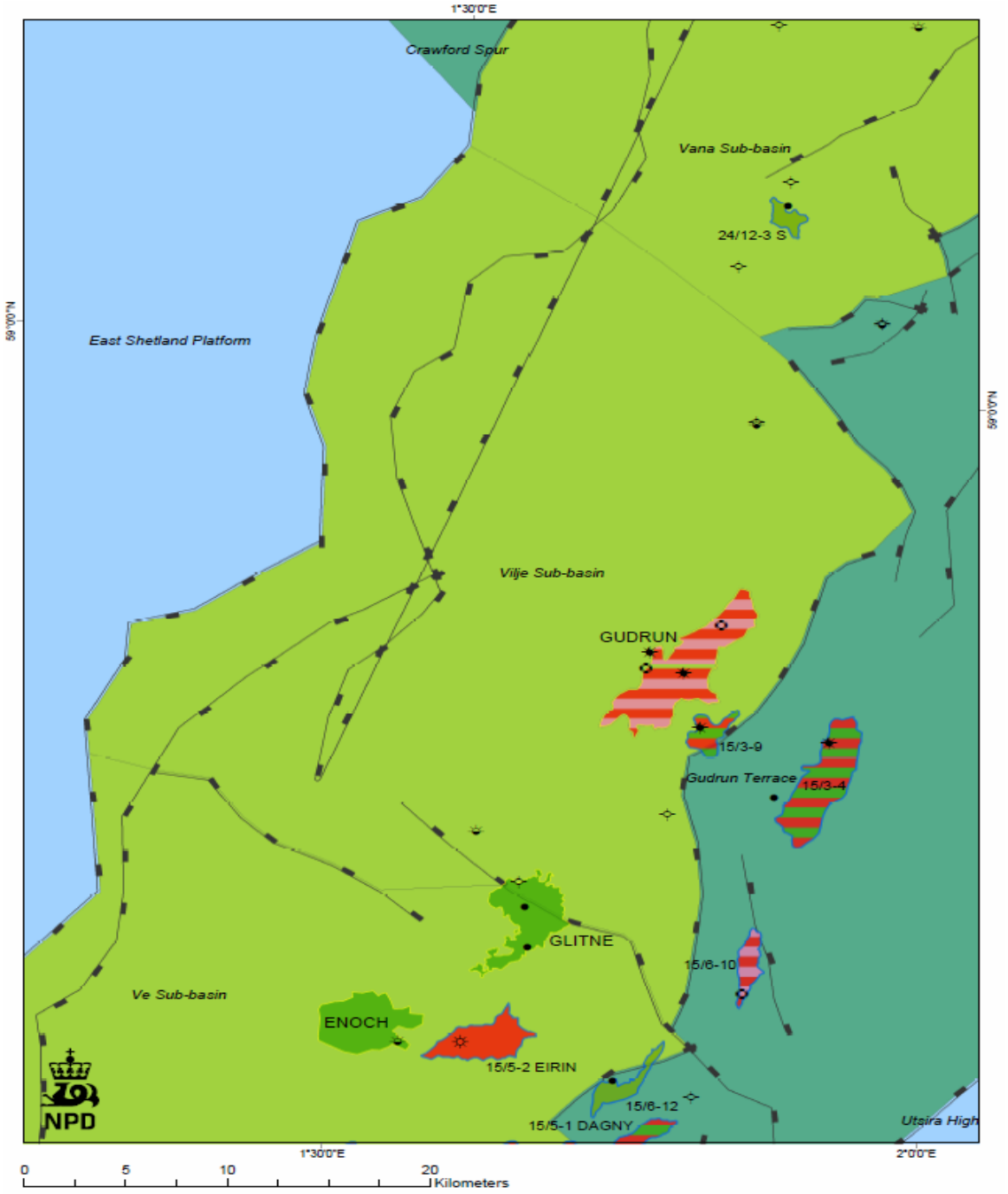

Figure 1: The structural element map of the study area within South Viking Graben (NPD 2012).

2. GEOLOGICAL SETTINGS

2.1 Introduction

The South Viking Graben is located in the Central North Sea and forms the restricted rift basin in the south of the Viking Graben. This chapter will emphasize on the geological settings of the South Viking Graben, particularly the events which were active during the Upper Jurassic. The structural development and evolution and the reservoir facies and depositional model are also discussed respectively.

2.2 Late Jurassic/Upper Jurassic Rifting and Transgression

Late Jurassic is the most important time interval in the development of the North Sea Petroleum system due to three reasons. Firstly, it was the time of deposition of Kimmeridge Clay Formation and its lateral equivalents, which are the source rock for the majority of North Sea fields (Cornford, 1998 in Fraser et al., 2002). Secondly, its complex tectonic history is responsible for the formation of structures, which act as hydrocarbon traps for Upper Jurassic and lowermost Cretaceous syn-rift reservoirs and also pre-rift reservoir rocks of Devonian to middle Jurassic age. These pre and syn-rift hydrocarbon accumulations are accounting for 80% of the discovered reserves of the North Atlantic Margin, including the North Sea (Knott et all., 1993 in Fraser et al., 2002). Thirdly, Upper Jurassic has about 20% of all hydrocarbon reserves in the Central and Northern North Sea and still has potential for new petroleum reserves to be discovered. And there are still reserves in stratigraphic, structural and combination traps yet to be found (Johnson and Fisher, 1998; Boldy and Fraser, 1999 in Fraser et al., 2002). Discovery of Aldous Major South/Avaldsnes is in Jurassic sandstone of North Sea in 2011 confirms these statements.

Succession of Upper Jurassic rocks is preserved in the grabens of the rift system and reaches a thickness of up to 3000m. The top of upper Jurassic rocks, which is being estimated from the base Cretaceous surface lies between 2500 and 5000m below seabed in these graben areas. This succession belongs to the Humber Group (Richards et al., 1993, in Fraser et al., 2002) and its lateral equivalent in Norwegian sector is Viking group (Vollset, J, and Doré,, 1984 in Fraser et al., 2002). It comprises of mudstone dominated Heather, Kimmeridge clay and Draupne formations. Sandstone dominated intervals which contain hydrocarbons include shallow marine Fulmar and Piper formations, the deep marine Magnus Sandstone Member

and Brae Formation and the coastal-deltaic Sognefjord and Fensfjord formations (Fraser et al., 2002).

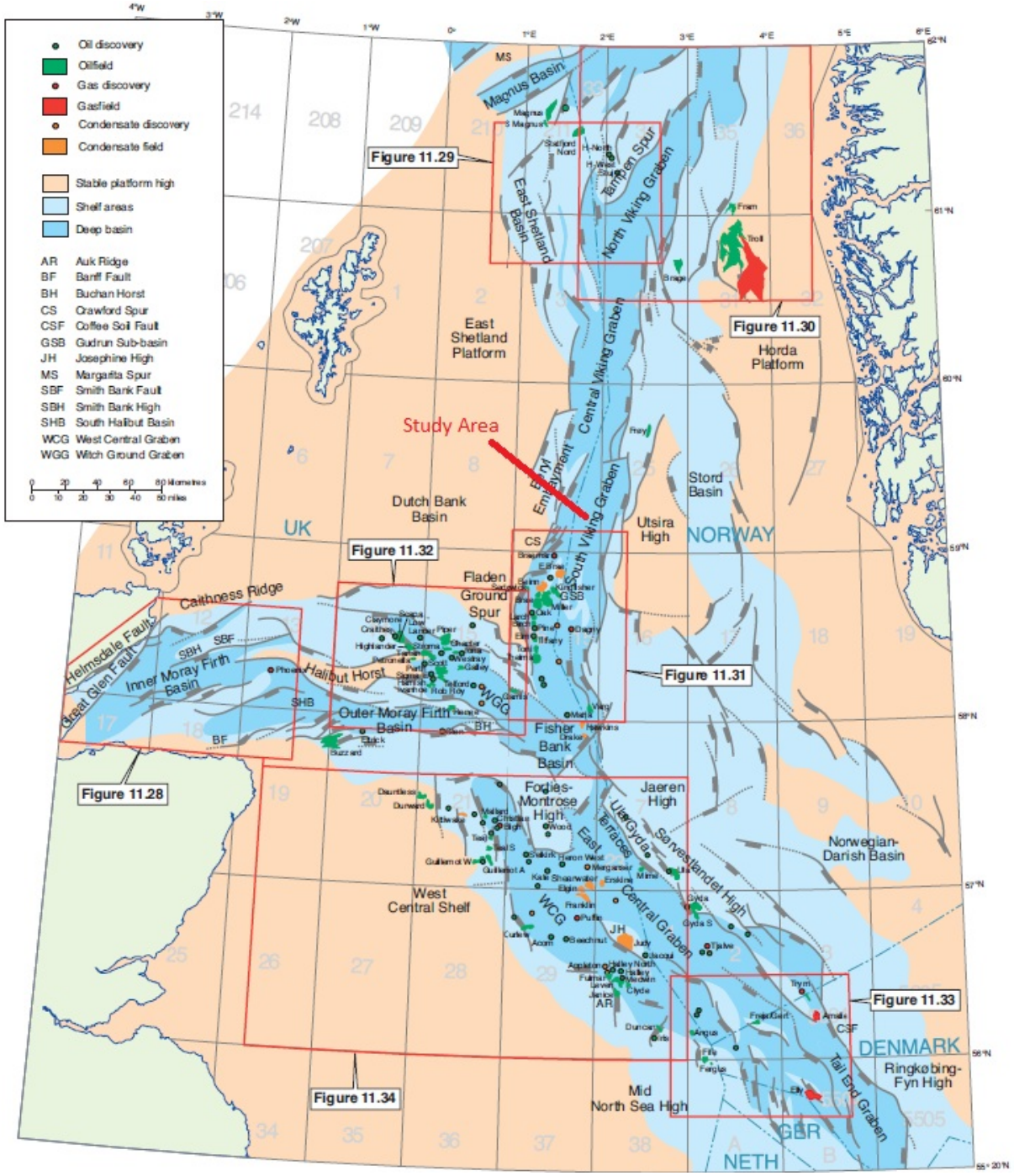

Figure 2.1: Location map and late Jurassic regional setting (Fraser et al., 2002).

The Upper Jurassic Play is distinguished by two contrasting reservoirs coastal-shelf sandstones and deep-sea submarine-fan sandstones in the form of slope aprons and basin-floor fans (Erratt et al., 1999 in Fraser et al., 2002). Regional development of restricted oceanic

circulation conditions together with irregular and fragmented basin-floor and high sedimentation rates contribute to the formation of anoxic conditions during the deposition of the Kimmeridge Clay formation which act as potential source rock.

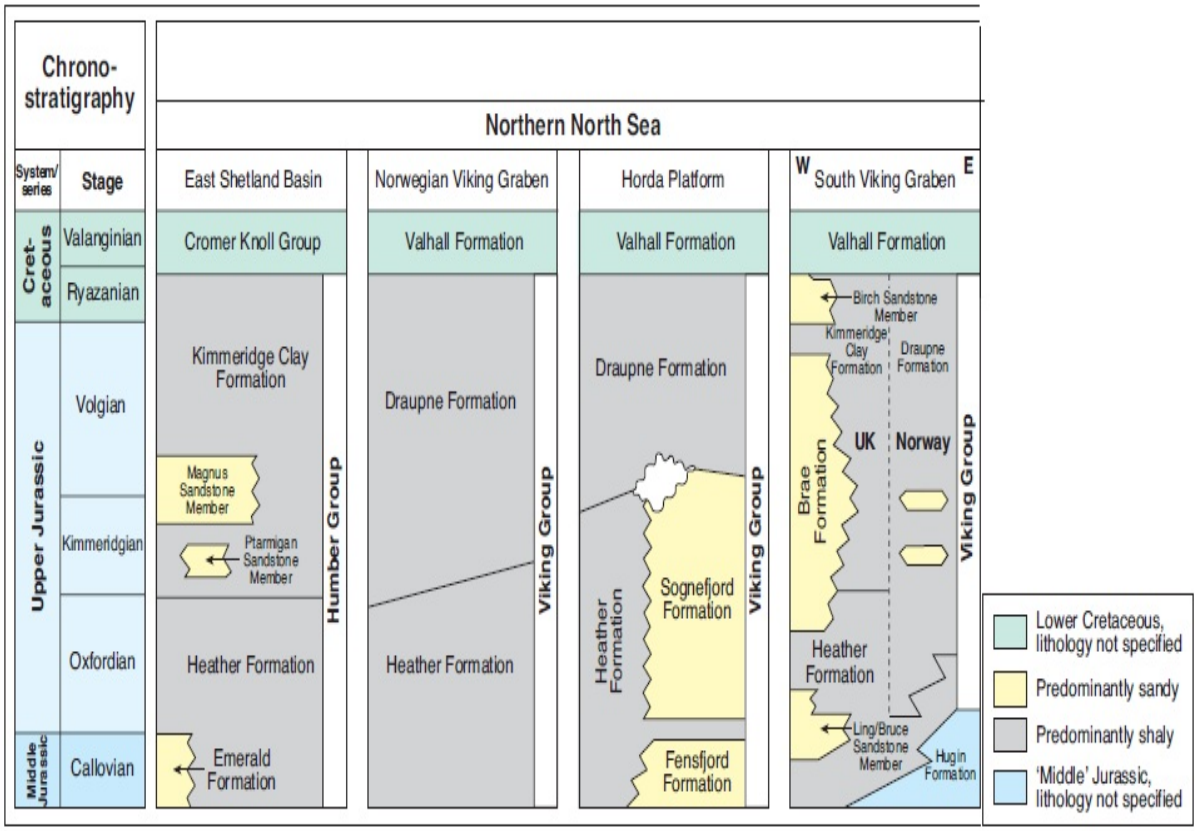

Figure 2.2: Lithostratigraphic chart of northern North Sea. From Fraser et al., (2002)

This source rock also act as top seal to the older shallow-marine/shelf sandstones or interfingers with and overlies, basin-margin, submarine-fan sandstone bodies. These perfect configurations are the major factors in the success of the play (Knott et al., 1993; Dore et al., 1999; Roberts et al., 1999 in Fraser et al., 2002).

2.3 Structural Development and Evolution

The near-base Cretaceous surface shows the pre-existing basement trends and overall structural style of the three rift arms of the Viking Graben, the central Graben and the Moray Firth basins (Ziegler, 1982; 1990a in Fraser et al., 2002). The most important extensional phase occurred over a period of about 10 Ma between the mid-Callovian and the early Kimmeridgian (Underhill, 1991a; 1991b; Rattey and Hayward, 1993) in (Fraser et al., 2002).

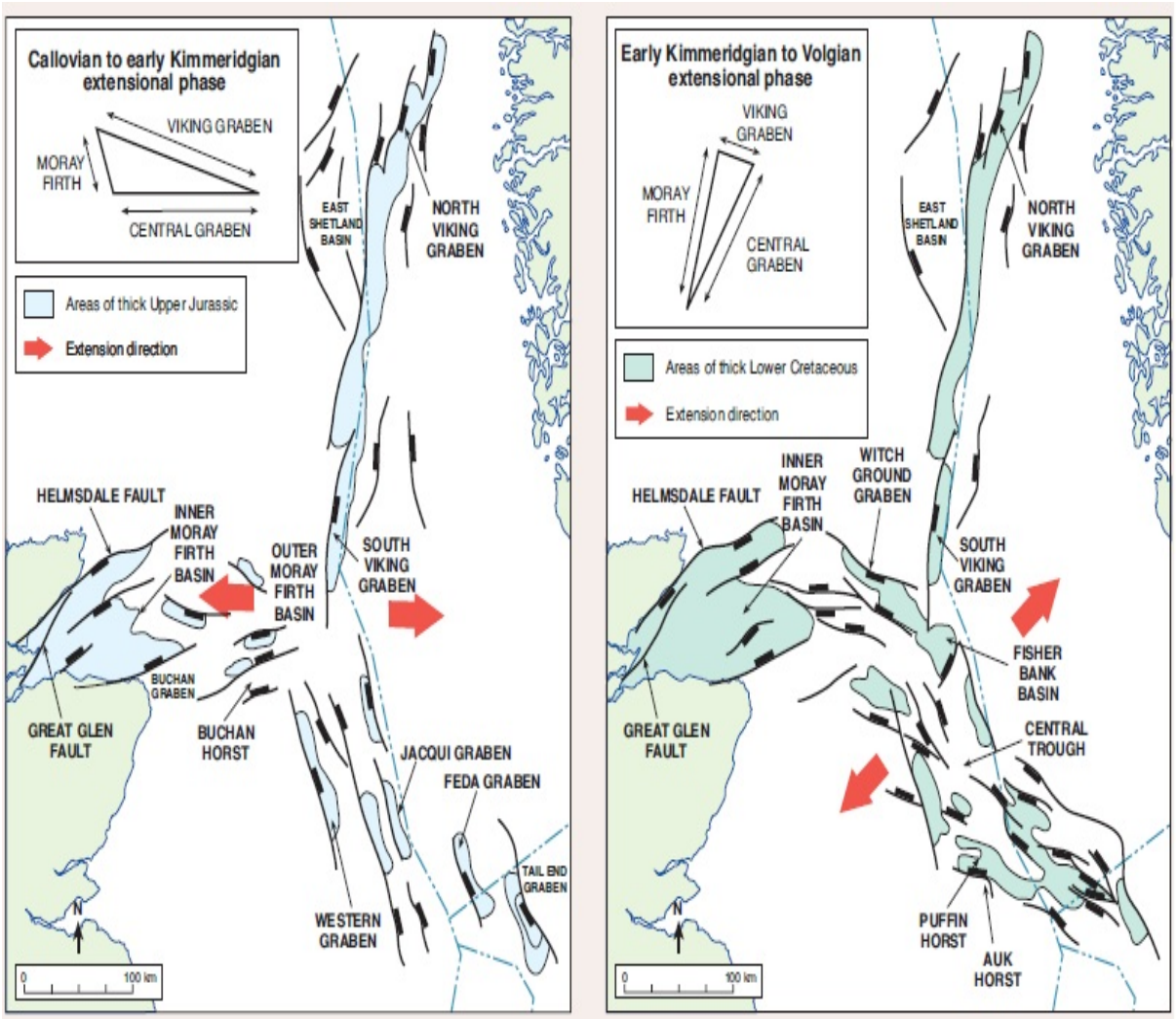

Figure 2.3: Two phase model of orthogonal opening of the North Sea rift (Errat et al., 1999) in (Fraser et al., 2002).

The interaction of three pre-existing lineaments i.e., the north-south Pre-Cambrian trend, the north-easterly Caledonite trend and the east-south-easterly Tornquist trend controlled the beginning of major Late Jurassic basement extension. Deflation of the Mid-Jurassic North Sea thermal zone was another controlling factor (Zielger, 1990a, Underhill and Partington, 1993 in Fraser et al., 2002). Orientation and interplay of extensional faults and their associated relay ramps provide the way to deliver the coarse grained clastic sediments into adjacent basins. The combination of main basement trends of Caledonian and Tornquist origin explains the triad failed-rift system. The Viking Graben is gradually offset by Tornquist alignments and basin margin faults have Caledonite trends (Fraser et al., 2002).

2.3.1 Structural Elements

The Viking Graben has Northward trend with five north-north-easterly trending structural elements, which are arranged in left stepping en-echelon pattern. All elements have half graben geometry and they are bounded on one side by a large normal fault (Fraser et al., 2002). The late Jurassic extension controlled the sedimentation and formed the major faults with tilting of already formed sedimentary sequences. Each fault segment is itself a separate fault block with hanging wall uplift and footwall subsidence (Jackson and McKenzie, 1983; Yielding, 1990 in Fraser et al., 2002), which is the cause of formation of structural traps in the North Viking Graben. Uplift of footwalls caused their crestal erosion and degradation of fault-scarp (Underhill et al., 1997 in Fraser et al., 2002). This erosion was so intense in some parts that it exposed pre-Jurassic sequences and juxtaposed the Permo-Triassic or Devonian reservoirs against Upper Jurassic source rocks (Johnson and Fisher, 1998 in Fraser et al., 2002).

2.4 Reservoir Facies and Depositional Model

According to Fraser et al., Upper Jurassic reservoir rocks developed in two depositional environments i.e., shallow-marine/coastal-shelf systems as in Ula/Gyda and Sognefjord formations and deep-marine slope-apron and fan systems such as Brae formation. Two main basin formation processes were active at that time, first was the beginning of the rift related faulting whose propagation was along the axis of Viking Graben from North to South. Secondly, there was a regional rise in relative sea level which drowned the earlier thermal dome (Zielger, 1982; 1990a; Underhill and Partington, 1993 in Fraser et al., 2002). During late Jurassic, development of facies belts occurred parallel to the developing graben faults (Mitchener et al., 1992; Milton, 1993 in Fraser et al., 2002).

2.4.1 Shallow marine/Coastal Shelf Depositional System

Due to rapid relative sea level rise coastal-shelf depositional system developed and at the basin margins, good reservoir quality, shallow marine sands were deposited. These sands are now called Emerald, Fulmar, Heno, Hugin, Piper, Sognefjord and Ula formations. These

shallow marine sandstones are highly bioturbated and structure less. They show arrange of ichnofacies which helps in reconstruction of the depositional environment and paleobathymetry of such deposits (Pemberton et al., 1992; Taylor and Gawthorpe, 1993; Martin and Pollard, 1996).

According to Fraser et al, six facies associations are identified which are grouped into four assemblages as

1. Mud dominated offshore shelf deposits
2. Very fine to fine, highly bioturbated, argillaceous, distal lower shoreface to offshore transition sandstones
3. Fine to medium grained, lower to upper shoreface sandstones with parallel, low angle and hummocky cross-stratification
4. Fine to coarse grained, well sorted and superficially massive sandstones, locally pebbly and cross stratified upper-shoreface deposits.

2.4.2 Deep-marine submarine-fan and slope-apron systems

Deep marine turbiditic sandstones occurred (isolately) within the Draupne Formation (Intra Draupne Sandstones and its lateral equivalents, in the Viking Graben, Kimmeridge clay Formation (Brae Clastics) and the East Shetland Basin. These sandstone bodies can be attributed to rift related footwall uplift and erosion. Deeper parts of basin were starved of sediments and anoxic conditions supported the deposition of organic rich source rocks (Stow and Atkin, 1987 in Fraser et al., 2002). These sandstones occur in Brae, Tiffany/Toni/Thelma and Miller fan systems in the South Viking Graben, the Magnus fan systems in East Shetland basin and also occurred in hanging walls of Viking and Central Graben. In the South Viking Graben Brae trend forms a 100 km-long and 2-15 km narrow conglomerate and sand-prone belt along the hanging wall of the western boundary fault (Fraser et al., 2002).

In proximal areas which are adjacent to fault scarp, thick conglomerate intervals are present. These intervals grade basinward from turbiditic sandstones to basinal mudstones. The deep marine sandstones which were deposited within the Draupne Formation may form combined structural-stratigraphic traps (Stow et al., 1982; Stow, 1983, Turner et al., 1987) in (Fraser et al., 2002).

The Intra-Draupne Formation Sandstones have been encountered in a number of wells in the Tampen and Oseberg areas and along the flanks of the Utsira and Jæren Highs (www.npd.no). These sandstones are considered to be of turbiditic origin (Harms et al., 1980) and are described as part of Draupne Formation. The East Brae reservoir consists of four lithotypes as differentiated by Aggett, 1997. (1) High density turbiditic sandstones (2) Low density turbiditic sandstones (3) Remobilized deposits and (4) 'Background' hemipelagic deposits). The East Brae reservoir consists of typically good to excellent quality sandstones in thick packages and is separated by thinner shales.

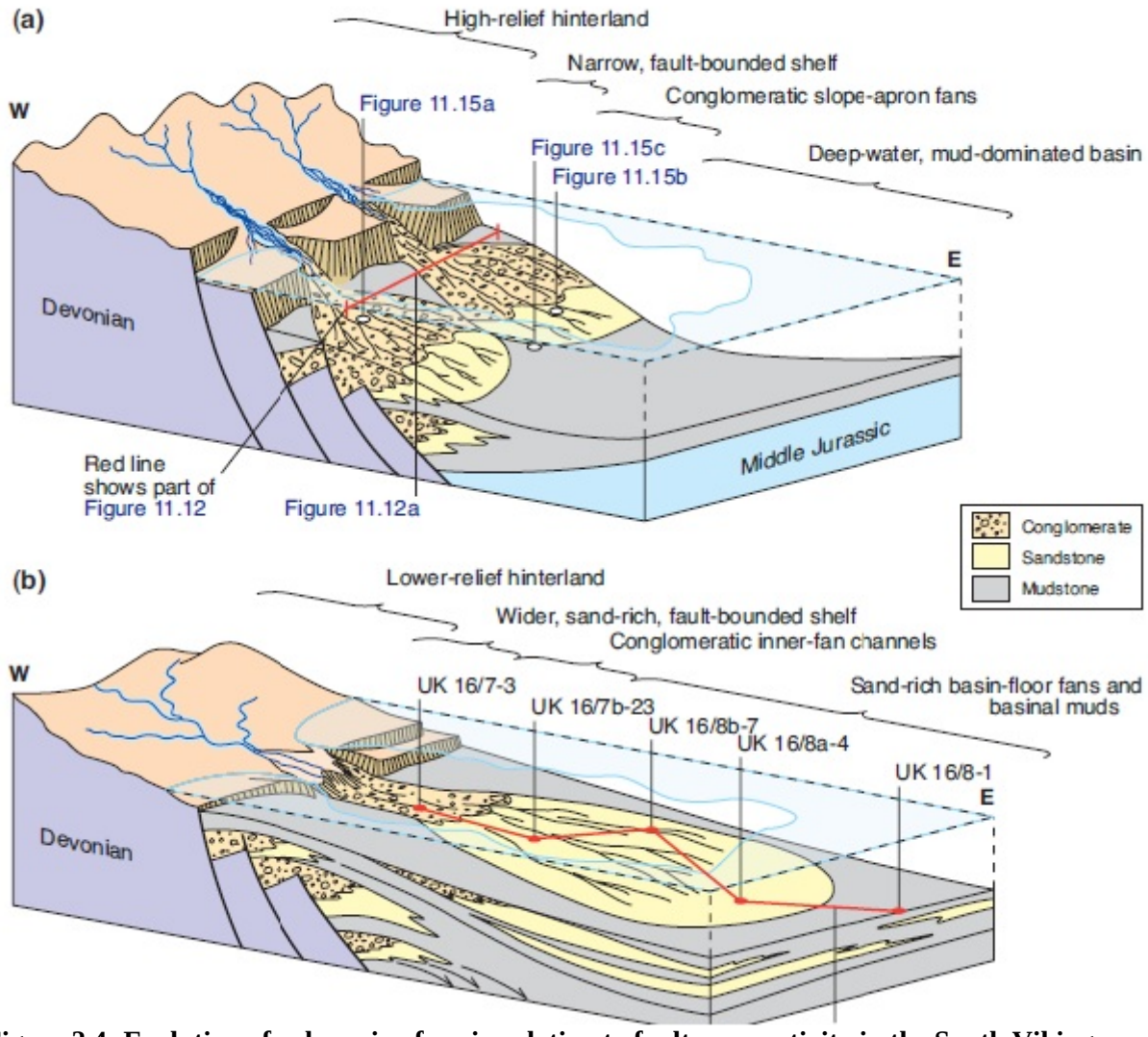

Figure 2.4: Evolution of submarine fans in relation to fault scarpactivity in the South Viking Graben (a) gravel rich slope-apron fans showing steep active faults (Brae, Tiffany, Thelma and Toni reservoirs. (b) Sand-rich basin-floor fans (Central Brae, Miller and Kingfisher reservoirs) from Fraser et al., 2002.

3. THEORATICAL BACKGROUND

3.1 Introduction

The success of finding hydrocarbons in exploration work relies on discoveries of sandstone reservoirs with enough porosity and permeability to support commercial development. Reservoir quality risk assessment is very important in plays and prospects in which sandstone reservoirs have been exposed to higher temperatures (>100^0C) and/or high effective stress for a longer period of geologic time (Taylor et al., 2010).

Reservoir quality is an important uncertainty in wildcat drilling (Bloch, 1994a; Wilson, 1994 in Lander and Walderhaug, 1999). During greater burial depth several diagenetic processes occur. This chapter describes the main digenetic processes and porosity preserving mechanisms which affect the sandstone bodies.

3.2 Diagenesis

After deposition, diagenetic processes occur to modify the composition of sediments. The main diagenetic processes include; near surface diagenesis, mechanical compaction, chemical compaction and formation of authigenic minerals and cements (Bjørlykke and Jahren, 2010). Mechanical compaction is the main mechanism to reduce the porosity at shallow depths and chemical compaction is pronounced at greater depths.

3.2.1 Shallow Burial

At shallow burial depth (between 1-10m), sediments react with the atmosphere and water by fluid flow and diffusion. Dissolved solids are transported by these two mechanisms. Oxidizing conditions occur in the upper few centimeters of seabed and reducing conditions prevail in deeper part of basin. At certain depth where there is no free dissolved oxygen in the pore water, sulphate reducing bacteria uses the sulphates and generate sulphides like pyrite. The initial composition of clastic sediments is altered by the addition of newly formed components within the basin like biogenic carbonates and silica, authigenic minerals like carbonates, phosphates, glauconite, sulphides and iron etc, and the formation of kaolinite by the leaching of feldspar and mica (Bjørlykke and Jahren, 2010). Bioturbation also changes the

textural composition of the sediments. It destroys the laminations of the clay, increases the vertical permeability and hence enhances the reservoir quality. Siliceous organisms like diatoms and siliceous sponges which are composed of opaline silica, can act as source for micro-quartz coatings on detrital quartz grains at greater burial depths. Biogenic carbonate is the main source of calcite cement. In the Mesozoic era, evolution of pelagic planktonic calcareous organisms occurred and increased the supply of carbonate to deeper parts of the basin, before this, all of the carbonate produced by the benthic organisms was confined to the shallow water facies. Upper Jurassic and younger sandstones are heavily cemented by calcite due to the rain of calcareous algae and foraminifera on the seafloor. Siliceous sponges made up of amorphous silica, are dissolved at higher temperatures and are changed to opal CT and quartz (Bjørlykke and Jahren, 2010).

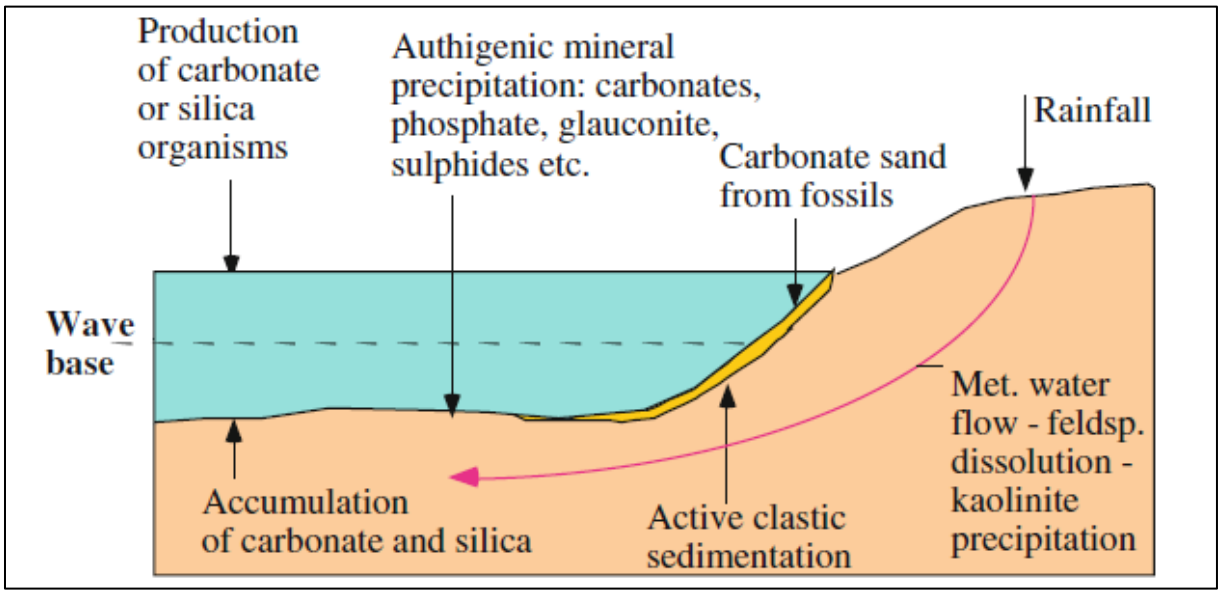

Figure 3.1: Digenetic processes in shallow marine environments. Meteoric water flushing and water from delta top causes dissolution of feldspar and mica. Early carbonate cement is important addition to the composition of sandstone. And presence of siliceous organisms such as sponges can help in enhancing the reservoir quality by providing the dissolved silica at low temperatures to form micro quartz coating preventing the quartz overgrowth and enhancing the porosity (Bjørlykke and Jahren, 2010).

Rainwater dissolves CO_2 and SO_2 from the air and alters slightly into carbonic acid (H_2CO_3) and Sulphuric acid (H_2SO_4), seeps into ground and is mixed with ground water. This meteoric water starts to dissolve carbonates first and then other unstable minerals like feldspar and mica. According to Bjørlykke and Jahren (2010), leaching of minerals like feldspars and mica and then precipitation of kaolinite are controlled by the flux of groundwater which is flowing through the rock per unit of time. Na^+ and K^+ are leached away from silicate minerals like

feldspar and mica come into solution. This reaction can be explained by the following equations:

$$2K(Na)AlSi_3O_8 + 2H^+ + 9H_2O = Al_2Si_2O_5(OH)_4 + 4H_4SiO_4 + 2K^+(2Na^+)$$

Feldspar — Kaolinite — Dissolved Silica — Dissolved Cations

$$2KAl_3Si_3O_{10}(OH)_2 + 2H^+ + 3H_2O = 3Al_2Si_2O_5(OH)_4 + 2K^+$$

Muscovite — Kaolinite

From these reactions it is obvious that dissolution of feldspar and mica, and precipitation of kaolinite is only continuous when Na+ , K+ and silica are removed constantly and it will only be possible when there is enough supply of fresh water which is undersaturated with respect to feldspar and mica. Feldspar grains weathered away during this process leave behind a clay coating that forms an outline of feldspar grain. Dissolved silica and aluminum generated, combines to precipitate the kaolinite. This process leads to small increase in porosity but reduce the permeability. The pores between the kaolinite crystals are too small and that could be a reason for the reduction of oil saturation in kaolinite-rich sandstones. Silica released from dissolution of feldspar does not precipitate as quartz but it remains in the solution because temperature is low near the surface. When concentration of silica becomes very high in porewater, kaolinite becomes unstable and smectite is precipitated instead (Bjørlykke and Jahren, 2010).

When sediments stay in a zone where meteoric water flushing is intense, feldspar leaching amount will be high. Based on the observation of thin sections, it can be concluded that kaolinite precipitation occurs at a relatively late stage because it is a pore-filling mineral that is surrounded by quartz cement subsequently. But detailed textural studies and isotopic evidence reveals that formation of kaolinite is in early stage and it can be enclosed in quartz cement (Bjørlykke and Jahren, 2010).

Observations from isotopic composition ($\delta^{18}O$) of kaolinite explains that its precipitation occurred at low temperatures in the range between 30-60^oC (Glassmann, 1989). But these temperatures are expected to be higher that could be experienced in meteoric water flushing and there is another possibility that some kaolinite may be recrystallized at higher temperatures which resets the isotopic composition. Another mineral dickite, (which looks like kaolinite) has the same composition as of kaolinite but thicker more blocky crystals.

Studies indicate that dickite sometimes replaces some kaolinite when temperature exceeds 100^{o}C. There is abundant authigenic kaolinite present in the North Sea Basin in the shallow reservoirs (1.5-2 Km) and there is little or no quartz cement in sandstones and this provides the evidence of formation of kaolinite at shallow depths. Dissolution of feldspar and mica generates secondary porosity but the precipitation of authigenic clays like kaolinite reduces the porosity so there is small net gain in pore space. Authigenic kaolinite occurs as pore-filling mineral and this reduces the permeability. The smaller pores (<0.005 mm) which are present between the kaolinite crystals are too small to be filled with oil because of the high capillary entry pressure which is required to infiltrate these pores. Thus, there is higher water saturation in the reservoir rock (Bjørlykke and Jahren, 2010).

3.2.2 Mechanical compaction of loose Sand

When well sorted sand is deposited and is present between (0-2 Km) depth. It remains loose if not cemented by carbonate cementation. Studies of experimental compaction of loose sand with an initial porosity 40-42% reveals that porosity can be reduced to 25-35% at stresses of 20-30MPa corresponds to 2-3 Km of burial depth of normally pressured rocks. The experimental data also shows that under same circumstances, well sorted coarse-grained sand are more compressed than fine-grained sand (Chuhan et al. 2002). Overpressure reduces the vertical effective stress and helps in preserving the porosity due to mechanical compaction.

In Sedimentary basins with normal geothermal gradient, grain framework is stabilized by quartz cementation and hurdles the further mechanical compaction at a burial depth of about 2km (70-80^{o}C). At further greater depths, compaction occurred by both effective stress and temperature. The degree of porosity loss by mechanical compaction determines the intergranular volume (IGV) at the onset of chemical compaction (Bjørlykke and Jahren, 2010). In North Sea, sandstone IGV is measured and it falls between 38 to 28% (Walderhaug, 1996) and after precipitation of 10% of quartz cement net porosity will be very different.

3.2.3 Burial of sandstone reservoirs to Intermediate Depth (2.0-3.0 Km, 50-120^{o} C)

Sedimentary basins where continuous subsidence occurred, sandstone reservoirs buried to shallower depths than 2.0-2.5 km are still loose and become poorly cemented but exceptions

occur in basins with high geothermal gradients and early carbonate cementation. This phenomenon is well documented in North Sea basin and parts of the gulf coast basin (Bjørlykke et al., 1992).

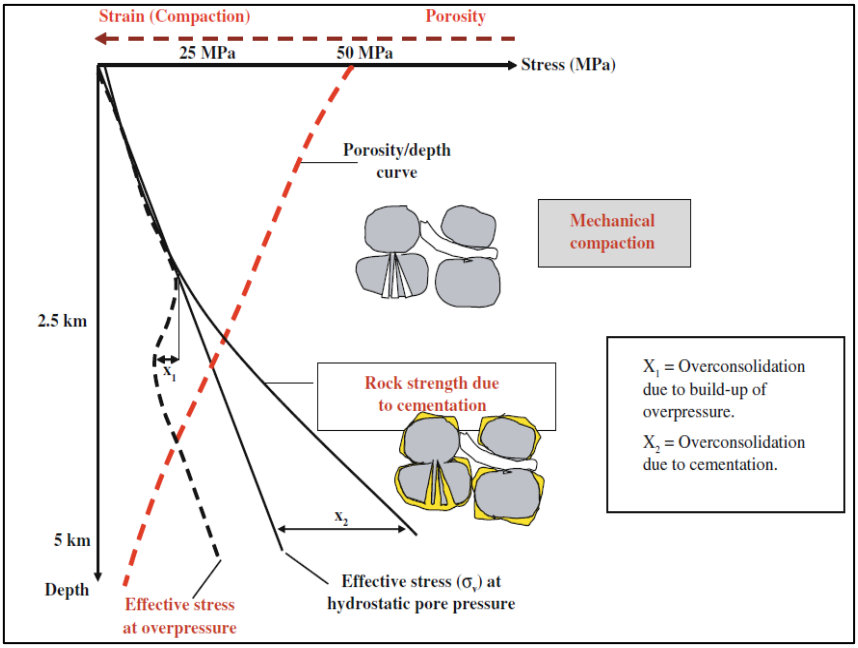

Figure 3.2: Mechanical compaction at shallow depths as a function of effective stress by grain reorientation and grain breakage at temperature lower than 80°C but at greater depths where temperature exceeds 80°C the rock compact chemically by quartz cementation (Bjørlykke and Jahren, 2010).

The amount of quartz cementation in sandstone is basically dependent upon the detrital grain surfaces available for quartz precipitation and time-temperature integral (Walderhaug, 1994). At a certain depth, high geothermal gradients and slow subsidence rate will increase the amount of quartz cement. In Upper Jurassic sandstone reservoirs of the North Sea, amorphous silica from Rhaxella sponges dissolves and generates super saturation of silica relative to quartz. This process is responsible of precipitation of minute quartz crystals on the surface of clastic quartz grains. This micro-quartz coating prevent or decelerate the precipitation of later quartz cement and is the main reason of high porosity preservation and good reservoir quality at depths up to 5km in sandstone reservoirs. The micro-quartz precipitation at lower temperatures (60-80°C) is only possible when the porewater is highly supersaturated with respect to quartz by the dissolution of Opal A or Opal CT. Rhaxella evolved in the Upper Jurassic so older sandstones like the Middle Jurassic Brent sandstones does not contain this type of micro-quartz (Bjørlykke and Jahren, 2010).

At temperatures between 100-120^{o}C, small amount of kaolinite recrystallizes to dickite with the same chemical composition as of kaolinite but with slightly thicker crystals and it can also be distinguished from kaolinite on XRD. We can use the common name kaolin or kandite for these clay minerals. Carbonate cemented intervals can act as barriers to fluid flow and is important for reservoir quality evaluation and if they are laterally extensive, it can be useful. These types of low permeability layers can prevent the flow of gas from below the oil/water contact and from above the gas/oil contact into oil producing well. This phenomenon is called coning. Albatization occurs by the replacement of k-feldspar or plagioclase by albite in sandstones buried to about 3 km. Albite is more stable than K-feldspar because Na^{+} is dominant cation in the porewater while the potassium concentration is reduced due to removal by the clay mineral reactions. Smectite is present in some muddy and volcanic sandstone which are flushed with limited amount of meteoric water. Smectite dissolves and is replaced by mixed-layer minerals and illite between temperatures 70 to 80^{o}C. Sandstone with smectite has low or poor reservoir quality. Dissolution of smectite and precipitation if illite and quartz can cause a sharp increase in the seismic velocity, and rock density and this transition of mineral phase transition can be shown on horizontal reflector on seismic and can be taken as fluid contact misleadingly i.e., gas/oil or oil/water contact (Thyberg et al., 2009).

3.2.4 Deeply Buried Sandstones (>3.5-4Km,>120oC)

When quartz cementation process starts and quartz overgrowth takes place, all the porosity will be lost by quartz cementation until temperature remains above 70-80^{o}C. This is observed from the analysis of different sedimentary basins that there is a greater reduction in porosity and permeability in sandstone reservoirs where burial depth is in the range of 3-3.5km to 4-4.5km with temperature value between 120^{o} to 160^{o}C. The reason of this reduction in porosity and permeability is due to the precipitation of quartz cement and digenetic illite. The main factor in the precipitation of quartz cement is the availability of surface area of grains to form quartz cement and as this process proceeds reduce the porosity and surface area available for quartz cementation decreases (Bjørlykke and Jahren, 2010).

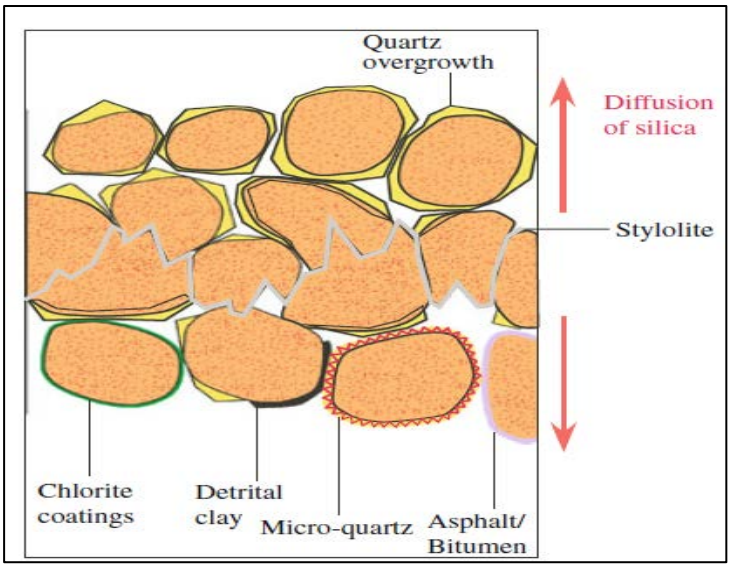

Figure 3.3: Schematic illustration of stylolite. The dissolved silica is transported away from the clay-rich stylolite by diffusion. The rate of precipitation of quartz cementation is a function of the surface area available. Grain coatings like chlorite, illite, detrital clay, iron oxide, micro-quartz and bitumen prevent or slow down the quartz cementation and preserve good porosity in sandstones (Bjørlykke and Jahren, 2010).

While modeling and prediction of quartz cementation and porosity loss in a sandstone, the temperature history is very critical. Because between the temperature range of 100 and 140^{o}C the rate of quartz cementation can double four times, quartz cementation increases 16 fold. And the increase in effective stress is linear with depth (under hydrostatic conditions) and increases from 30-40% with corresponding depth interval of 3-4km. Here, the main factor which controls the quartz precipitation is temperature. Quartz cementation is insensitive to variation in effective stress. Diffusion is the main mechanism which transports the dissolved silica from grain contacts or along stylolites to the grain surfaces where quartz cementation occurs in the form of quartz overgrowth (Figure 3.3)

3.3 Porosity Preservation Mechanisms

During the burial of sandstone, quartz cementation is found to be the main porosity reducing factor when temperature ranges between 70-80^{o}C and quartz cementation will continue until temperature remains above this limit and also until the remaining porosity is filled by cementation. There are certain coatings of minerals which, if developed on the grain surfaces

prior to quartz cementation can hinder the formation of quartz over-growth and help in preserving the porosity.

There are different mechanisms which help in preserving the porosity in deeply buried sandstones depths greater than 4km. In this chapter the main emphasis is on micro-quartz coating because it is found as the porosity preservation factor in several other studies and during this observation it is found to be the main control on porosity.

3.3.1 Micro-Quartz Coating and Preservation of Porosity

According to Bjørlykke and Jahren, 2010 amorphous silica formed by the dissolution of Rhaxella sponges generates high super saturation of silica relative to quartz. This dissolved silica precipitates as a coating of minute quartz crystals (micro-quartz coating) on the surfaces of detrital quartz grains. Formation of this micro-quartz coating helps in preventing the precipitation of later stage quartz cementation (over-growth) and is found to be the main cause for higher porosities and good reservoir quality at depths up to 5Km. The precipitation of micro-quartz can occur at lower temperature of 60^{o}C because at that moment pore water is highly supersaturated with respect to dissolved silica through the dissolution process of Opal A and Opal CT, and at the same time quartz growth rate is slow resulting in nucleation of many small crystals. At higher temperatures, unstable silicates like Opal A, Opal CT and smectite have already dissolved. At this point, pore water is saturated with respect to silica and insufficient to precipitate quartz on the micro-quartz surfaces (Aase et al., 1996). Evolution of Rhaxella occurred in Upper Jurassic so the older sandstones did not contain micro-quartz coating like Middle Jurassic Brent sandstones. Due to its smaller crystal size, it is difficult to identify microcrystalline quartz in thin section using standard light microscopy but it can be easily identified using scanning electron microscope (SEM) secondary electron images. Micro-quartz coat consist of a layer of about 1-15µm prismatic quartz crystals with c-axis haphazard direction. The c-axis orientations of micro-quartz crystals (Haddad et al., 2006) can prevent their change into bigger syntaxial quartz overgrowths.

3.3.2 Clay Coatings

The clay coats are very important in preserving the porosity in sandstones and are identified in a lot of studies (Ehrenberg, 1993, Storvoll et al., 2002a, Bloch et al., 2002). These authors

demonstrate that sandstones that have poorly developed clay coatings are very highly quartz cemented whereas the same sands with extensive clay coatings have very low amount of quartz cement. The authigenic chlorite coatings are the most important and effective in retarding the extensive quartz cementation in sandstones. The main reason being that chlorite form continuous layers around the detrital quartz grains which helps in preventing the quartz overgrowth (Taylor et al., 2010). At Haltenbanken, offshore mid Norway, the Tilje and Garn Formations are reported to have extensive chlorite and illite coatings (Ehrenberg, 1993, Storvoll et al., 2002). These coatings are believed to be the reason for the good reservoir quality in the oil and gas discoveries on the Haltenbanken, and porosities are preserved up to 25% at greater burial depths of more than 5km depth. The precursor of chlorite formation in marine sandstones is from the alteration of an earlier iron silicate phase which were formed on the sea floor could be the iron and magnesium rich smectite. Illite is also reported to form an effective coating which prevents the quartz overgrowth (Heald and Larese, 1974) and precursor of illite could be smectite.

3.3.3 Hydrocarbon Emplacement

Many authors has suggested that early hydrocarbon emplacement inhibited the quartz overgrowth and helped in preserving the porosity (Emery et al., 1993, Gluyas et al., 1993, Marchand et al., 2000, 2001). But studies of the fluid inclusion data from quartz demonstrate that in sandstones quartz cementation continues after oil has been emplaced in the reservoir (Walderhaug, 1990, Karlsen et al., 1993). According to Ramm and Bjørlykke, 1994, there is very little correlation found between good reservoir quality and presence of hydrocarbons in the North Sea and reservoir quality remained the same across the water contact. Hydrocarbon emplacement does not affect the rate of precipitation of quartz cementation in sandstones (Walderhaug, 1994a).

3.3.4 Fluid Overpressure

Porosity reduction related to mechanical compaction is mainly driven by increase in effective stress. The vertical effective stress is being reduced by fluid overpressure at the grain contacts. Due to overpressure, the porosity is preserved in the sandstone reservoirs at greater

burial depths. Otherwise, it would be destroyed during the compaction process. The porosity is preserved by early overpressure during the diagenesis until the quartz cementation starts at about 80^{o}C (Walderhaug, 1994b). While according to Taylor et al., 2010, the development of overpressure at later stage has little effect on porosity.

4. METHODS AND DATA

Introduction

This study has been divided into three levels of investigation with different resolutions related to the tool to be used to evaluate the processes which are responsible in preserving the porosity and permeability of sandstone reservoirs. During the analysis Optical microscopy, Scanning electron microscopy (SEM), well correlation and Petrophysical evaluation techniques are employed. In addition WDSS, maps and a lot of information available through the Norwegian Petroleum Directorate's website (www.npd.no) is incorporated during the study. Information gathered from the NPD's website is presented in Table 4.1.

4.1 Well Correlation and Petrophysical Evaluation

4.1.1 Well Correlation

Well correlation has been performed between seven wells. Main purpose is to separate different Lithostratigraphic units based on the Gamma Ray (GR), Bulk Density (RHOB) and Neutron Porosity (NPHI) logs. The correlation is focused on the Upper Jurassic synrift interval of the Draupne Formation/Brae Formation. The geophysical measurements are taken by lowering a probe into the well. These recorded measurements are very helpful in describing the porosities, lithology and the hydrocarbon content. For example, deep resistivity log (ILD) gives very high value in the hydrocarbon zone because of its penetration into the uninvaded zone of the formation. These logs can be further used to explain petro physical properties of rock units by making cross-plots.

Well correlation is based on the values from GR, RHOB and NPHI logs. Particularly RHOB and NPHI logs are run together in the reverse order, they make crossover against the gas zone. In addition to these two logs the DT and ILD are employed to separate the carbonate cemented intervals in a sandstone unit. The identification and demarcation of different lithostratigraphic units is easier in the study area. The values of gamma ray log are high (often above 150API) in Draupne Formation as compared to the underlying Heather Formation which made it distinctive. The well correlation has been carried out using PETREL software. Some details about the different logs with their basic principles is given below.

Well	Location	Field	Depth(m)			B.H.T (^{o}C)	Pay Zone	Fluid Type	Oldest Penetrated Formation & Age
			M.D (m RKB)	K.B	Water Depth				
15/3-1S	Vilje Sub-basin	Gudrun	5132	25.0	109.0	-	Upper Jurassic Middle Jurassic	Gas/Condensate	Sleipner FM Middle Jurassic
15/3-3	Vilje Sub-basin	Gudrun	5116	25.0	109.0	149	Upper Jurassic Middle Jurassic	Gas/Condensate	Skagerrak FM Triassic
15/3-7	Vilje Sub-basin	Gudrun	4818	18.0	109.0	154	Upper Jurassic Middle Jurassic	Oil/Gas	Sleipner FM Middle Jurassic
15/3-8	Vilje Sub-basin	Gudrun	4592	23.5	109.0	145	Upper Jurassic	Oil/Gas	Intra-Draupne FM Upper Jurassic
16/3A-1	Vilje Sub-basin	East Brae	4690	-	-	123.72	Upper Jurassic	Gas/Condensate	Kimmeridge Clay Upper Jurassic
16/3B-5	Vilje Sub-basin	East Brae	4327	-	-	123.72	Upper Jurassic	Gas/Condensate	Brae Clastics Upper Jurassic
16/3B-7	Vilje Sub-basin	East Brae	4420	.	.	123.72	Upper Jurassic	Gas/Condensate	Kimmeridge Clay Upper Jurassic

Table 4.1 An abstract of well summary sheet from the Fact Pages from (www.npd.no).

4.1.2 Geophysical Well Logs:

Logging is a technique used to record the physical properties of the rocks penetrated by a well. Drilling mud is used to balance the water pressure in the formation and also the pressure of oil and gas which we encounter during drilling. This mud also transports back the rock fragments cut by bit to the surface for observation (drill cuttings). Type of drilling mud used is also very important as it influences the recordings. Muds with seawater or fresh-water can be used and the salinity of mud influences the resistivity. Oil based muds are also being used in the industry. The pressure of the drilling mud must be greater than the formation water pressure to squeeze the mud into the formation (Bjørlykke, 2010).

A borehole is logged by sending a probe with a measuring instrument down into the well after we pull up the drilling tool. A list of well logs with some detail is given below

1. Resistivity Log
2. Gamma Ray log
3. Neutron Porosity log
4. Acoustic (Sonic) log
5. Caliper log

Resistivity Logs:

Resistivity logs are the result of measurements of the resistance between 2 and 4 electrodes which are in contact with the rocks in the well. Resistivity (In ohms) is measured as a function of the cross section ($m^{2)}$ of the rock and the distance (m) between the electrodes. The resistivity R = ohm.m^2/m, so the unit is Ohm.m. Resistivity is the inverse of conductivity. Clay minerals and salts such as NaCl and KCl have significant conductivity. All conduction take place through liquid phase and resistance depend upon the pore liquid and its salt content. Oil and gas have higher resistivity than water, so we can use resistivity logs to locate the OWC and GWC in a reservoir, i.e. hydrocarbons are resistive while formation water is conductive (Bjørlykke, 2010).

Gamma Ray Logs

Gamma ray logs measure the natural radioactivity, produced in the rock. Potassium (K), Thorium (Th) and Uranium (U) produce gamma radiations in sedimentary rocks. Shale mostly contains most of these elements and gamma readings of shale are always higher than the sandstones. Gamma ray logging toll is equipped with scintillation counter capable of distinguishing different energy levels(expressed in MeV of gamma radiation from rock) so that it can distinguish between the relative contributions of K(1.46 MeV), U(1.76 MeV) and Th(2.62 MeV). These logs are called spectral gamma ray logs. The gamma ray index is calculated from the minimum gamma ray readings in clean sand. The maximum reading is recorded in the shales. And then volume of shale can be calculated (Bjørlykke, 2010).

Neutron Logs

This log is based on a probe which emits neutrons at high velocity. The neutron rays are absorbed by the rock and particularly by water in the rock. This is due to collisions with atomic nuclei and absorption of the neutron radiation is a function of hydrogen atom concentrations (Hydrogen Index). Since most of the hydrogen in rocks is present as water, neutron logs provide an expression of the water content and thereby porosity of the sediments. These are very useful in determining the porosity of shales. Gas is less dense and has few hydrogen atoms per unit volume than water and oil and has lower hydrogen index.

Neutron log can be used to detect gas and distinguish it from oil. Calculation of porosity from neutron logs (neutron porosity) gives very low porosity, when the pores are filled with oil and gas because they contain less hydrogen per unit volume compared to water. This is called the gas effect. Neutron porosity is represented by NPHI (Bjørlykke, 2010).

Sonic or Acoustic Logs

A probe sends out acoustic pulses which travel through the rock surrounding the well to the other end of the logging tool and velocity of sound in the rock is recorded. The velocity is denoted by time Δt, a signal takes to travel a certain distance which is the inverse of velocity (slowness). This is called interval transit time and is presented on the log in scale of 40-140 μs/ft. The interval transit time is the reciprocal of the sonic transit velocity (Bjørlykke, 2010).

4.2 Petrophysical Analysis

Petrophysical analysis is done on Interactive Petrophysics (IP) software. All the well logs used in the Petrel were imported into IP. This software helps in plotting the data of logs in the form of cross-plots and additionally gives the advantage of third dimension of color coding to be displayed. For this purpose Bulk Density (RHOB), Sonic (DT), Gamma Ray (GR) and Resistivity (ILD) logs were employed. For the analysis on Interactive Petro physics (IP) Density_ Porosity log generated on Petrel by using the Log Calculator. Because most of the samples observed were quartz arenites so the density of matrix taken 2.65 g/cm^{3,} which is the density of quartz. The bulk density is taken equal to the values measured by the density log (RHOB). The density of fluid varies between 1.3 to 2.02 g/cm^3 in different wells. But this is set to 1g/cm^3, which is the density of brine water (Champel, 2006).

The density porosity can defined as:

$$\text{Density\_Porosity} = (\rho matrix - \rho b)/(\rho matrix - \rho f)$$

Gamma Ray Index calculated from the following equation

$$I_{gr} = (GR_{log} - GR_{clean})/ (GR_{sh} - GR_{clean})$$

$$V_{sh} = 0.33\ (2^{(2 - Igr)} - 1) \quad \text{(Larionov, 1969 for older rocks)}$$

$$\text{Total-Porosity} = \text{Sqrt}\ (NPHI^2 + RHOB^2)/2$$

$$\text{Effective-Porosity} = \text{Total-Porosity} * (1 - V_{sh})$$

Where,

$\rho matrix$ = density of matrix

ρb = bulk density

ρf = fluid density

I_{gr} = Index Gamma Ray

GR_{clean} = minimum Gamma Ray reading from log

GR_{sh} = maximum Gamma Ray reading from log

V_{sh} = Volume of shale

The value of GR_{log}, NPHI and RHOB used from the logs directly.

4.3 Optical Microscopy

4.3.1 Thin Section Analysis and Textural Characteristics

Twenty one thin sections have been analyzed to get estimation of the mineralogical and textural variations in sandstone samples from Intra-Draupne Formation Sandstone and Brae Formation with a standard polarization microscope; Nicon Optiphot-Pol petrographic microscope. All the thin sections were polished and seventeen of them were impregnated with blue epoxy and remaining four with transparent (colorless) epoxy. Thin section study has been carried out to make estimation about mineral content (lithology), average grain size of samples, sorting and grain shape. Other characteristics like quartz overgrowths and sponge spicules are also noted during the analysis. Pictures from thin sections are also included to support the study taken with high magnification microscope; Nicon-Microphot –SA. The grain size measurements are based on the scale of Udden-Wentworth (Wentworth, 1922) grain size scale. Whereas the maturity of sandstone from the sorting and roundness measurements of samples is calculated employing the Folk, 1951, scheme.

4.3.2 Point Counting Analysis

All the twenty one samples have been point counted to get an estimation of the composition and porosity of the samples. An automatic counter (Swift) attached with a mechanical stage, POL is used with the standard polarizing microscope for point counting. Across the thin section a grid is projected by combining the mechanical stage and point counting attachment by moving the section through the field of vision along a straight line at equal intervals. For each thin section three hundred points are counted in ten rows with thirty counting each row by counting rock composition (quartz, feldspar and lithic fragments), matrix (detrital and authigenic clays), cements (quartz and calcite) and porosities (primary and secondary). The rock composition calculated has been plotted in a ternary diagram, using the TriPlot program (Copyright ©Graham and Midgley 2000).

4.3.3 Intergranular Volume

From the point counting results IGV was calculated according to definition of (Paxton et al., 2002) Intergranular Volume (IGV) = (total cement + depositional matrix) + intergranular porosity. The results from calculated IGV were presented as Bar chart diagram and divided into components like cements, matrix (detrital + authigenic clays) and primary porosity.

4.4 Scanning Electron Microscopy (SEM)

Scanning Electron Microscopy (SEM) technique is used for high resolution analysis of carbon coated thin sections and gold coated stub mounted samples of both formations. The analysis performed in a JEOL JSM 6460LV scanning electron microscope equipped with a LINC INCA EDS spectrometer, Gatan Mini CL and MonoCL3. To distinguish between different materials of variable elemental composition backscattered electron imagery (BEI) technique is employed. With the help of Energy dispersive x-ray microanalysis (EDS) the energies of emitted x-rays can be displayed as a series of peaks, spectra which is distinct for individual elements within the material (Bishop et al., 1992).

Both type of samples, the carbon coated thin sections and gold coated stub mounted samples, are photographed and evaluated both in SEM and EDS. CLI (Cathodoluminiscence) images are also taken to analyze quartz overgrowth and pervasive grain crushing. Visual estimation of micro quartz coating performed of all the stub mounted samples in SEM to obtain a quantitative analysis. The main emphasis is to analyze mineralogy and quartz overgrowth in thin sections and authigenic clays, mineral coatings, quartz overgrowth in stub mounted samples.

4.5 Uncertainties

4.5.1 Well Correlation and Petrophysical Analysis

The correlation of formations has been performed according to the information gathered from well reports, published literature and the fact pages on NPD's website (www.npd.no). There could be some uncertainties while putting tops for the wells from Brae Formation because no

published data were found. The assumption about bulk density value of 2.65 g/cm^3 is very simplified because the sandstone interval in all the wells having different thickness and clay stone intercalations.

There are certain parameters which may affect the calculation of density porosity like gas effect and borehole carvings because presence of gas in a formation can give high density porosity. And also enlarged and rough boreholes can affect the measurements taken from the instrument. This can cause the values of bulk density (RHOB) to lower readings than actual values. In this case porosities derived from density could be extremely high. But this effect can be detected by the crossover of RHOB and NPHI logs.

4.5.2 Thin section Analysis (Optical Microscopy)

There are uncertainties during the point counting of thin sections while counting secondary porosity and quartz overgrowth. Because secondary porosity was created during the dissolution of feldspars and unstable grains. During this process grains are partially dissolved and in other case authigenic clays precipitated in pores. So point counting of secondary porosity could be uncertain. Quartz overgrowths sometimes are not much obvious and dust lines formed which describe the surface of onset of quartz overgrowth are not visible which could lead to the difficulties in separating overgrowths from grains. Also the samples were point counted from the middle part of thin sections to correctly count the porosity values because the grains could be plucked at the edges, generating false porosity in the sample. Some of the points counted thin section were impregnated with white epoxy so to distinguish between missing grains and porosity was difficult. These all uncertainties can influence the calculated IGV values.

4.5.3 Scanning Electron Microscopy

During the SEM analysis of stub mounted samples it is difficult to quantify the real mineral content because the area of observation is very small. During the BEI mode of observation on thin sections quartz and albite look identical because of the same amount of electrons emission both minerals display the same grey shade. And albite content estimation undermined.

5. WELL CORRELATION AND PETROPHYSICAL EVALUATION

5.1 INTRODUCTION

This chapter describes the petrophysical properties which are being recorded by the well logs with an emphasis on the reservoir intervals in the seven wells. This investigation particularly based on the assessment of the synrift sandstones which are interbedded with the deep marine shales. And all the sandstone reservoir intervals are buried deeper than 4000m, which falls in the limit of deep burial in this area with corresponding temperature of 120^0C and with 30^0C/Km geothermal gradient. All the wells are present in Vilje Sub basin of the South Viking Graben in North Sea. The main purpose of well correlation is to identify lithostratigraphic units and to correlate them with the thin section slides and stub mounted samples.

5.2 Results

The results of lithostratigraphic correlation and petro physical evaluation are presented separately. The purpose of this approach is to evaluate the correlation between the zones with anomalous porosity, to demarcate lithology and hydrocarbon zone.

5.2.1 Well Correlation

The Lithostratigraphic well correlation was carried out to find the variation in lithological units across the wells. The main purpose of well correlation is to correlate the Upper Jurassic section from Gudrun Field and East Brae Field. The Draupne Formation is mainly marine claystone, which is very rich in organic carbon and Gamma Ray values are very high (>100 API units). The Draupne Formation consists of interbedded lithologies of sandstone, claystone and limestone stringers of various thicknesses from laminas to stringers and massive layers. (www.npd.no). Its sandstone units are considered to be of turbiditic origin (Harms et al., 1980)".

The Brae Formation is predominantly medium grained sandstone, which were also deposited by high density turbidity currents. This sequence of East Brae reservoir is interpreted as the basin floor lateral equivalent of the North Brae feeder system to the south west. The North Brae and East Brae reservoirs are considered as the part of the same sub-sea fan, i.e., North

Brae is proximal part of the fan and is conglomeratic while East Brae is interpreted as the sandy basin floor equivalent (Brehm., 2003). The East Brae reservoir is enclosed in the kimmeridge Clay Formation, which is the source rock in this area (Branter. 2003). According to Turner et al., 1987 The Brae Formation is both underlain and overlain by the Kimmeridge Clay Formation. The Upper Jurassic sandstone reservoirs of both deep marine Draupne formation and Kimmeridge Clay Formation are mainly evaluated in this study. Thin section and stub mounted samples are studied from the wells 15/3-8(Gudrun Field) and 16/3B-5(East Brae Field) and are marked with corresponding depths (Figure 5.3).

Well	Location	Field	Depth(m)			B.H.T (°C)	Pay Zone	Fluid Type	Oldest Penetrated Formation & Age
			M.DR KB	K.B	Water Depth				
15/3-1S	Vilje Sub-basin	Gudrun	5132	25.0	109.0	-	Upper Jurassic Middle Jurassic	Gas/Condensate	Sleipner Fm. Middle Jurassic
15/3-3	Vilje Sub-basin	Gudrun	5116.0	25.0	109.0	149	Upper Jurassic Middle Jurassic	Gas/Condensate	Skagerrak Fm. Triassic
15/3-7	Vilje Sub-basin	Gudrun	4818	18.0	109.0	154	Upper Jurassic Middle Jurassic	Oil/Gas	Sleipner Fm. Middle Jurassic
15/3-8	Vilje Sub-basin	Gudrun	4592	23.5	109.0	145	Upper Jurassic	Oil/Gas	Intra-Draupne Fm Upper Jurassic
16/3A-1	Vilje Sub-basin	East Brae	4690	-	-	123.72	Upper Jurassic	Gas/Condensate	Kimmeridge Clay Upper Jurassic
16/3B-5	Vilje Sub-basin	East Brae	4327	-	-	123.72	Upper Jurassic	Gas/Condensate	Brae Clastics Upper Jurassic
16/3B-7	Vilje Sub-basin	East Brae	4420	-	-	123.72	Upper Jurassic	Gas/Condensate	Kimmeridge Clay Upper Jurassic

Table 5.1: An abstract of well summary sheet from (www.npd.no).

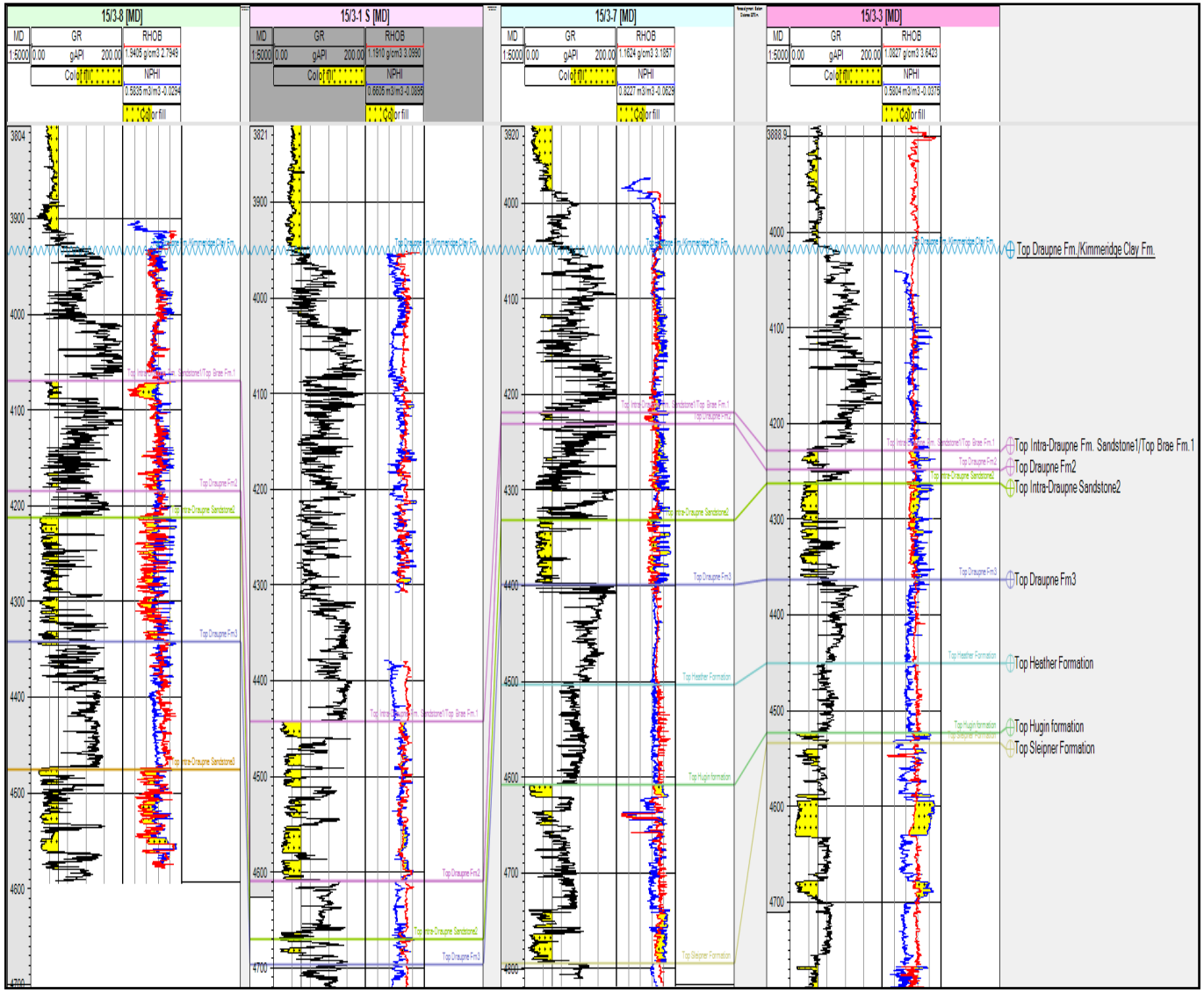

Figure 5.2: Lithostratigraphic Correlation of the Jurassic strata in the Gudrun Field

Well Correlation between 15/3-8 and 16/3B-5 is drawn (Figure 5.3). Thin section samples were made from the cored interval from both wells. Samples with corresponding depths were mentioned in the logs. Typical Boxcar trend (Emery and Myres, 1996) of gamma ray log, which is distinctive of turbiditic sandstone, is well displayed in both wells. The log response of bulk density (RHOB) and neutron porosity (NPHI) displayed in second panel next to gamma ray (GR) log. Both of the logs display crossover across the gas interval in the reservoir zone, when plotted in reverse order. The crossover is well displayed in well 16/3B-5, because of gas zone.

The lithostratigraphic correlation between all the wells from both Gudrun Field and East Brae Field displayed in figure 5.4. Wells were arranged EW across the South Viking Graben, showing the correlation between Upper Jurassic strata.

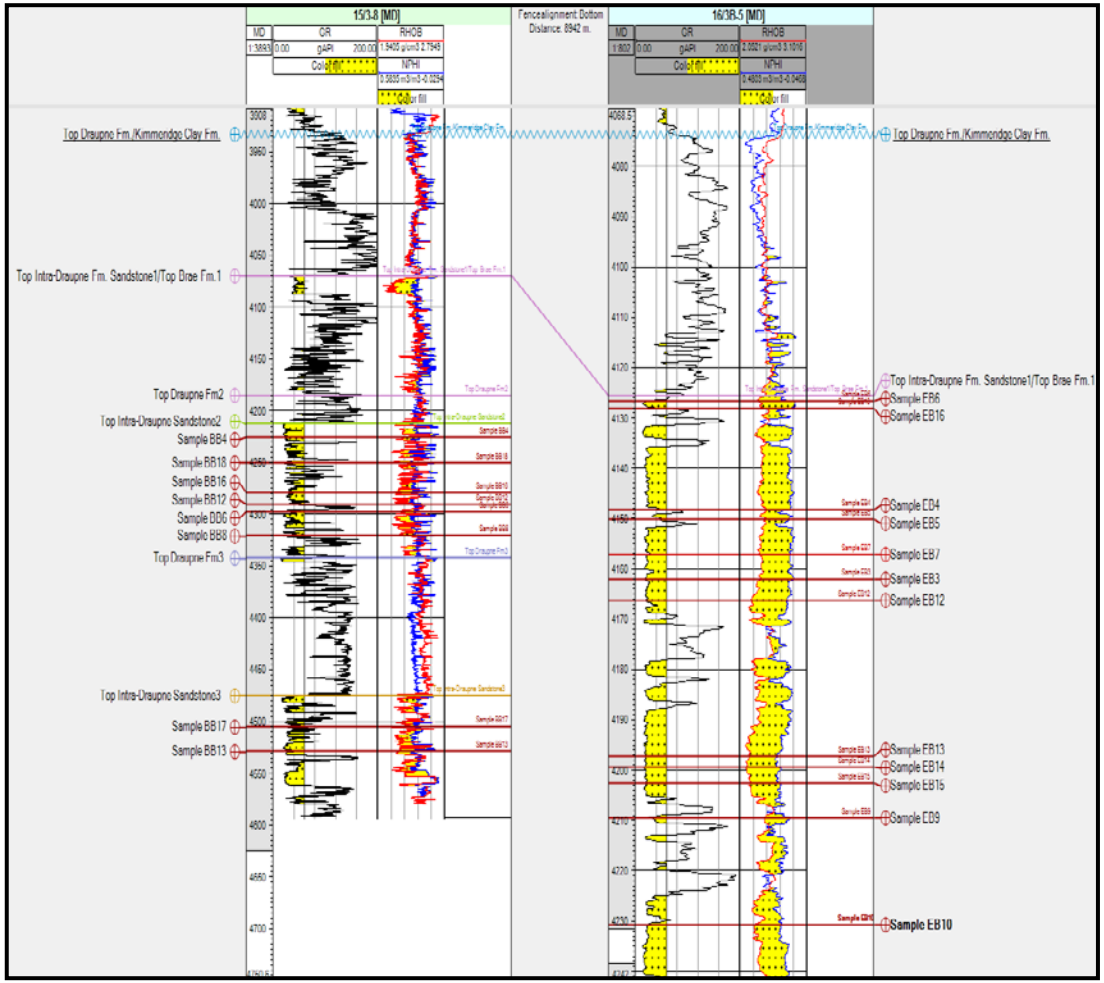

Figure 5.3: Well Correlation between 15/3-8(Gudrun Field) and 16/3B-5(East Brae Field) also displaying the thin sections with corresponding depths for both Intra-Draupne Sandstone Fm. (BB's) and Brae Formation (EB's). Typical Boxcar trend (cylindrical/block shape) of gamma-ray log (Emery and Myres, 1996) in turbiditic sandstones clearly seen. Crossover between RHOB and NPHI across the sandstone units in both wells corresponds to gas interval.

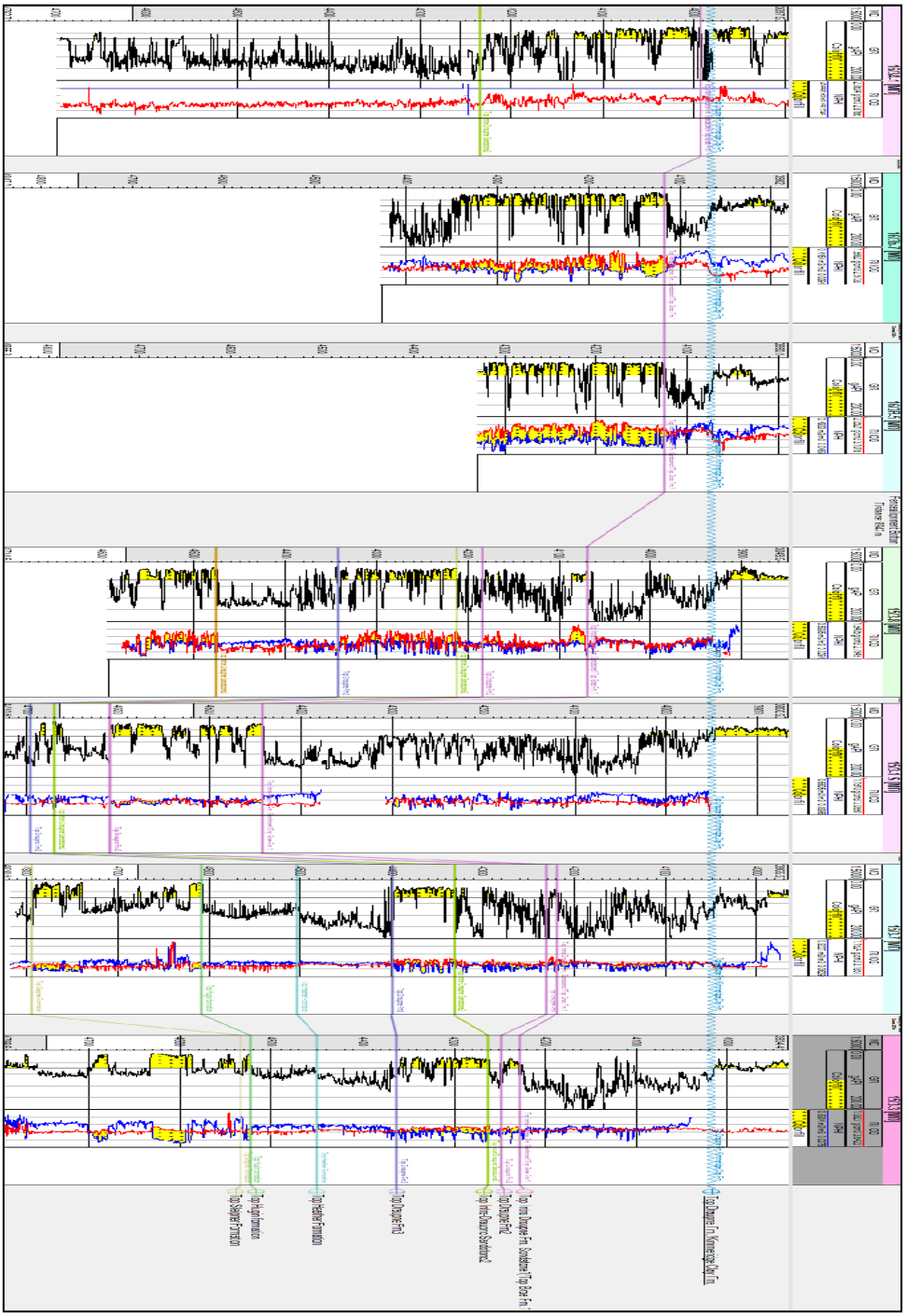

Figure 5.4: Lithostratigraphic Correlation of the Upper Jurassic strata in the East Brae and Gudrun Field

5.2.2 Petrophysical Evaluation

Petrophysical evaluation of the Upper Jurassic Synrift sequences has been performed to evaluate the lithology, porosity and fluid content by employing wire line log data. Different parameters are applied and plotted against each other to identify the lithologies and demarcation of high porosity zones in the wells. Hydrocarbon bearing sands are highly resistive than the water bearing sands. A cross plot between density-porosity versus depth color coded with deep resistivity shows porosity values range between 10 to 25% in the Intra-Draupne sandstone (Figure 5.5).

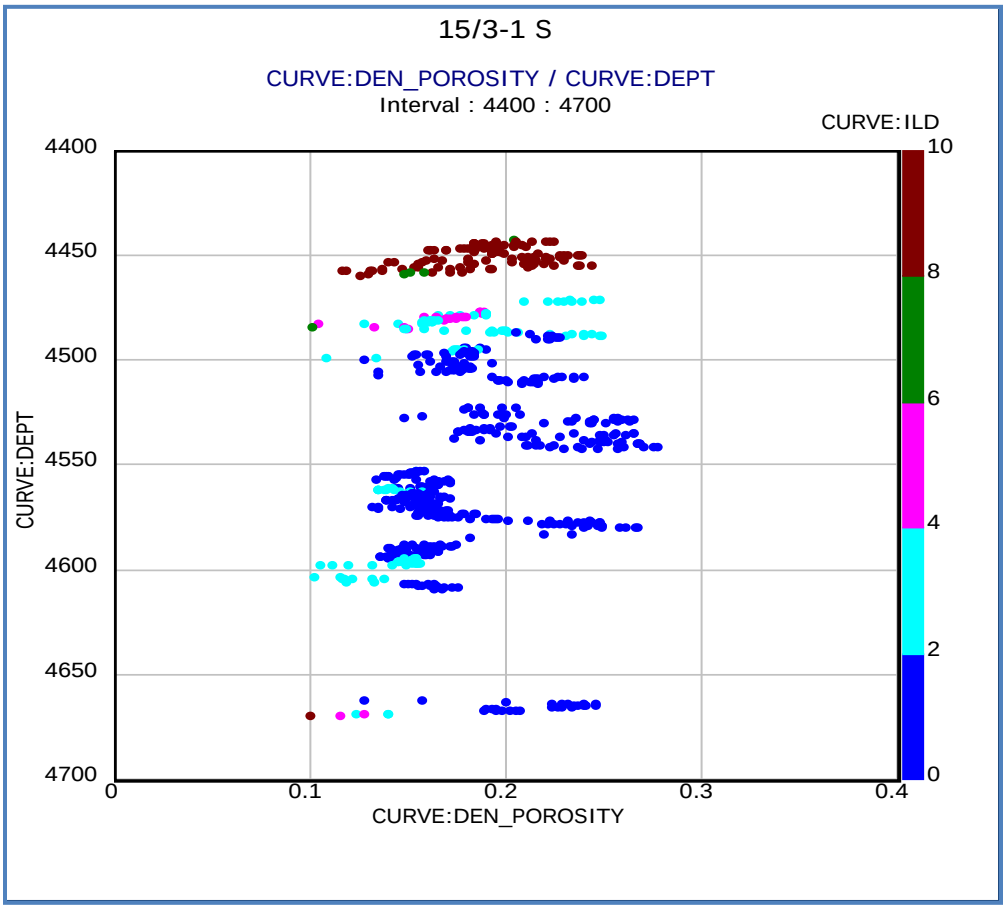

Figure 5.5: Density derived porosity (Density Porosity) plotted against depth color coded with deep induction resistivity (ILD) measurements. High ILD values in the upper part of plot can be correlated to hydrocarbon zone. While low ILD values are response of water bearing sand. This plot is made specifically to show porosity variation and ILD response in the sandstone interval of Draupne Formation.

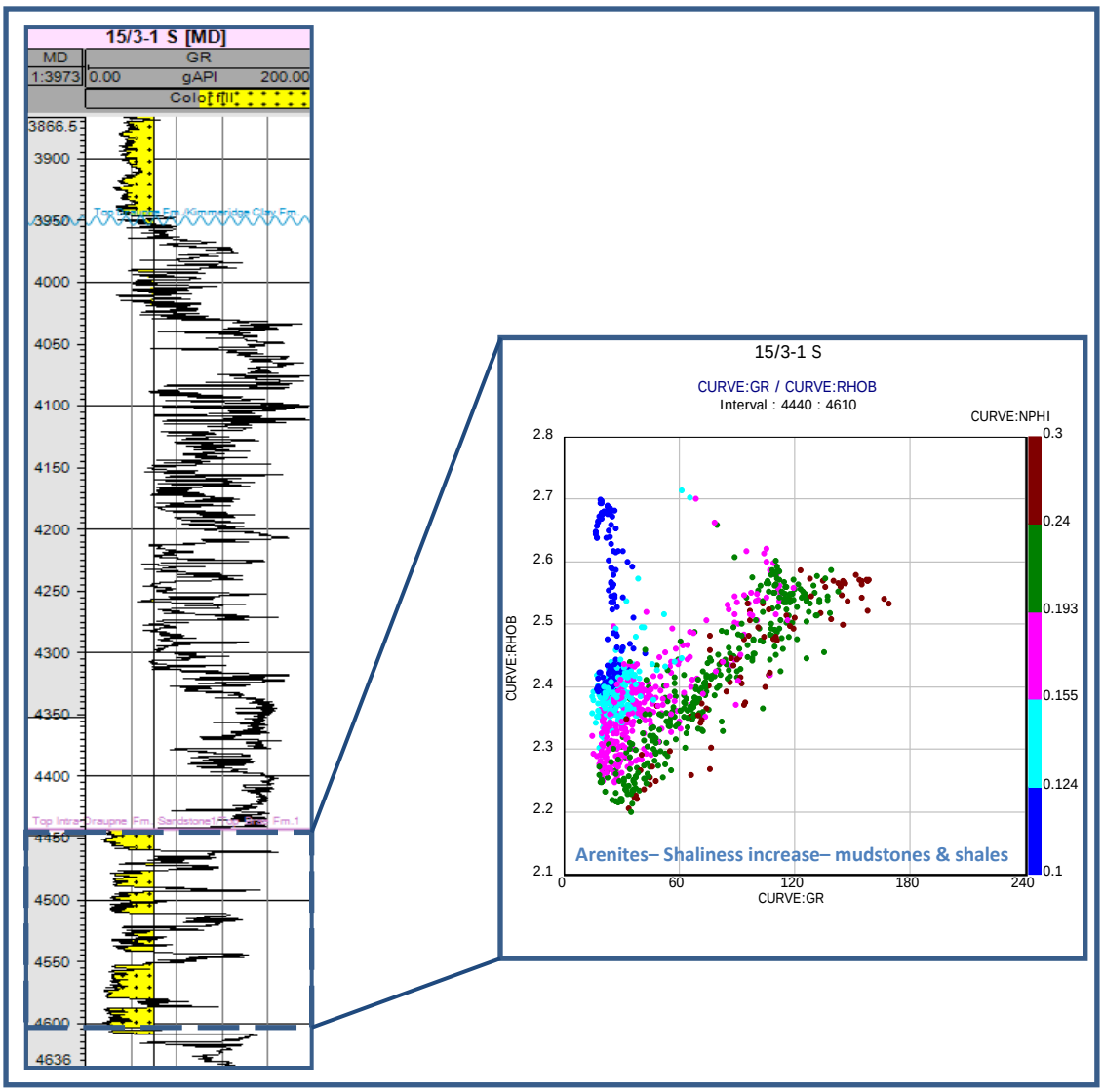

Figure 5.6: Log response of well 15/3-1S for the Upper Jurassic interval of the Draupne Formation. The gamma-ray log (GR is) in API units and measured depth (MD) in meters. On the left cross plot of gamma-ray (GR) versus bulk density (RHOB) color coded with neutron porosity (NPHI) for the Intra-Draupne sandstone interval. The interval with the bulk density values between 2.2 and 2.4 (g/cm^3) and having gamma-ray less than 60API demonstrated the high porosity sandstone interval. Also the small intervals of high gamma ray in log response are clearly discriminated on the cross plot.

Sandstone intervals of Intra-Draupne Formation have been identified on well log. A cross plot from this interval is also displayed (Figure 5.6). Anomalous high porosity values interpreted from low bulk density (RHOB) are identified.

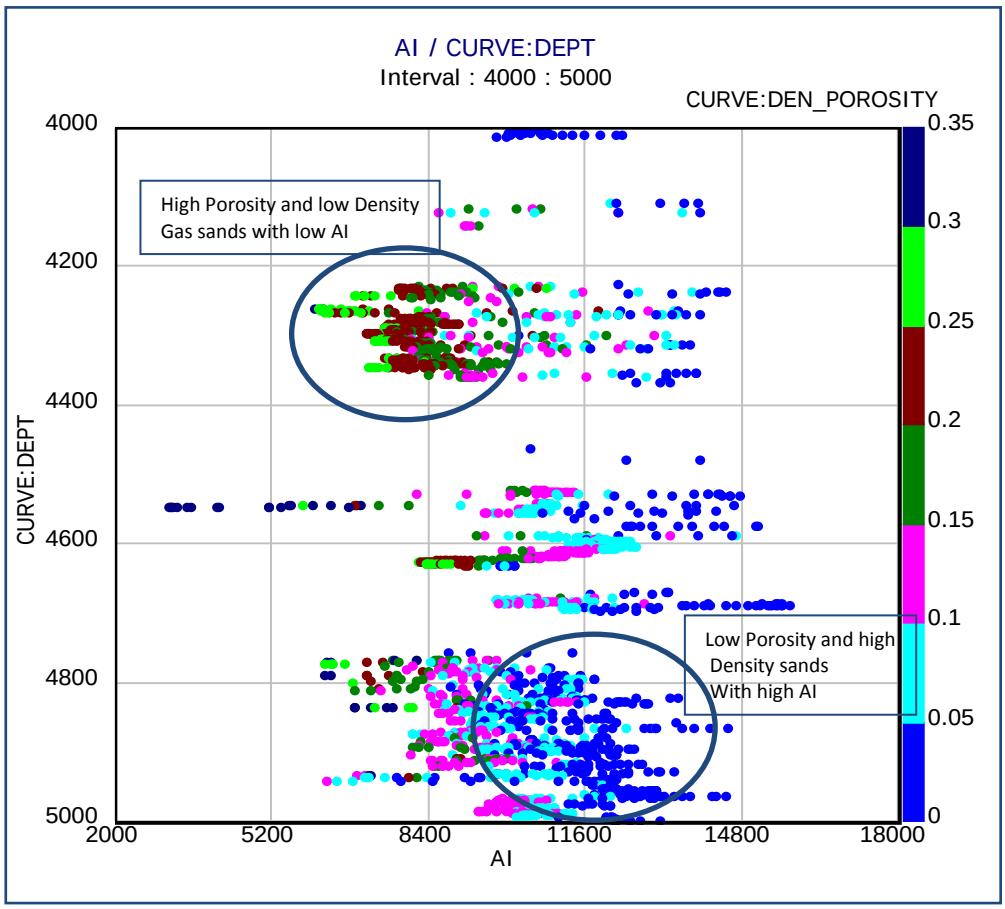

Figure 5.7: Acoustic Impedance, AI (g/cm^3 × m/s) versus depth (m) plot for the Jurassic sequence. The plot is color coded with density porosity.

5.2.3 Porosity variations Based on Petrophysical Data

During the analysis of deeply buried sandstone reservoirs, the porosity data shows large variations. To analyze this variation a plot of acoustic impedance versus depth color coded with density porosity displayed two distinct main classes of porosity (Figure 5.7).

The acoustic impedance is the product of density and seismic wave velocity (V_S). Both quantities are related to the porosity (Wyllie et al., 1956; Gardner et al., 1974; Raymer et al., 1980). The acoustic impedance is calculated from the sonic (DT) and bulk density (RHOB) logs. The range of density derived porosities is between 35% to as low as 0%. Two types of porosity anomalies have been observed in the Upper Jurassic sandstone reservoirs of the south Viking Graben. In the

upper part of the plot (Figure 5.7) between depth interval of 4200 and 4400m, low acoustic impedance values are corresponding to high porosity and low density gas sand interval indicating with porosity range between 20 and 30%. Since the value of V_P decreases in gas zone with corresponding lower acoustic impedance. In the lower part of the plot between depths interval of 4800 to 5000m high acoustic impedance (AI) values corresponds to the low porosity (less than 10%) and high density sandstones. Density derived porosity values vary between 0 to 30% according to the plot above for the deeply buried sandstones with depth greater than 4000m. Two main zones are identified based on density-porosity values. Sandstones with low porosities (up to 10%) are present in the greater depths while high porosity gas sands (up to 25%) are at shallow depth.

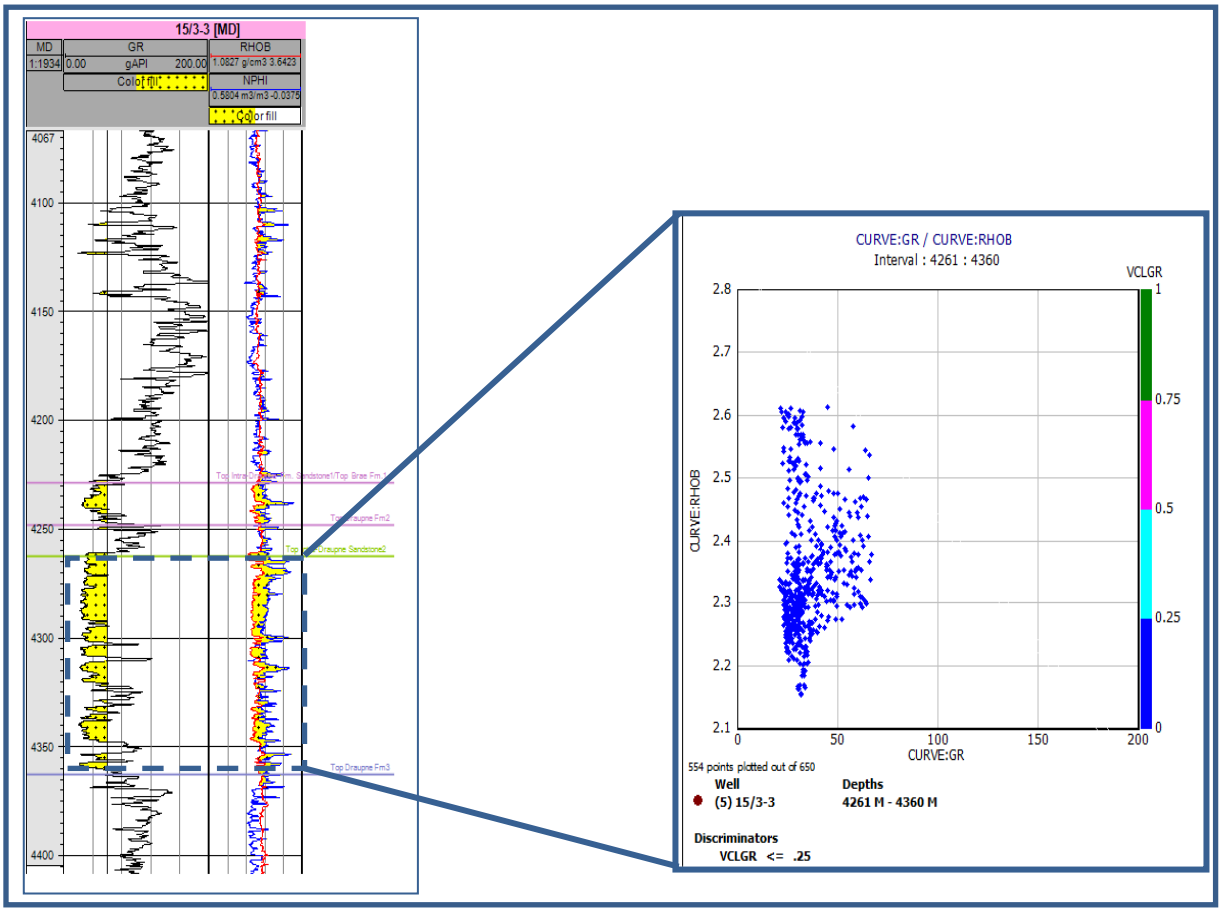

Figure 5.8: Log responses for the well 15/3-3. The Gamma Ray Log (GR) in API units, Bulk Density (RHOB) in grams per cubic centimeter, Neutron Porosity (NPHI) and measured depth (mMD). On the right, cross plot of gamma-ray versus bulk density color coded with VCLGR for the depth interval 4261 to 4360m. The bulk density (RHOB) values concentrated between 2.22 and 2.35 g/cm^3 corresponds to highly porous sandstone interval.

6. PETROGRAPHY: OPTICAL MICROSCOPY AND SCANNING ELECTRON MICROSCOPY (SEM)

6.1 Introduction: Optical Microscopy

Petrographic and mineralogical analysis the thin section samples are done from Intra-Draupne Formation Sandstone and Brae Formation to find the relationship between mineralogy and preserved porosity of the deeply buried sandstones from Gudrun and East Brae Field. A comparison of results from both formations is also done to investigate the processes which were involved in the deposition, diagenesis, compaction, cementation and the formation of authigenic minerals such clays, which has occurred during the history of the sandstones formation. Specially emphasized areas are grain coatings, quartz cementation and authigenic clays. Other processes that affect the porosity like overall grain composition are also analyzed in the thin sections. The data set consists of twenty one thin sections from two wells 15/3-8 and 16/3B-5 from Gudrun and East Brae fields respectively of the South Viking Graben, North Sea. Nine of samples are prepared from Intra-Draupne Formation Sandstone and twelve from Brae Formation. Point counting of all the samples has been done using a polarizing microscope. Data obtained from thin section analysis by point counting is further employed to calculate Inter-granular volume (IGV) and petrographic classification of sandstones by Dott, 1964.

6.2 Results

6.2.1 Point Count Analysis

Point counting is performed in a scheme with respect to detrital framework grains, matrix, cement, authigenic clays and porosity employing 300 points per sample. Results of the point count analysis are shown in the table 6.1. Samples which contain sponge spicules are also mentioned in the table. Grains consisting of microcrystalline (cryptocrystalline) quartz and cherts were put together with the quartz mineral grains using scheme from Bjørlykke and Jahren, 2010.

Graphical representation of point counting results is shown in figure 6.1. Grain category is the sum of quartz, feldspar and lithic rock fragments. Matrix contains authigenic clays (kaolinite and illite) and detrital matrix. Porosity is the sum of primary depositional porosity and secondary porosity formed by the leaching of feldspars and other grains. The largest amount of grains is

found in the sample BB5 of Intra-Draupne Formation Sandstone (73.3%). Quartz cement is present in all samples as syntaxial overgrowth with same crystallographic orientation as the detrital quartz grain. Most of the samples from the Intra-Draupne Formation Sandstone have carbonate cement with highest amount of 4.3% found in sample BB4. This is a typical sample representing early carbonate cementation hindering the compaction. Whereas samples from the Brae Formation contain carbonate cement in trace amount (0% -1%).

	Well	Sample	Depth (m)	Temp. (C°)	Grains			Matrix		Cement		Sponge Spicule	Porosity		IGV %	Grain size (mm)
					Qtz.	Felds	Lithi. Frags	Authi. Clays	Det. + Opaque	Quartz	Calcite		1.*	2.*		
Intra-Draupne Sandstone	15/3-8	BB4	4199.7	130.6	65.6	0.9	2.0	2.6	6.6	3.6	4.3	Yes	12.8	1.6	29.9	0.22
		BB18	4225.7	131.3	59.3	0.6	1.6	6.6	1.0	3.3	1.0	Yes	25.3	1.3	37.2	0.25
		BB16	4253.8	132.1	59.0	1.6	2.6	6.6	3.9	7.0	2.0	No	15.3	2.0	34.8	0.23
		BB12	4264.9	132.4	65.0	2.9	3.0	9.6	1.0	3.0	1.6	No	12.3	1.6	27.5	0.18
		BB6	4273.2	132.6	61.3	0.9	1.6	8.3	1.0	3.6	1.3	No	18.0	4.0	32.2	0.21
		BB11	4274.9	132.6	62.0	1.0	3.3	10.3	1.6	2.6	1.0	No	16.2	2.0	31.1	0.22
		BB8	4296.0	133.2	73.3	1.3	0.6	6.6	1.0	2.3	2.3	No	10.0	2.3	22.2	0.33
		BB17	4479.6	138.3	60.3	1.0	0.3	5.0	0.9	9.6	0.3	Yes	18.0	4.3	33.8	0.31
		BB13	4503.4	138.9	60.3	2.3	1.3	3.6	0.0	3.9	1.0	Yes	18.6	9.0	27.1	0.18
Brae Formation	16/3B-5	EB6	4125.2	-	72.3	0.3	0,0	1.6	0.3	7.3	0.3	No	17.0	0.6	26.5	0.27
		EB16	4128.3	-	61.3	0.3	0.0	1.3	0.3	19.0	0.0	No	11.0	6.6	31.1	0.29
		EB4	4148.3	-	71.3	0.3	0.6	1.6	0.3	12.6	0.0	No	11.6	1.3	26.1	0.20
		EB5	4150.9	-	72.6	1.0	0.6	2.0	5.6	6.0	1.0	No	11.0	0.0	25.6	0.28
		EB7	4157.2	-	70.3	1.0	0.0	5.6	0.6	7.6	0.0	No	12.2	2.3	26.0	0.27
		EB3	4162.0	-	58.3	3.0	0.6	3.0	0.9	11.0	0.3	Yes	18.0	4.6	33.2	0.20
		EB12	4166.3	-	65.3	0.6	1.0	2.0	0.0	6.3	0.3	No	22.3	2.0	30.9	0.18
		EB13	4197.6	-	67.6	1.0	0.0	5.3	0.0	2.6	0.0	No	23.0	0.0	30.9	0.15
		EB14	4199.6	-	67.3	0.6	0.0	5.6	0.0	2.3	0.0	Yes	20.6	3.3	28.5	0.22
		EB15	4202.5	-	70.6	6.0	0.6	5.3	3.0	3.3	0.3	No	8.0	2.6	19.9	0.38
		EB9	4209.4	-	72.0	1.3	0.6	3.0	4.6	11.0	0.6	Yes	6.0	1.3	25.2	0.17
		EB10	4230.8	-	72.6	0.0	0.3	1.6	1.0	3.0	0.0	No	18.6	2.3	24.2	0.28

Table 6.1: Summary of Point Count Analysis of Samples from Intra-Draupne Formation Sandstone and Brae Formation

1.* Primary Porosity, 2.* Secondary Porosity

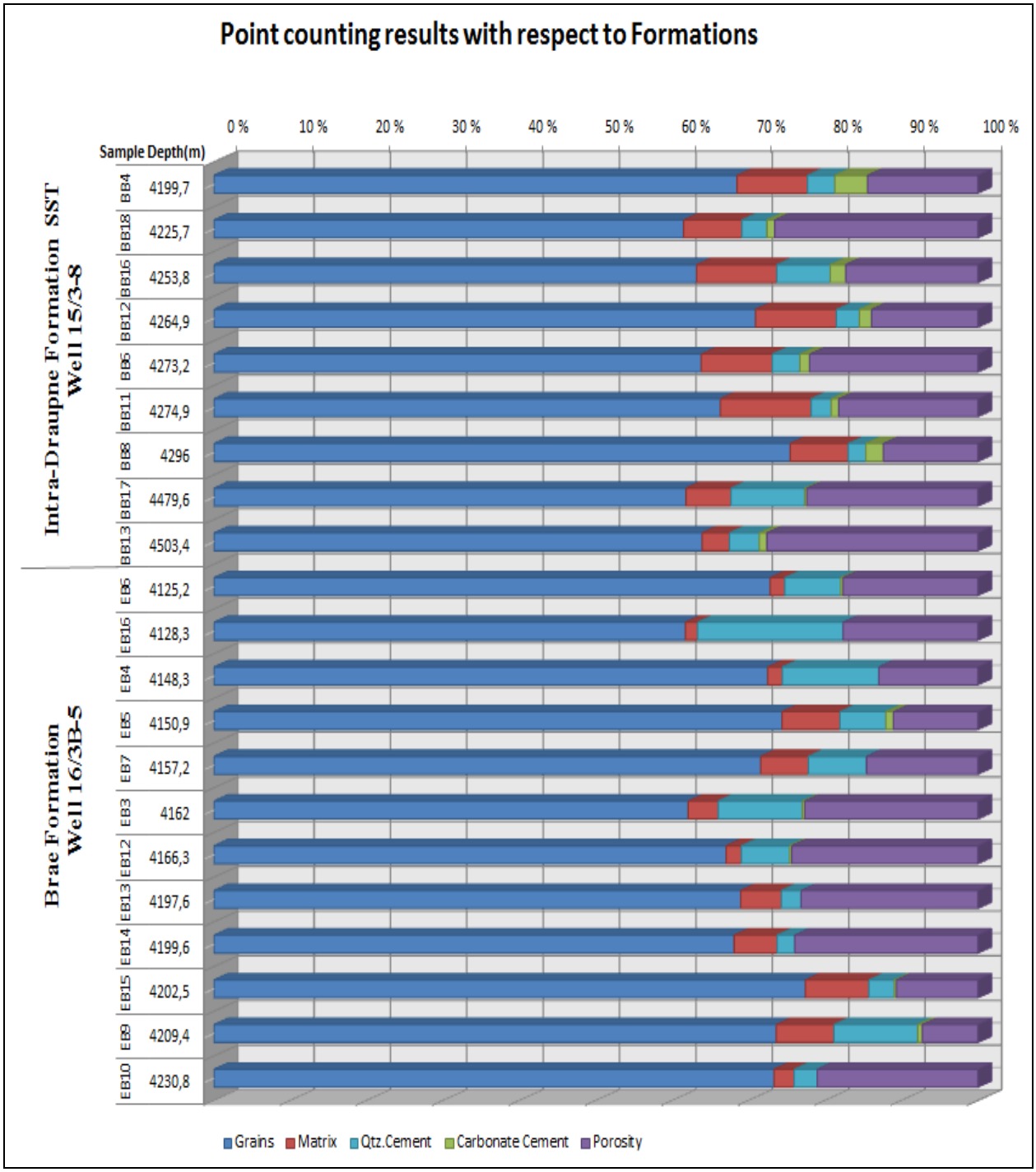

Figure 6.1: The point counting results divided into five constituents and displayed according to formation.

Petrographic Classification:

Point counted composition of the rock resolved into three components i.e. quartz, feldspar and lithic rock fragments has been plotted in the QFL diagram to classify the samples (Fig.6.2). From all the samples counted, major component is found to be quartz and also fine grained matrix is less than 15%. Therefore all the samples lie in the region of quartz arenites. The classification of Dott (1964) is used and most of the plotted samples lie within the quartz arenite area except one sample (some points overlap). According to Adams et al., 1986, the mineralogically mature sandstones contain more than 95% quartz grains. So both Intra-Draupne Formation Sandstone and Brae Formation are mineralogically mature.

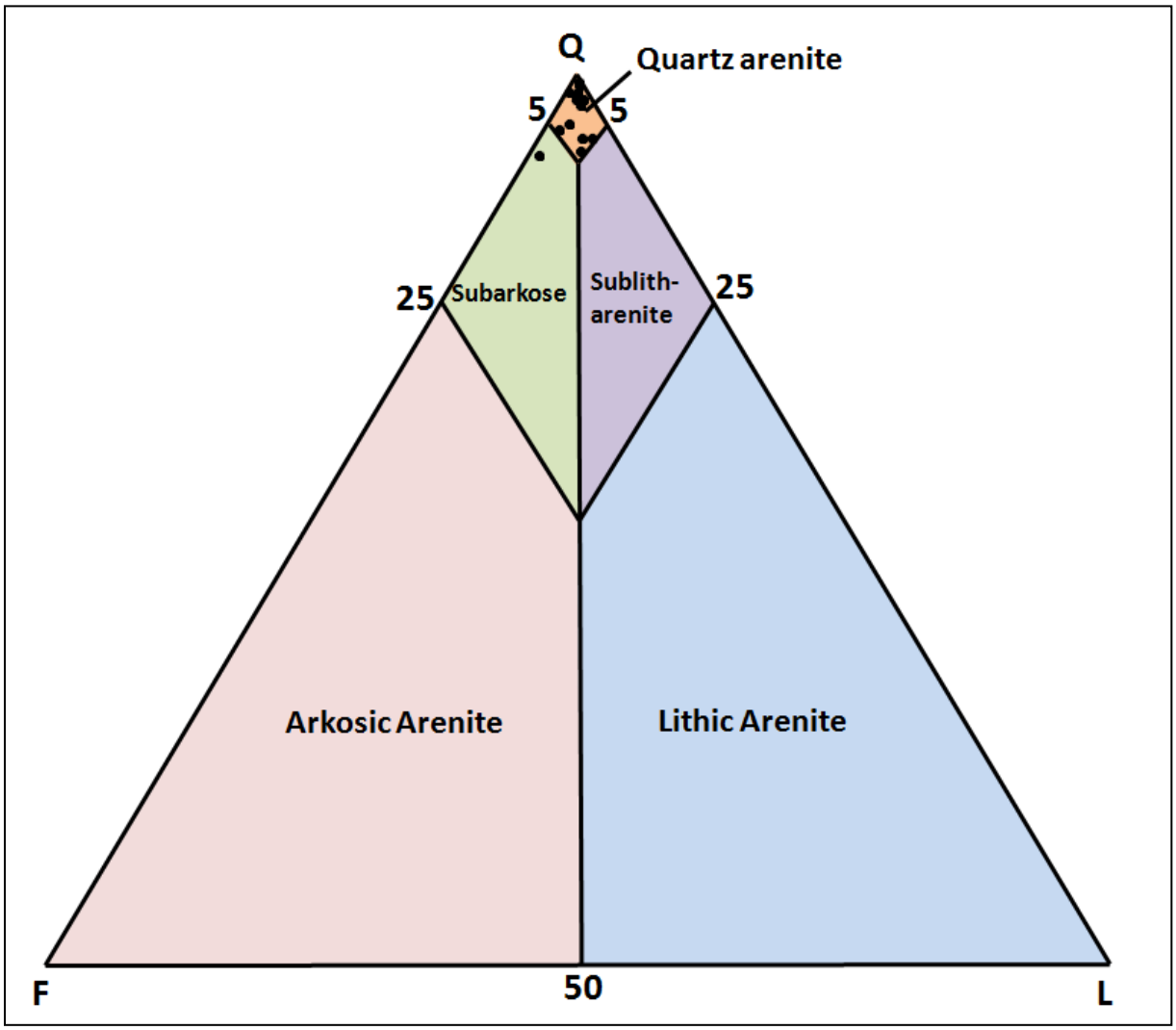

Figure 6.2 Petrographic classifications of sandstones (from Dott, 1964). Samples from Intra-Draupne Formation Sandstone and Brae Formation plotted together.

Primary Porosity and Quartz Cementation

Primary porosity is found to be the most abundant pore type during the point count analysis and ranges from 6 percent in cemented sandstones to as much as 25.3% as shown in histogram overview (Figure 6.3). The shape of the primary pores is triangular because grains are angular. The average porosity of Intra-Draupne Sandstone is 16.27% and 14.89% for Brae Formation.

Low porosity is observed in sample BB8 from Intra-Draupne Formation due to higher authigenic clay content and higher grain content. Samples from Brae Formation with low porosities are EB15 and EB9. Both samples have higher quartz grain content.

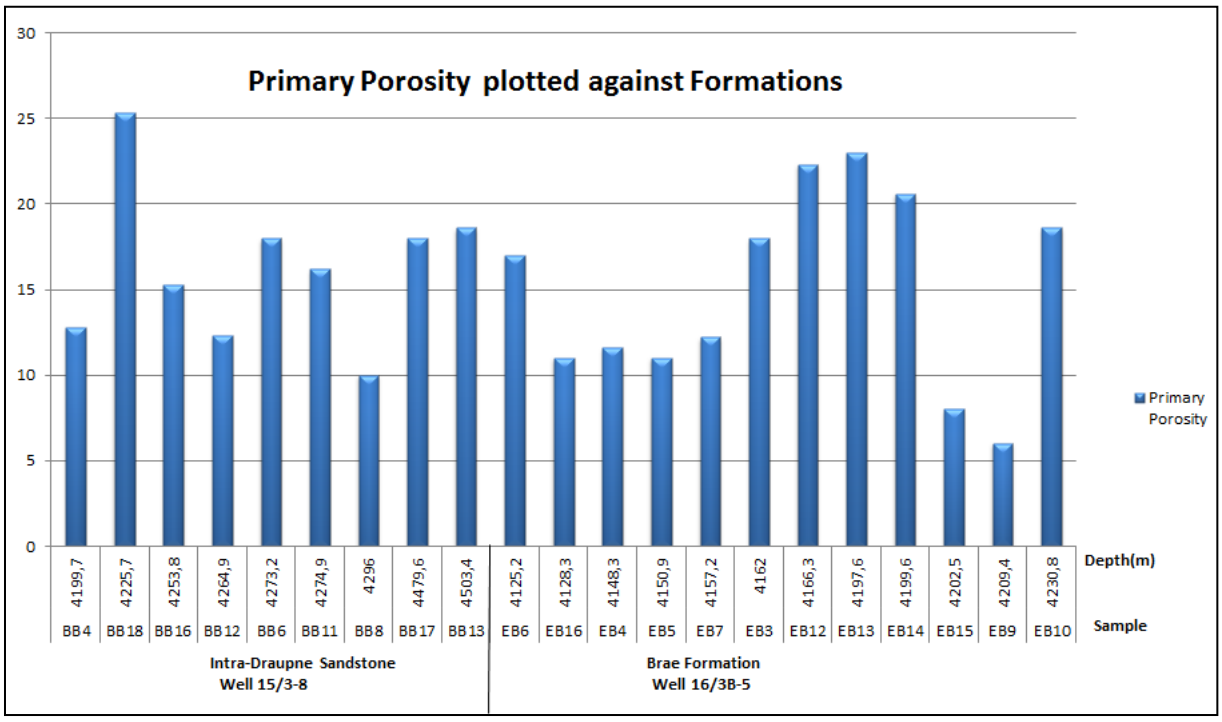

Figure 6.3: Histogram of the counted percentage of primary porosity. The values are shown according to formations with respective depths.

Variable content of quartz cement is observed from samples in both formations. Its amount varies between 2.3-12.6% of the total rock volume. The amount of Quartz cementation seems to be the reason for low primary porosity. Also, presence of low quartz cement in some samples indicates anomalously higher porosities (Figure 6.4). Samples with low quartz cement and higher porosity are BB18, BB6, BB11 and BB13 form Intra-Draupne Formation

Sandstone and EB13, EB14and EB10 from Brae Formation. This coupled relationship of quartz cementation and primary porosity can also be observed in EB4 and EB9 which are having higher quartz cement content and lower porosities.

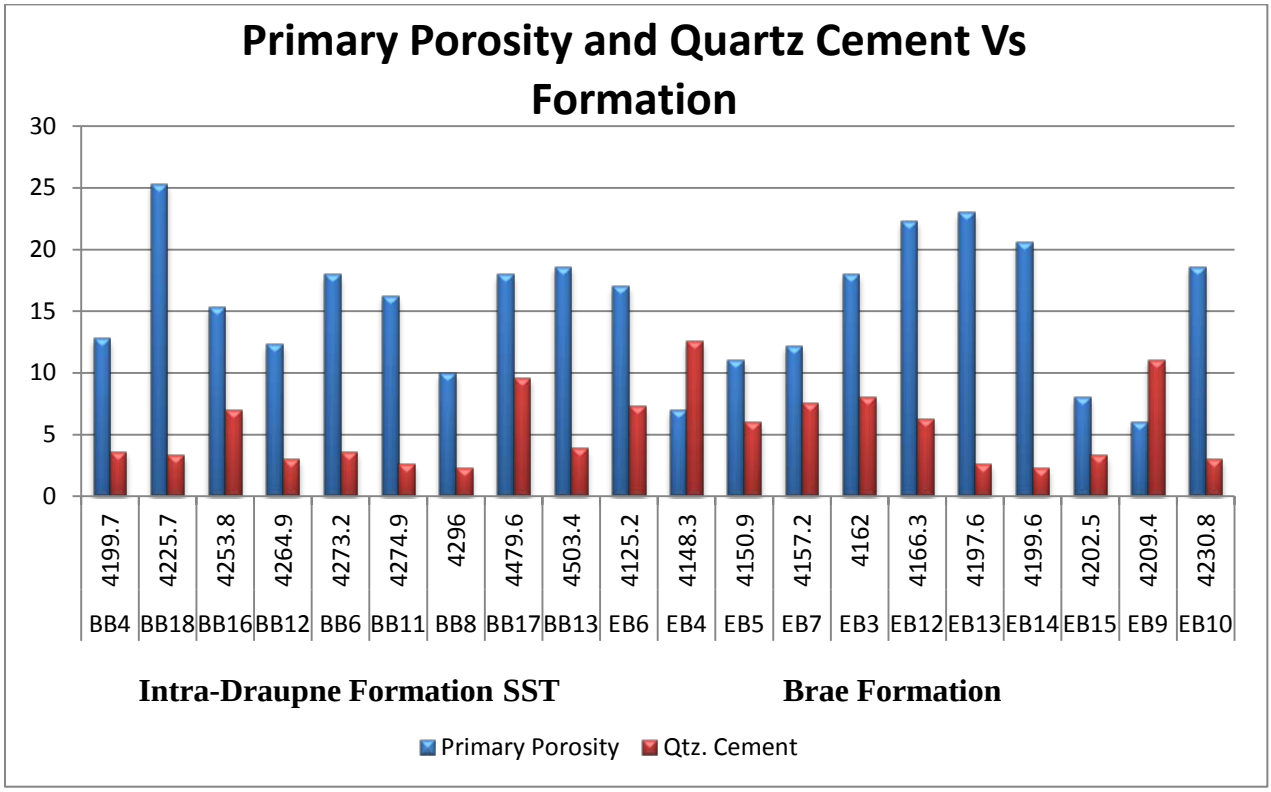

Figure 6.4: Histogram representations of primary porosity and quartz cement arranged in accordance with formation.

Most of the samples are quite porous with low quartz cementation due to the presence of extensive micro-quartz coating (to be discussed in the SEM part of the thesis) and also have higher amount of clay matrix (up to 11.9%). The samples which show least correlation between quartz cement and porosity are EB5 and EB7 within the Brae Formation. Both samples have higher quartz grain content and matrix content.

To find the relationship between quartz cement and porosity, a cross plot is drawn (Figure 6.5). The results show that high porosity sandstones exhibit quartz cement content between 2-4%, whereas the low porosity sandstones contain quartz cement up to 12.6%.

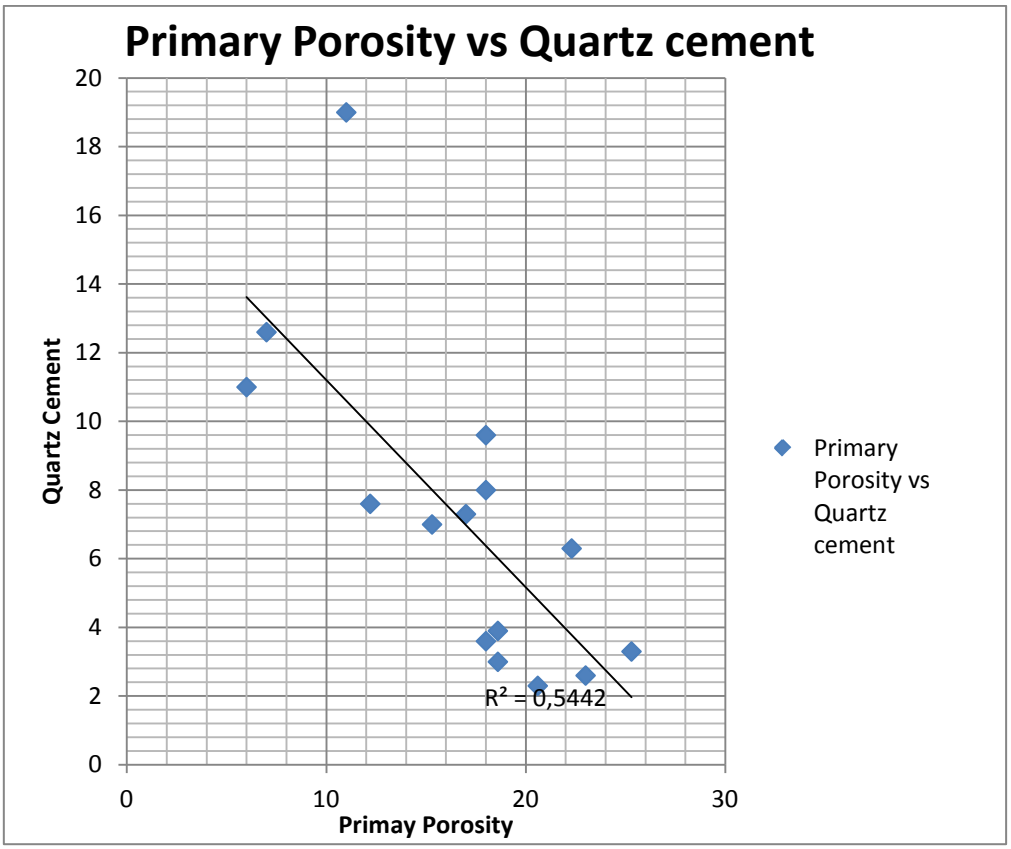

Figure 6.5: Cross plot between primary porosity and quartz cement

Feldspar Dissolution and Secondary Porosity Relationship

Secondary porosity can be generated in clastic rocks by the process of partial to complete post depositional leaching of framework grains (Heald and Larese, 1974 in Bloch, S., 1994). Results from point counting and SEM observations were integrated to look at a possible relationship between secondary porosity generated by the leaching of feldspar grains. And an attempt has been made to look at its influence on the resulting porosity and permeability of the sandstone reservoirs of the Intra-Draupne and Brae Formations.

The cross plot (Figure 6.6) made from the point count data from Intra-Draupne Formation shows a relationship between the presences of feldspars with the secondary porosity. Some of the samples show nearly equal amount of feldspars and secondary porosity but others do not

follow this pattern. There is certain increase in secondary porosity observed with low feldspar content. But most of the samples have same amount of feldspar and secondary porosity.

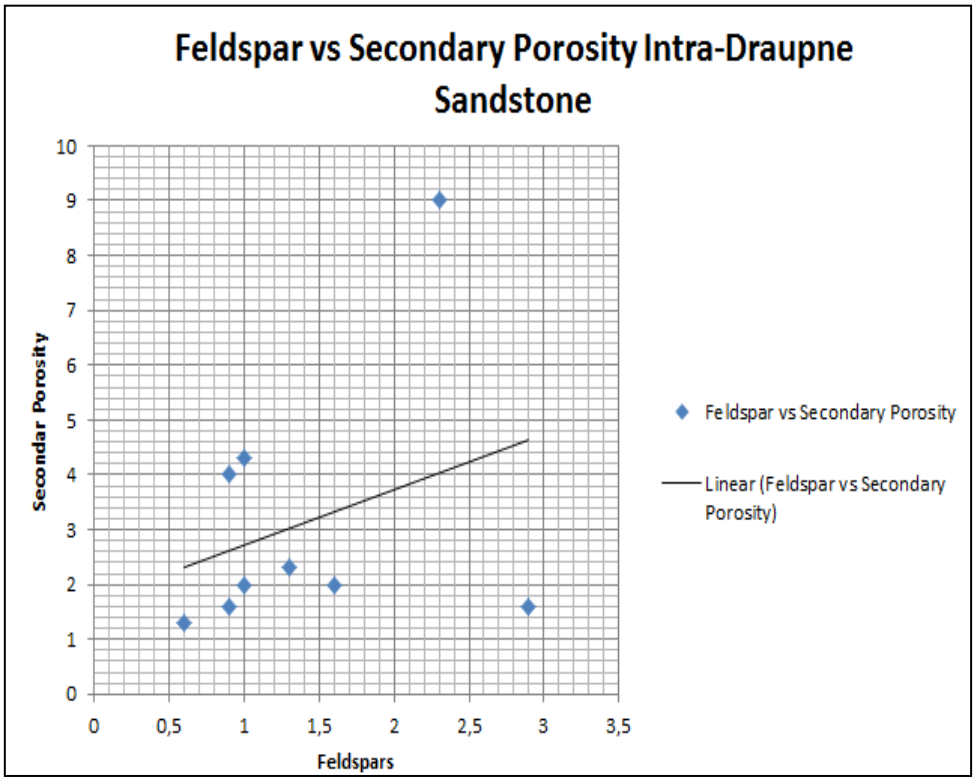

Figure 6.6: Cross plot between feldspars and secondary porosity Intra-Draupne Formation

The same attempt has been made with the data from Brae Formation (Figure 6.7). Most of the samples have feldspar content of about 1% but secondary porosity ranges between 0-3.3% and other samples with different behavior. If we plot data from both formations together, we will have the same result (Figure 6.8). Mostly, samples have feldspar content between 0-.6%, with secondary porosity ranging between 0-4.3%. Results from SEM also exhibit some partially leached feldspar grains generating secondary porosity.

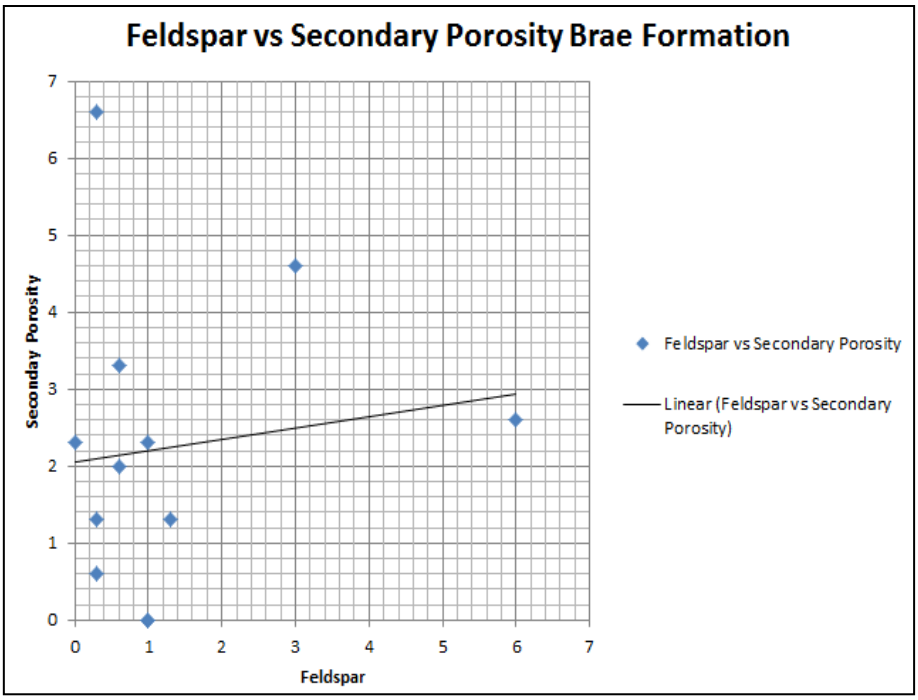

Figure 6.7: Cross plot feldspars and secondary porosity Brae Formation

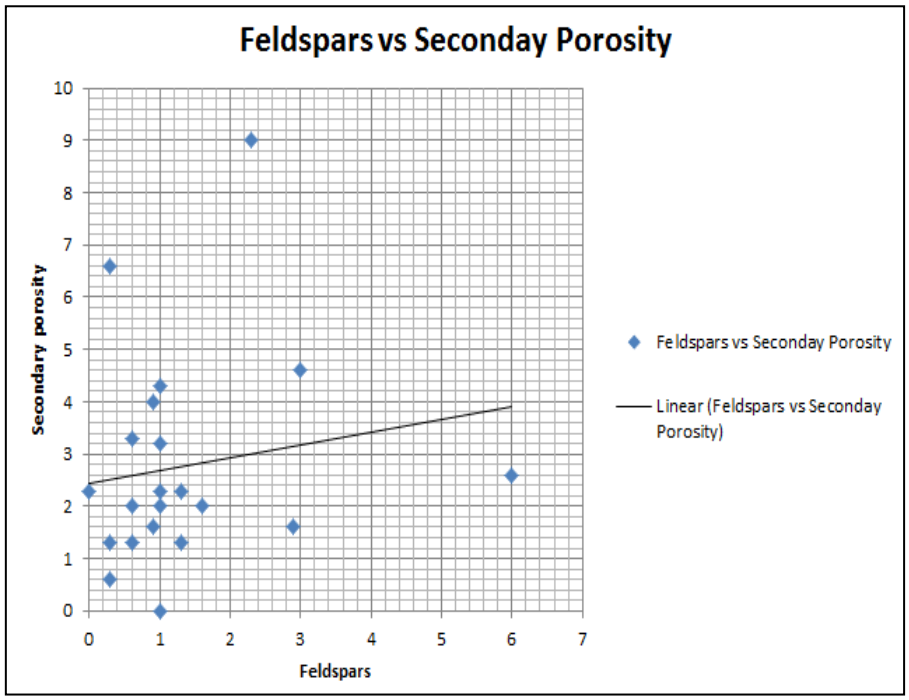

Figure 6.8: Cross plot between feldspars and secondary porosity for both Intra-Draupne and Brae Formations

Leaching of feldspar is always associated with the precipitation of authigenic clays like Kaolinite and Illite. The observations from Bjørlykke, K. O., 1984 explained that the generation of secondary porosity does not enhance the total porosity. Because the increased

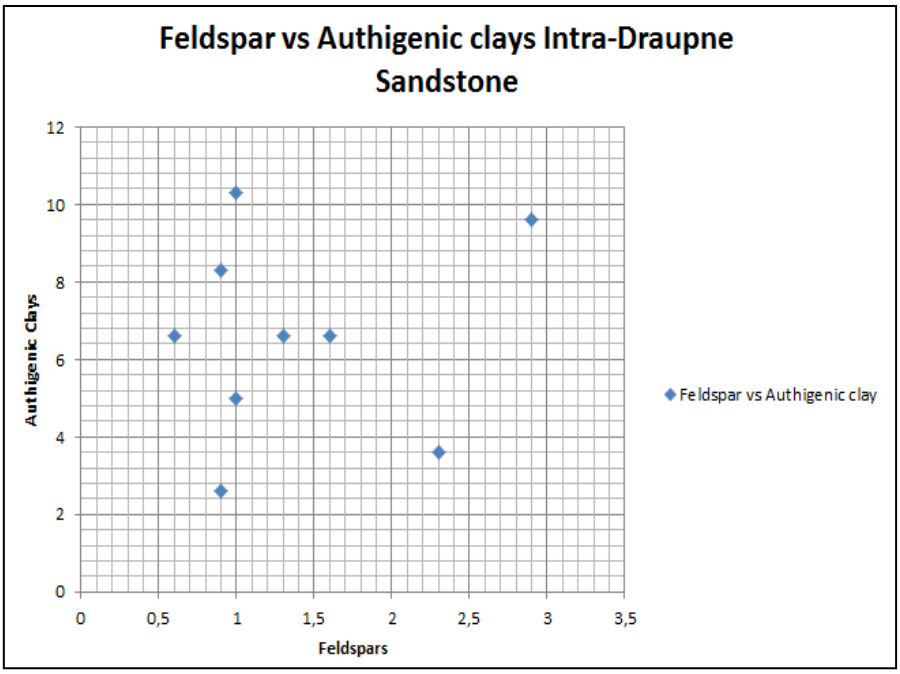

Figure 6.8: Cross plot between feldspars and authigenic clays Intra-Draupne sandstone

volume generated by the dissolution of mineral grains is balanced by the precipitation of authigenic clays in the pore space. The cross plots between feldspar and authigenic clays for both formations are shown in figure 6.8 and 6.9 respectively. Intra-Draupne sandstone has higher clay content up to 10.3% as compared to Brae Formation with corresponding feldspar range is the same. This can be correlated to leaching of feldspar grains and associated precipitation of greater amount of authigenic clays.

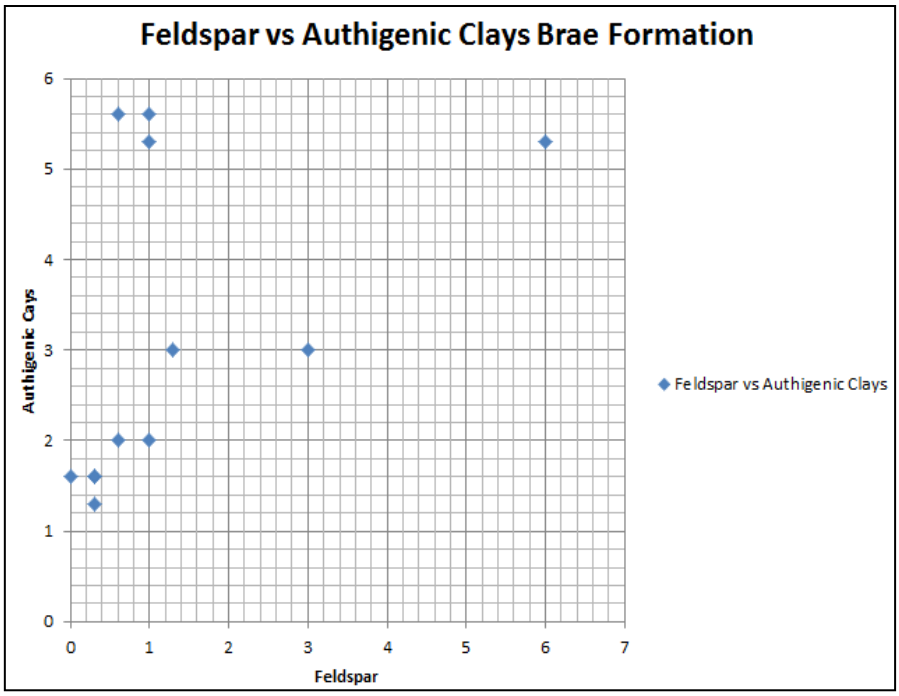

Figure 6.9: Cross plot between feldspar and authigenic clays Brae Formation

6.2.2 Intergranular Volume (IGV)

According to Bjørlykke and Jahren (2010), the IGV can be defined as "The degree of porosity loss by mechanical compaction determines the Intergranular volume at the onset of chemical compaction (quartz cementation)". To measure Intergranular volume point counting of petrographic thin sections is done. It is defined as the sum of intergranular porosity, cement and matrix (Maast et al., 2011). Secondary intergranular porosity is not the part of IGV.

Calculated IGV results are presented as the bar chart in figure 6.10 and arranged according to formations. The value of IGV varies between 22.2-37.2% for Intra-Draupne Formation Sandstone and is between 19.9-33.2% for Brae Formation. Average value of IGV is higher for Intra-Draupne Formation Sandstone than the Brae Formation and values are 30.71% and 27.35% respectively. Intra-Draupne Formation Sandstone has relatively higher authigenic clays (kaolin+illite) and carbonate cement but lower quartz cement. While Brae Formation has higher quartz cement and lower content of both authigenic clays and carbonate cement. So presence of higher carbonate cement and authigenic clays could be the reason of higher

average of IGV in Intra-Draupne Sandstone. Early carbonate cementation jam the frame work grains apart and helps in less compaction and greater IGV value.

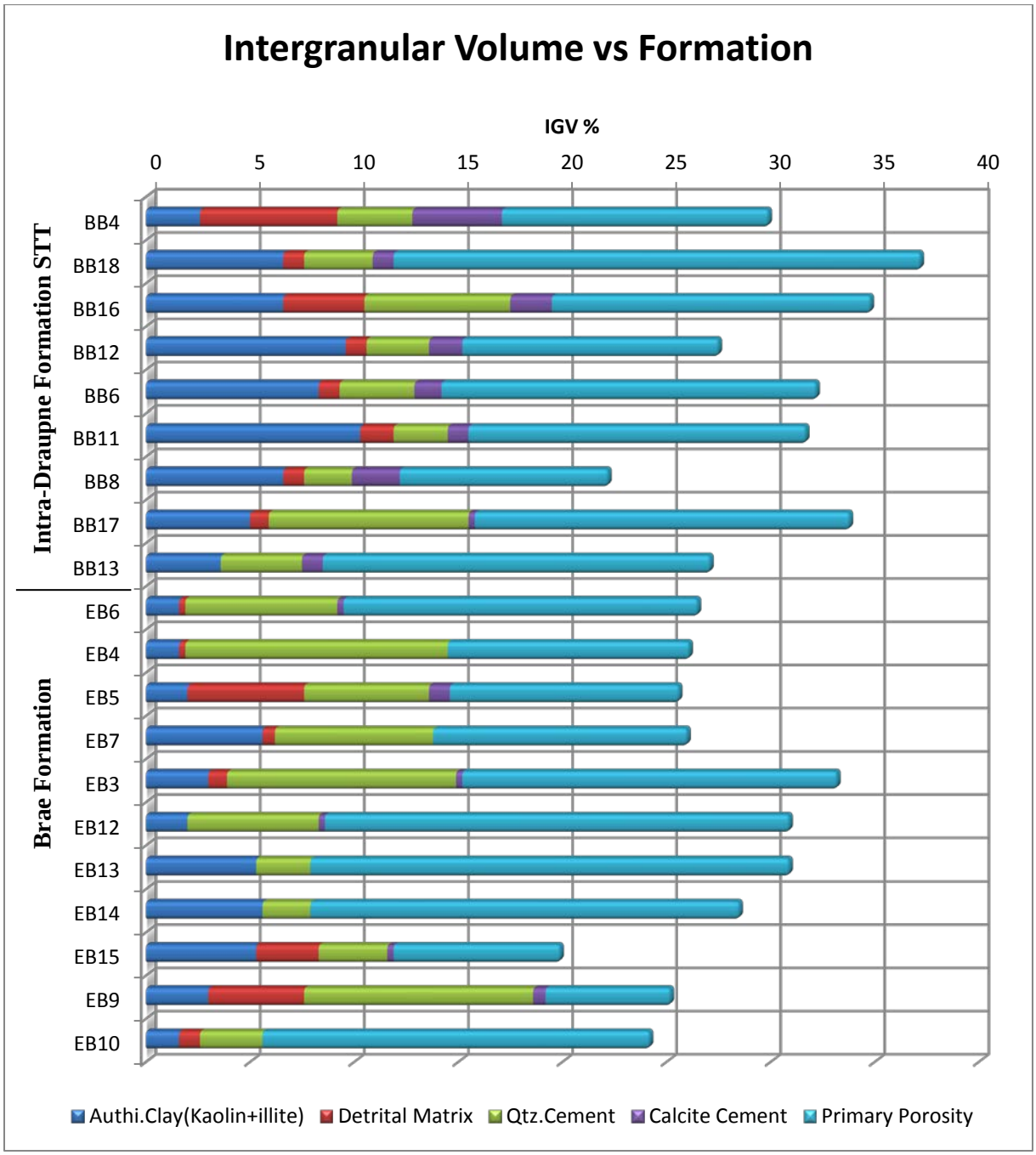

Figure 6.10: Bar chart overview of different components contributing to IGV in Intra-Draupne Formation Sandstone and Brae Formation.

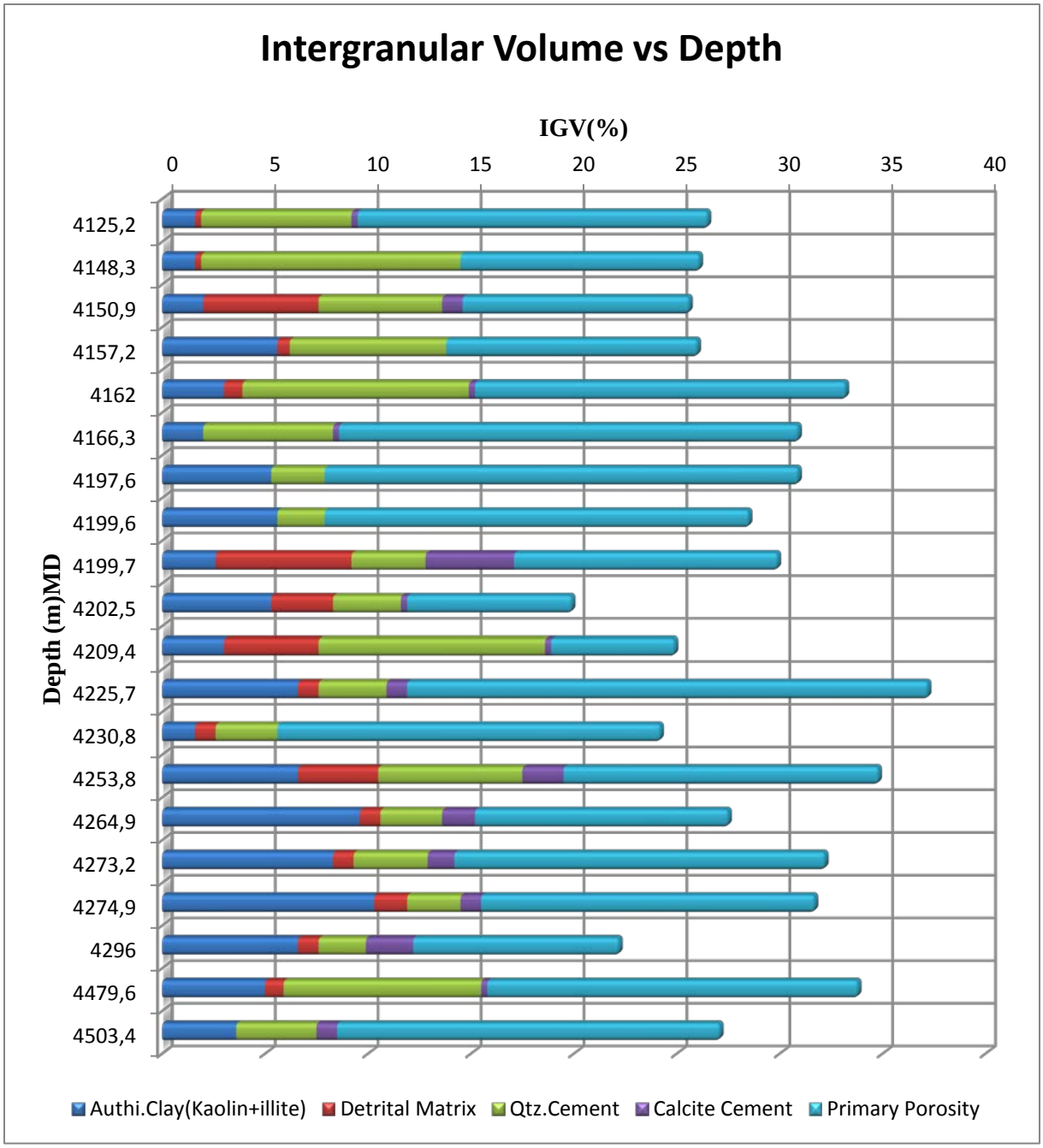

Figure 6.11: Bar chart overview of IGV percentage presented according to depth.

The calculated values of intergranular volume from point count data arranged according to the depth (Figure 6.11). The IGV values vary between 19.9-37.2%. Deeper samples are expected to have lower IGV but some samples have higher IGV values. The reason is higher authigenic clays content and primary porosity count as compared to shallower ones. Grain plucking during the preparation of thin section samples could generate the pseudo porosity so higher porosity count results in the higher IGV values.

IGV and Secondary Porosity

According to Bjørlykke and Jahren, 2010, at shallow depths meteoric water infiltrates and causes leaching of minerals like feldspar and mica and precipitate kaolinite. This leaching process can cause secondary porosity to develop and extra-large size pores can be generated. At greater burial depths, with temperature about 130^{o}C, the remaining K-feldspar and kaolinite react with each other and precipitate illite. So this transformation may enhance the secondary porosity so much that it may affect the IGV by generating larger pores. Figure 6.12 shows the linear relationship between IGV and secondary porosity.

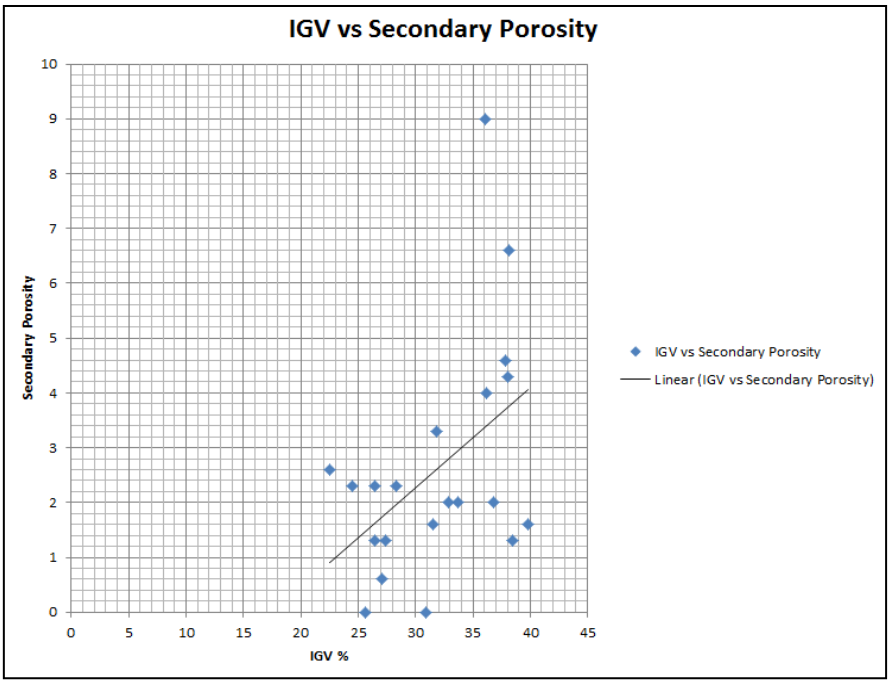

Figure 6.12: The correlation between IGV and secondary porosity

This relationship shows that generation of secondary porosity can cause increase in IGV, if this secondary porosity is well developed and get connected with the primary porosity it can enhance the total porosity.

IGV and Depth Relationship

During this analysis samples from Intra-Draupne Sandstone and Brae Formation are observed with depths ranging between 4125.2 to 4503.4 m. Most of the samples have IGV value between 25-39%. Marcussen et al., (2010), calculated IGV values for Etive Formation and found that it does not decrease as depth greater than 2260m and IGV ranges between 27.2-40.2% in Etive Formation. The similar observation is made here for samples from Intra-Draupne Formation Sandstone and Brae Formation. It is observed that for same burial depth IGV can vary, for example at around 4200m IGV values are between 22.5-31.8%.

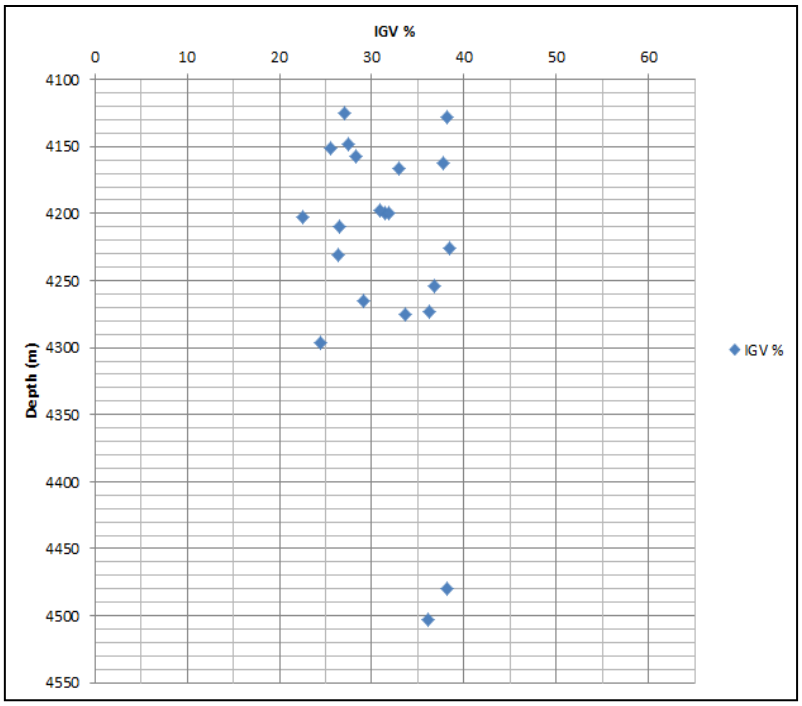

Figure 6.13: Intergranular Volume and depth relationship

The relationship between quartz cementation and intergranular volume has been drawn (Figure 6.14). It seems that there is no apparent trend present between the two quantities. Quartz cementation is the major factor in decreasing the porosity at greater depths but it does not decrease the IGV.

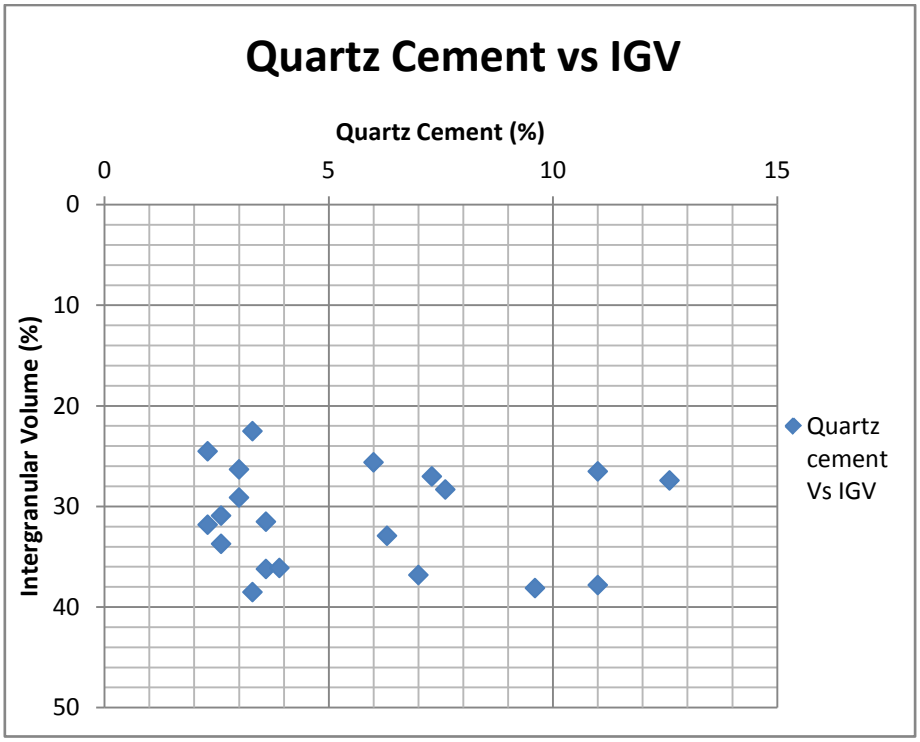

Figure 6.14: Relation between quartz cement and intergranular volume

6.2.3 Textural Maturity of Sandstone

To estimate the textural maturity of Intra-Draupne Sandstone and Brae Formation, the results from sorting and roundness of the samples were observed under the microscope. According to Folk, 1951, there are four stages of textural maturity described by the three sequential events (1) Clays removal (2) sorting of the sand grains (3) high roundness achievement. The four stages of textural maturity are:

6.2.3.1 Immature Stage

Large amount of clays are present and fine mica, poor sorting and grains are angular.

6.2.3.2 Submature Stage

Very little or no clay present, poor sorting and grains are angular

6.2.3.3 Mature Stage

No clay present, well sorting and grains are subangular

6.2.3.4 Super Mature stage

No clay present, well sorted and grains are rounded

According to Folk's (1951) criteria, the sorting and angularity of samples were observed. And results are presented in the table in Appendix A. Most of the samples from Intra-Draupne Formation Sandstone are angular to subangular and poor to moderately sorted, so it's texturally submature sandstone. During point count analysis less detrital quartz and more feldspar observed as compared to Brae Formation, which confirms its submaturity. While majority of samples from Brae Formation are surrounded with moderate sorting, this made it strong candidate for texturally mature sandstone.

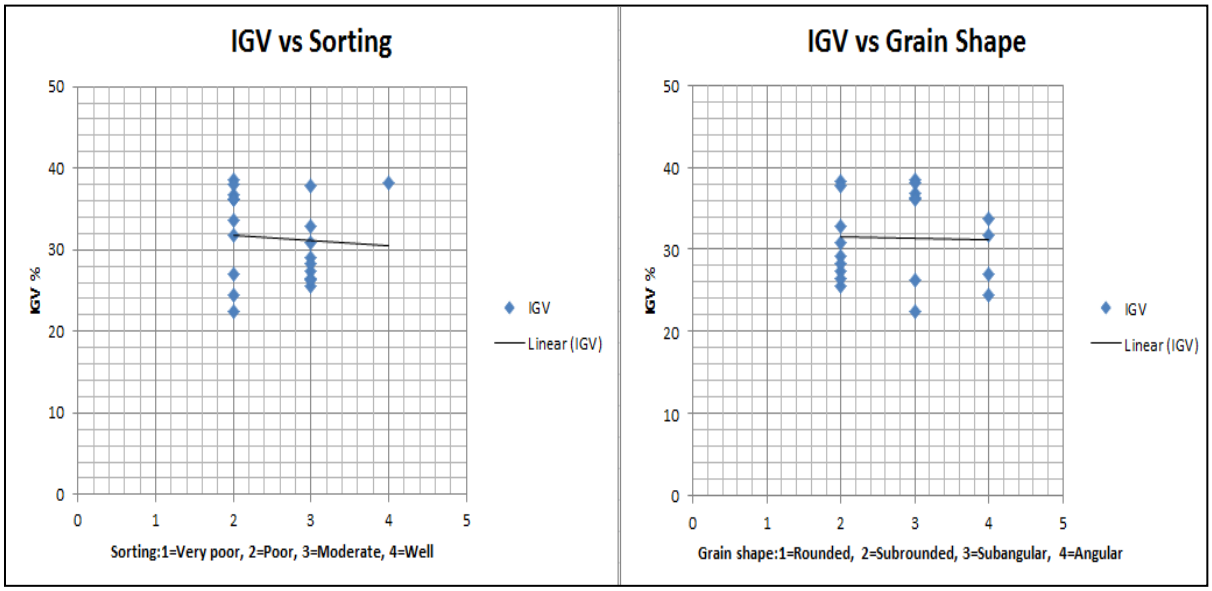

Figure 6.15: a) Calculated IGV versus degree of sorting b) IGV versus grain shape.

The visual estimate of grain sorting and grain shape performed of all the thin sections samples under the microscope. Calculated IGV values were plotted against the sorting and grain shape (Figure 6.15).

6.2.4 Thin Section observations under microscope

The thin sections from Intra-Draupne Formation Sandstone and Brae Formation are photographed in an optical microscope with attached camera. The images taken are used to support the observations made during the point count and textural analysis.

The Intra-Draupne Formation Sandstone has mostly quartz as basic grain frame work with lesser amount of feldspars and clays. The sandstone has both primary and secondary porosity. Secondary porosity developed mainly due to feldspar dissolution. Some samples have extensive quartz over growth developed with clear dust lines (Figure 6.16a). Mainly illite is observed as pore filling clay mineral (Figure 6.16b&d). Polycrystalline quartz grain is also present with sutured boundaries between small crystals. Quartz grains are sub-angular to sub-rounded (Figure 6.16a&c).

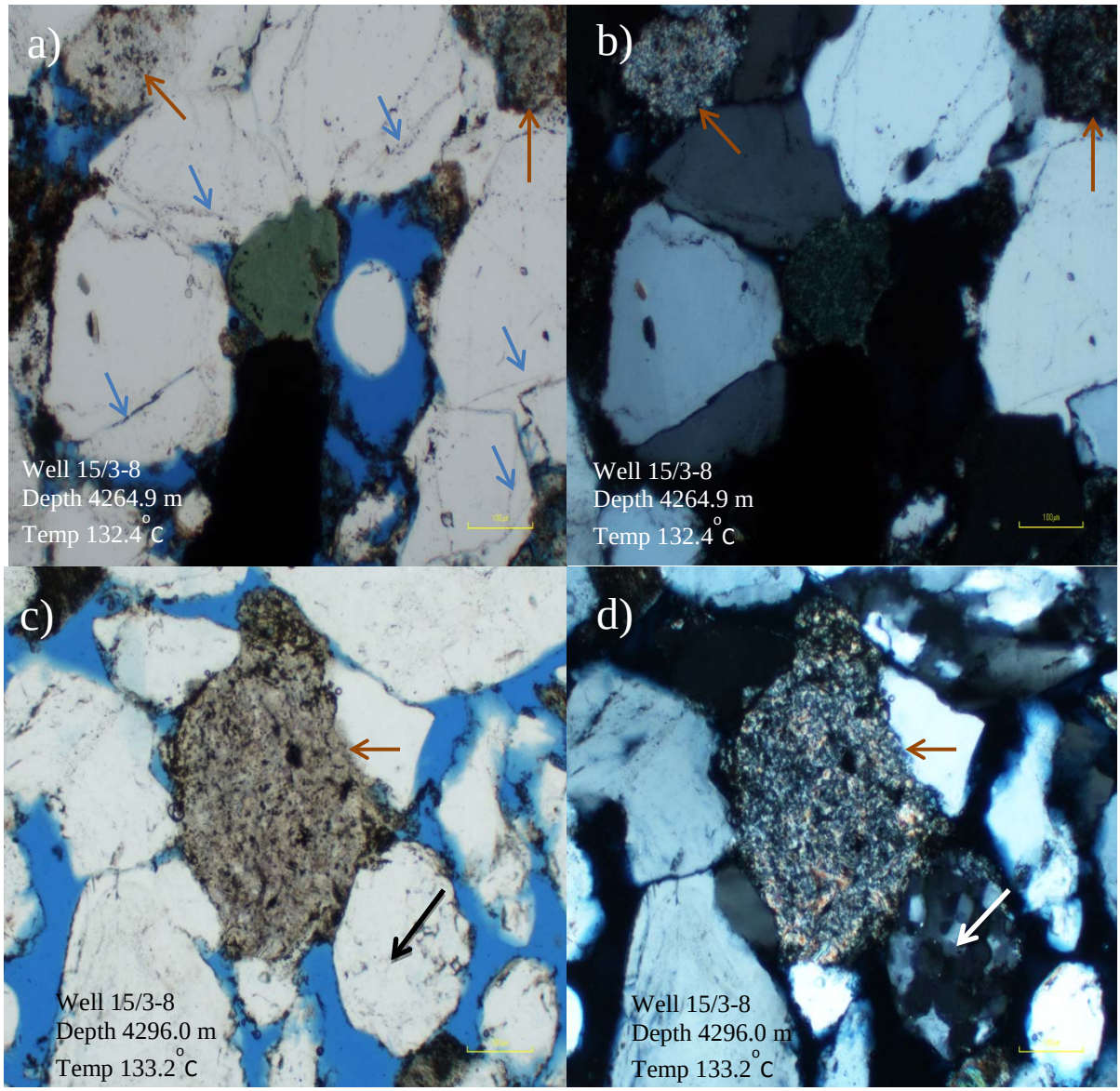

Figure 6.16: Thin section photomicrographs from Intra-Draupne Formation Sandstone, Well 15/3-8, Gudrun Field, South Viking Graben. The yellow scale bar in the lower right corner equals to 100µm. Blue epoxy between the grains showing porosity (a) Quartz grains with extensive quartz overgrowth seen in plane polarized light (PPL), Well-developed dust lines (blue arrows) shows quartz overgrowth. Pore filling illite (brown arrows) (b) Same image as a) with crossed polars, the light yellowish illite in the upper part is more visible (c) Quartz grains with pore filling illite (brown arrow) in PPL view. (d) Same image as c) shown crossed polars, polycrystalline quartz grain (white arrow) also observed.

The Brae Formation also characterized as quartz arenite in classification with grain frame work dominated by quartz. Have extensive porosity mostly primary depositional porosity. Both illite

and kaolinite are observed as pore filling clay minerals (Figure 6.17b&d). Quartz grains are sub-rounded to sub-angular (Figure 6.17b&c).

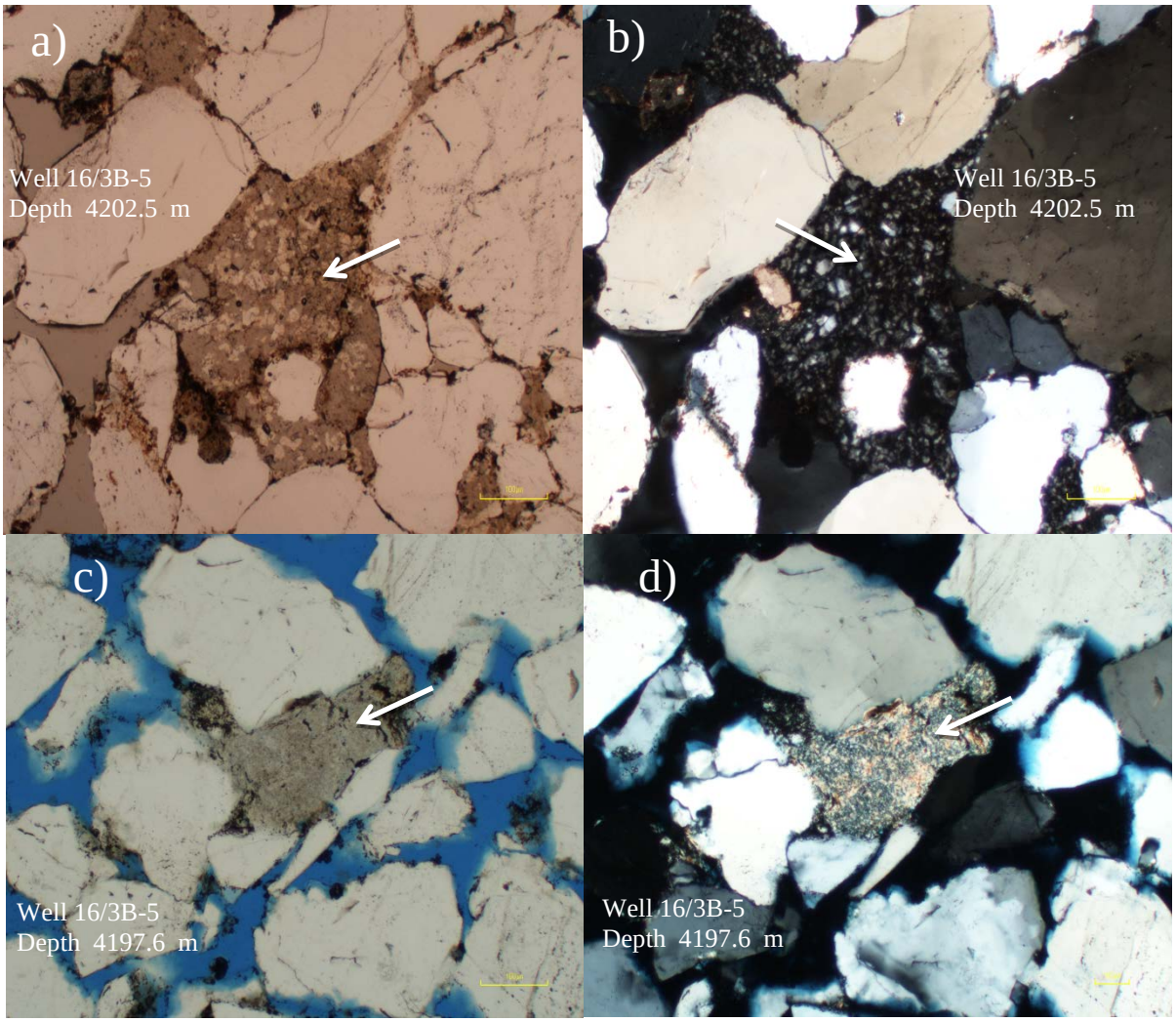

Figure 6.17: Photomicrographs of thin sections taken from optical microscope Brae Formation, Well 16/3B-5, East Brae Field, South Viking Graben. The yellow scale bar in the lower right corner equals to 100 µm. (a) Pore filling kaolinite (white arrow) in between quartz grains with plain polarized light. (b) Same image as a) with crossed polars, grey color pore filling kaolinite (white arrow). (c) Extensive porosity between quartz grains with pore filling illite (white arrow) in PPL view (d) Same image as c) with crossed polars, yellowish to grayish color illite.

The remnant rhaxellid sponge spicules (Maast et al., 2011) have been identified (Figure 6.18) during the point count analysis and which considered to be responsible in generating the micro quartz coatings on detrital quartz grains. These micro quartz coatings hinder the quartz cementation and preserve the porosity (Aase et al., 1996).

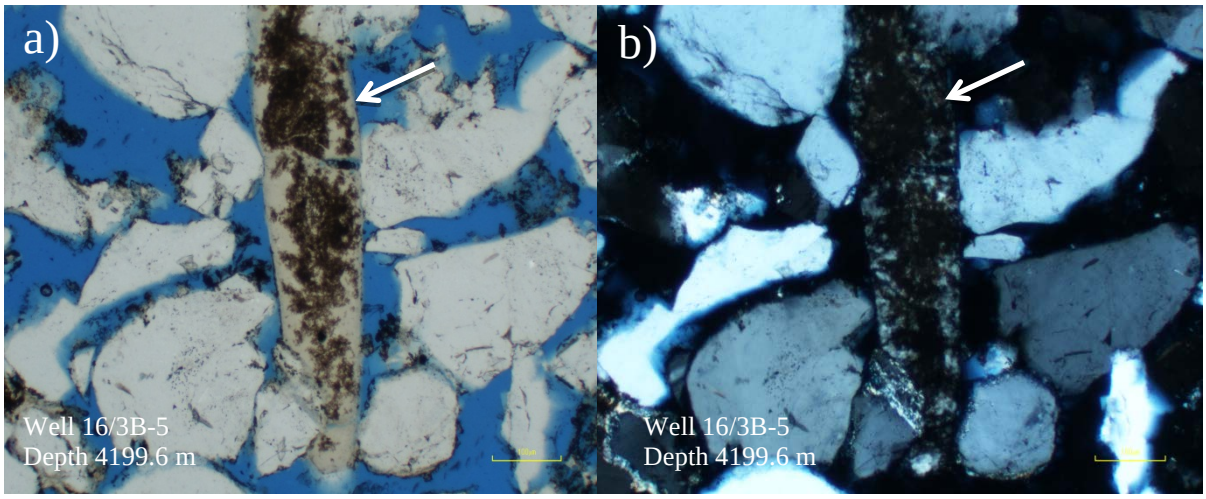

Figure 6.18: Thin section images from Brae Formation, Well 16/3B-5, East Brae Field, South Viking Graben. The yellow color scale bar equals to 100 µm. Sponge spicule marked by white arrow, made up of quartz and show lower birefringence color with surrounding quartz grains.

6.3 Introduction: Scanning Electron Microscopy (SEM)

Scanning electron microscopy technique is employed to investigate the mineralogy of the samples into more detail with emphasis on mineral content, porosity, cementation, mineral coatings and authigenic clays. This investigation is performed to cross check the results, which are being obtained in the optical microscopy. Following observations are made on the basis of this investigation

6.3.1 Quartz overgrowth and porosity

Both stub mounted samples and thin section slides are analyzed to look for quartz over growth and porosity present in the samples from Intra Draupne sandstone and Brae Formation. This is also a quality check for optical microscopy analysis.

Intra-Draupne Formation Sandstone

Intra-Draupne Formation Sandstone contains sandstone beds with less quartz overgrowth and good porosities as compared to Brae Formation. Stub mounted samples are observed (Figure 6.19). Point count results from optical microscopy showed the same behavior.

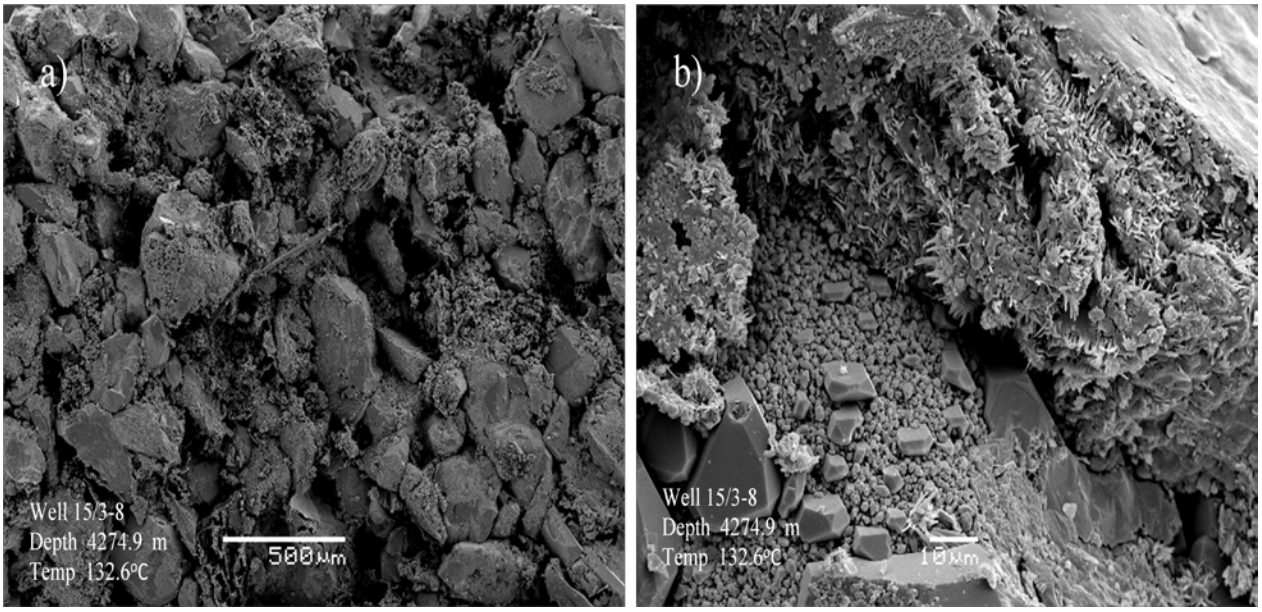

Figure 6.19: (a) Overview of sample from Intra-Draupne sandstone Formation, showing extensive porosity and low quartz cementation. (b) Close-up of quartz overgrowth and coatings present. Where micro quartz coating present, it hinders the overgrowth.

Thin sections from Intra-Draupne sandstone formation have also been examined using the cathode luminescence (Figure 6.20). Exposing thin section to CLI, the quartz overgrowth clearly distinguished from detrital quartz grain. Since detrital quartz grain luminate strongly than cement.

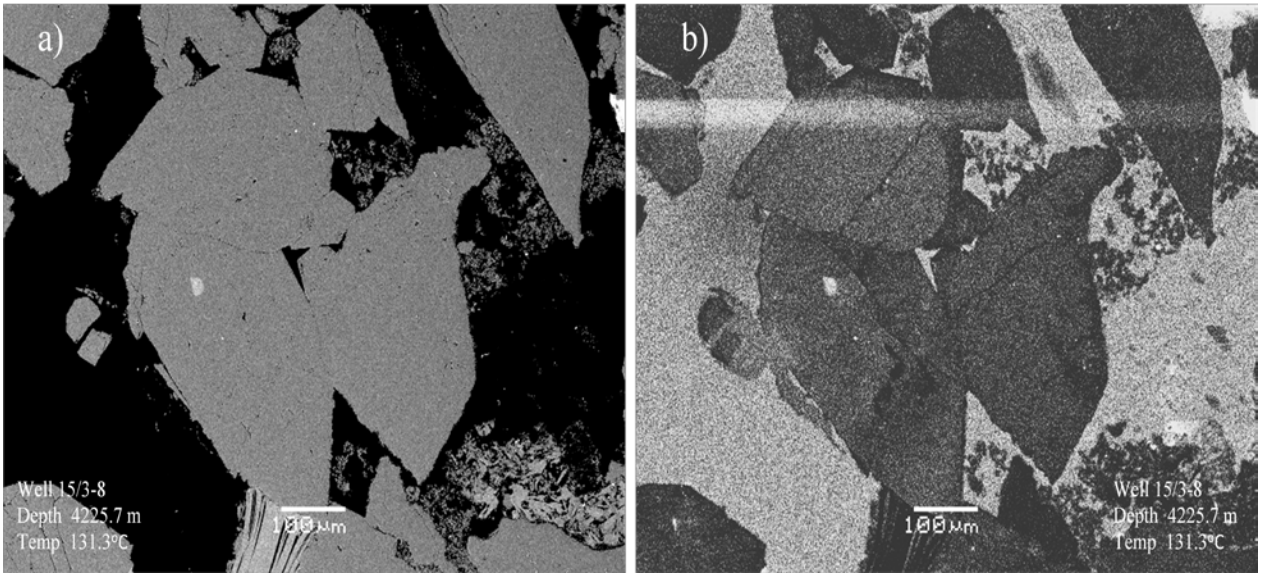

Figure 6.20: Example of quartz overgrowth in Intra-Draupne sandstone from thin section slide (a) Backscattered electron image of quartz cemented grains, depth 4225.7m well 15/3-8 Gudrun Field (b) The same picture is shown with cathode luminescence(CLI) , clearly showing the detrital grains without overgrowth.

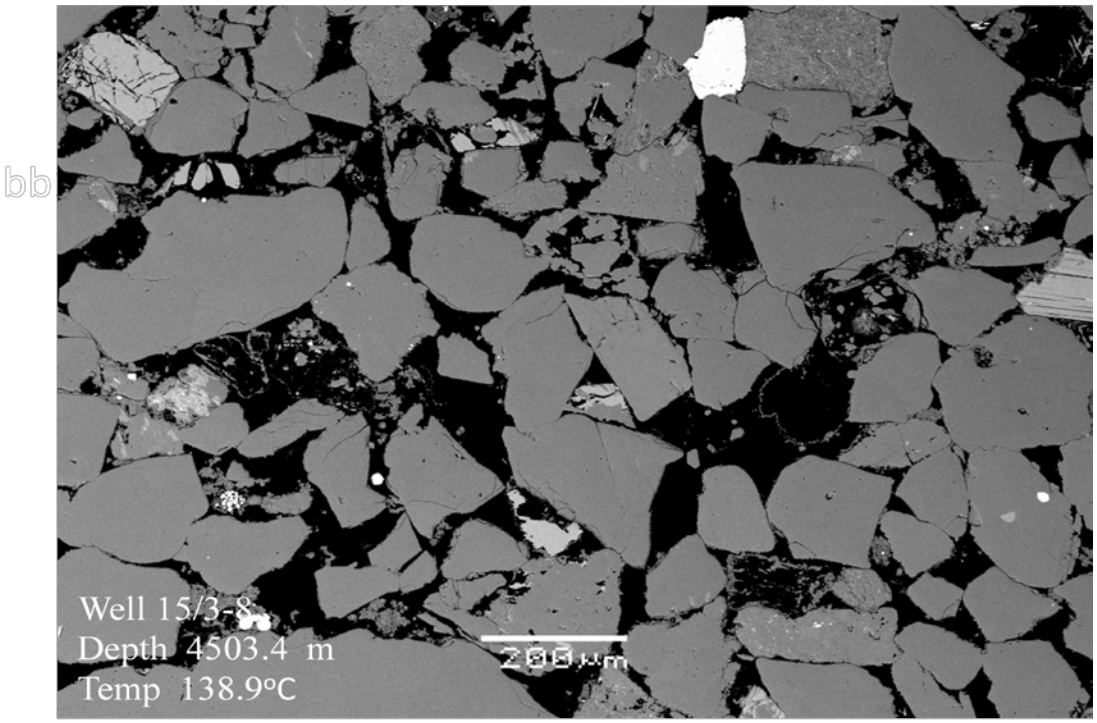

Figure 6.21: Overview of sample from Intra-Draupne sandstone showing extensive porosity and grains from well 15/3-8.

Brae Formation

Brae formation shows quartz cementation as over growth significantly as crystal faces developed. Thin sections from well 16/3B-5 are examined using the cathode luminescence (Fig. 6.22). Quartz overgrowth is clearly visible and can be distinguished from detrital quartz grain surface in CLI image of the same samples (Fig. 6.22a&c). Original quartz grain is illuminating strongly, creating a luminescence contrast from which we can easily distinguish detrital grain and overgrowth.

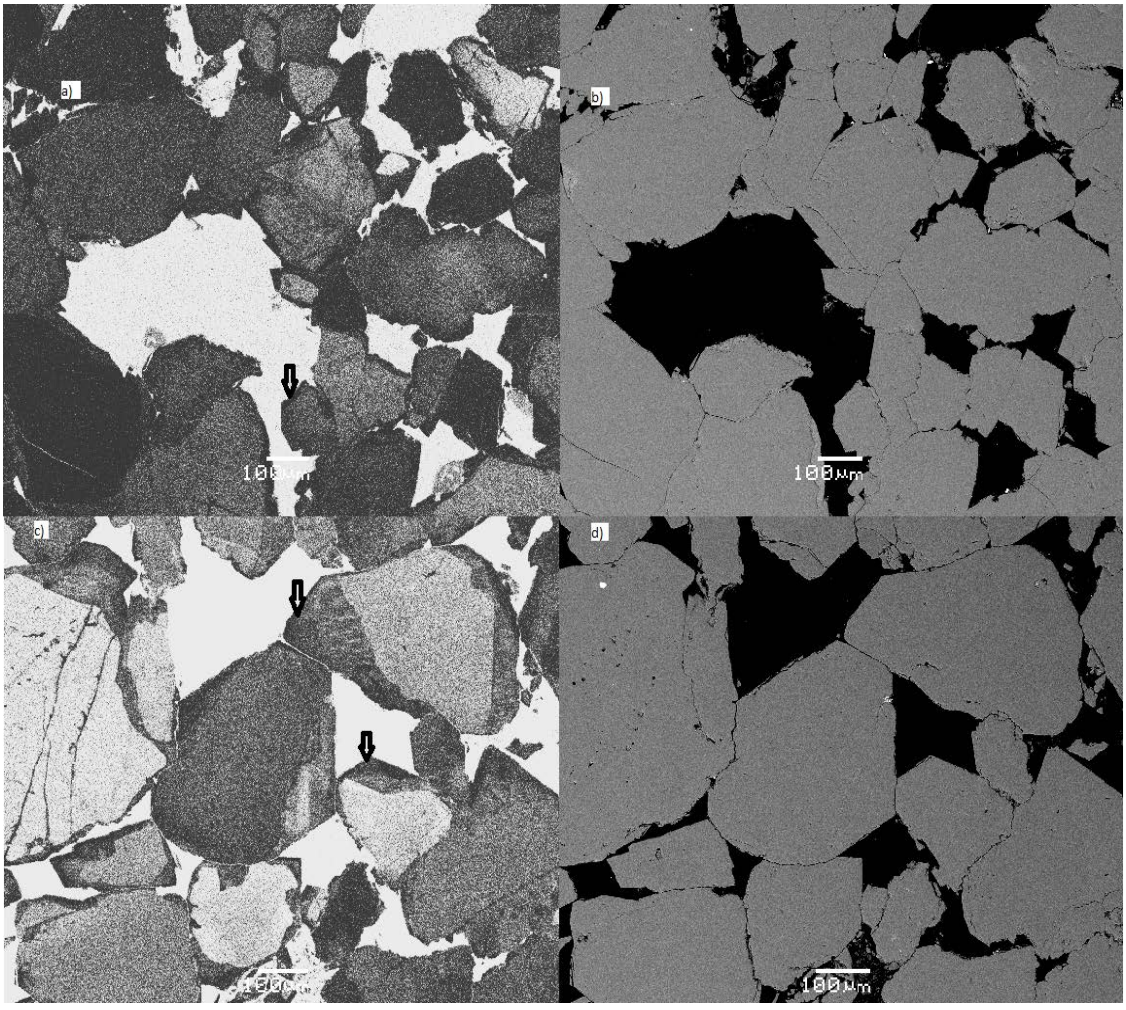

Figure 6.22: SEM image from Brae formation well 16/3B-5 vertically down arrows displaying quartz overgrowth (a) CLI image depth 4150.9m, arrow showing quartz overgrowth (b) BEI image from depth 4150.9m. quartz overgrowth (c) CLI image from 4125.2m, pervasive grain crushing. Microquartz coating delayed the quartz cementation but fresh quartz surfaces are exposed by pervasive grain crushing and quartz grow in pore space. Original detrital grain prior to quartz cement also shown with arrow (d) same BEI image as c.

The rock is compacted due to mechanical compaction and it was so severe that it causes pervasive grain crushing. Some grains show compaction related micro fractures as the one on the extreme left side of image 6.22c. According to Aggett (1997), a greater degree of quartz cementation is present which can be related to stylolization and controls the reservoir quality; also it looks that quartz cementation overprint the depositional fabric.

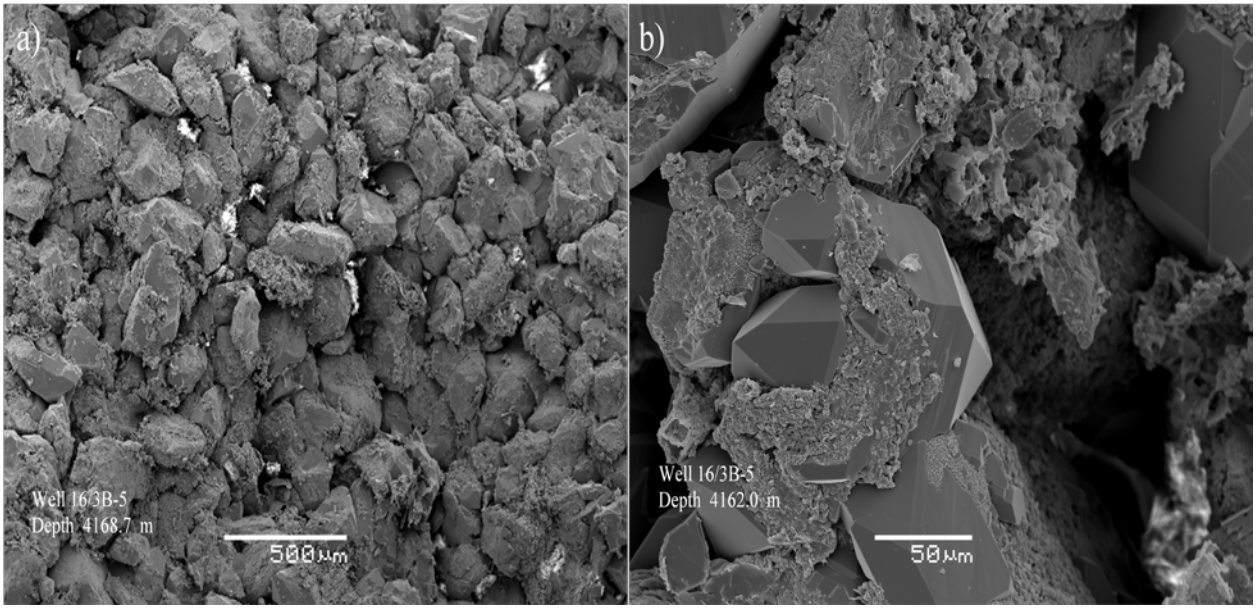

Figure 6.23: (a) Over-view of stub mounted sample from Brae Formation, sample displayed some porosity. (b) Grains partly covered grain with quartz overgrowth Brae Formation, Well 16/3B-5, East Brae Field.

6.3.2 Grain Coatings

Samples from Intra-Draupne sandstones and Brae formation are observed to find what type of grain coatings are present. Stub mounted samples from both formations have been analysed during the analysis.

Intra-Draupne Formation Sandstone

Most of the samples from Intra-draupne sandstone exhibit extensive microquartz coatings from well 15/3-8, which hinders the quartz overgrowth and helps in preserving the porosity. So it is

concluded that where microquartz coating is present, it prevents the further development of quartz overgrowth. The figure 6.24 a & b depicting the presense of microquartz and some porosity. This is a good method to get an overall estimate of grain coatings but we cannot estimate an accurate percentage from this. This attempt is taken to find the relationship between the presense of sponge spicules and content of microquartz. Sponge spicule of Rhaxella Perforata were observed in some samples from well 15/3-8, Gudrun Field and there record is being made in table 6.1.

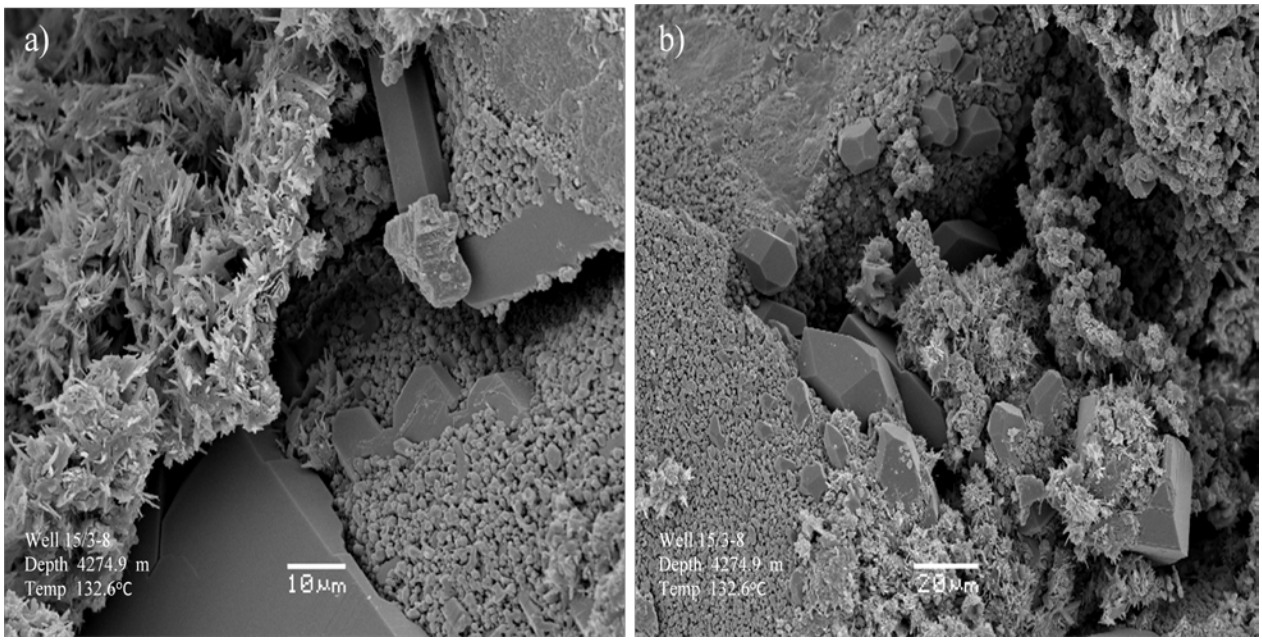

Figure 6.24: Example of micro quartz coating inhibiting quartz cementation, where coating is absent quartz nucleates as overgrowth. Authigenic illite precipitated between porosity Intra-Draupne Formation Sandstone Well 15/3-8, Gudrun Field.

The occurrence of remnant rhaxellid sponge spicule in Upper Jurassic sandstone of Intra-Draupne Formation Sandstone also supports the previous observations that indicate grain-coating microquartz are formed when spicules of Rhaxellid sponges are formed from the transformation of Opal A to quartz during shallow burial (Williams et al., 1985; Hendry and Trewin, 1995).

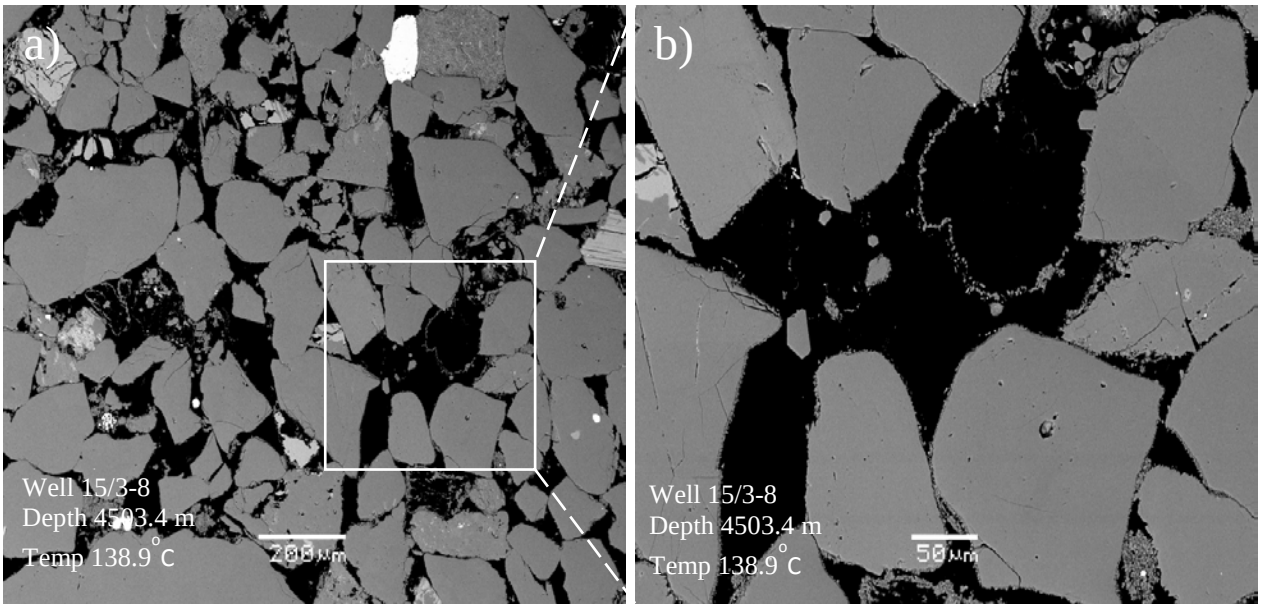

Figure 6.25: (a) SEM photomicrograph from Intra-Draupne Sandstone Formation exhibiting full coverage of grains by microquartz coating and preservation of good porosity (b) Closeup of image (a) shown on left, microquartz grain coat crystals can be observed around almost all the grains.

Microquartz coating is present in a wide range of facies associations. The first evidence of presense of rhaxellid sponges is from the Lower Calcareous Grit Formation of Yorkshire, United Kingdom(Hinde, 1890). In the South Viking Graben, a number of Upper Jurassic fields such as the East Brae (Leishman, 1994), Miller (Aase and Walderhaug, 2005), and Gudrun (Jahren and Ramm, 2000) are documented to contain microquartz. Reworked spicules can be found in Lower Cretaceous sandstones (Hendry and Trewin, 1995).

Brae Formation

Brae formation sandstone samples are basically low density and high density turbidites according to Aggett, 1997. Microquartz grain coating is observed in samples from different depths of well 16/3B-5 along with macroquartz growth figure(6.26). Microquartz coating helps in preserving the good reservoir quality in these samples and porosities of upto 28% are observed in core samples(Stephen, 2003) which can be correlated directly to this coating.

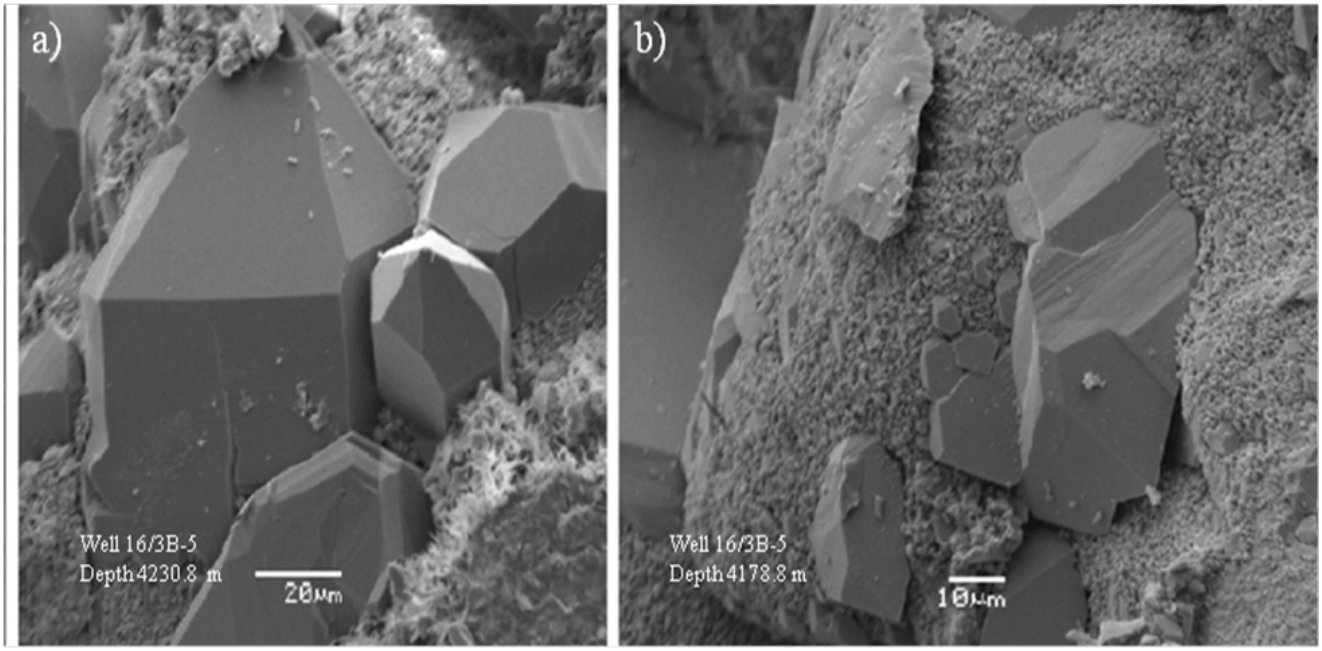

Figure 6.26: Grain-coating micro quartz preventing quartz cementation and preserving porosity while its absence formed the overgrowth from (a) Quartz overgrowth in well 16/3B-5 Brae Formation, East Brae Field. (b) Grain surface showing extensive micro quartz, Brae formation, and well 16/3B-5. Depths are shown in total vertical depth relative to sea floor.

The sponge spicule Rhaxella Perforata is described in previous studies as the source of providing solution for microquartz (Aase et al., 1996). Brae formation displayed alot of microquartz coating during the analysis of stub mounted samples in SEM (Figure 6.27&6.28) so this can be directly correlated to the presence of ponge spicules. Also in the SEM analysis of thin sections from Brae Formation sponge spicules are identified. Their different cross sectional views have been observed in different samples (Figure 6.29 b&d).

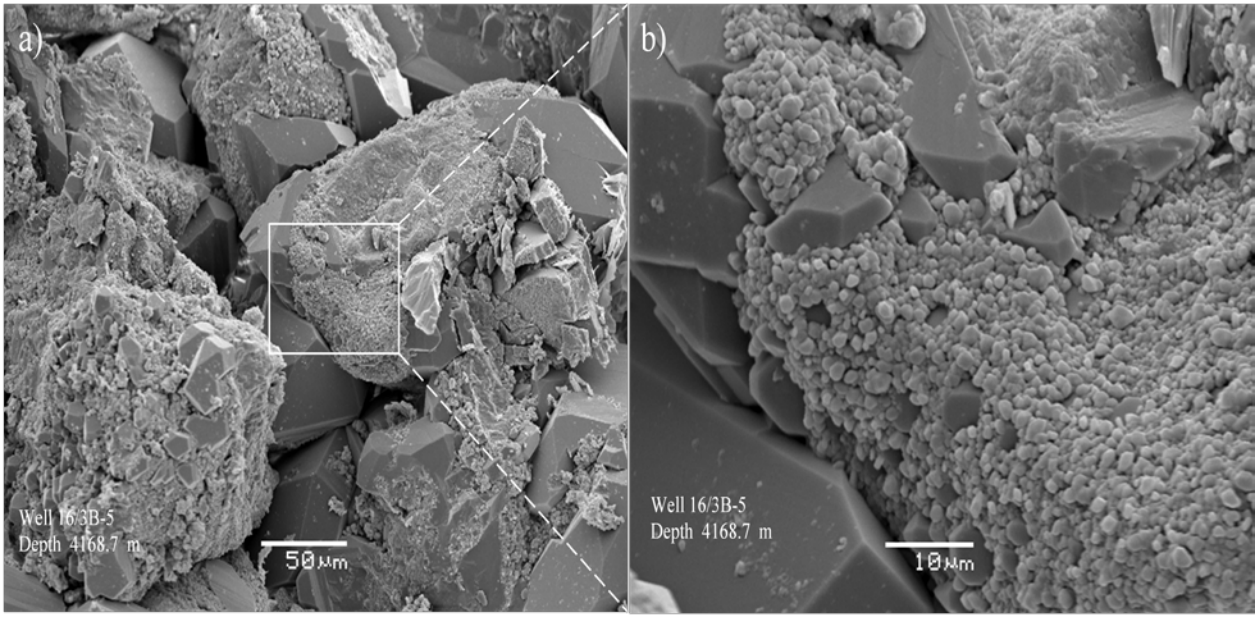

Figure 6.27: (a) Presence of grain coating hindered the quartz overgrowth, where coatings are absent quartz nucleate as overgrowth (b) Closeup of surfeace shown in figure (a) on left.

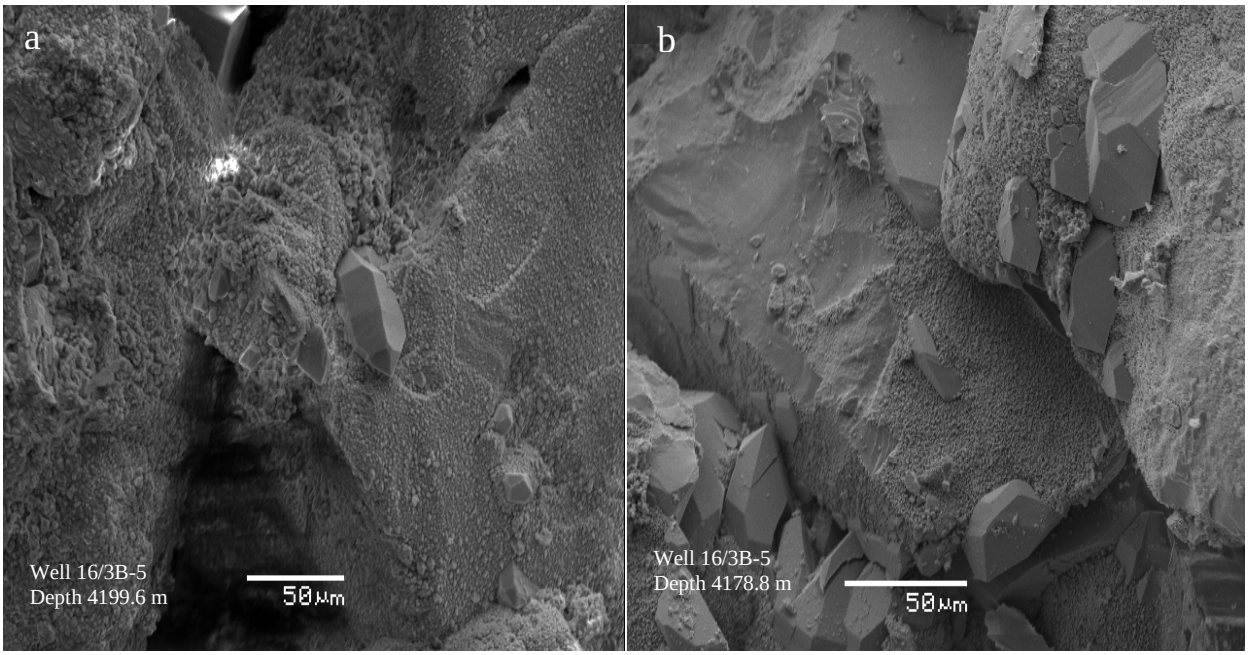

Figure 6.28: Extensive micro quartz coating preserving the porosity and hinders quartz overgrowth Brae Formation, Well 16/3B-5, East Brae Field.

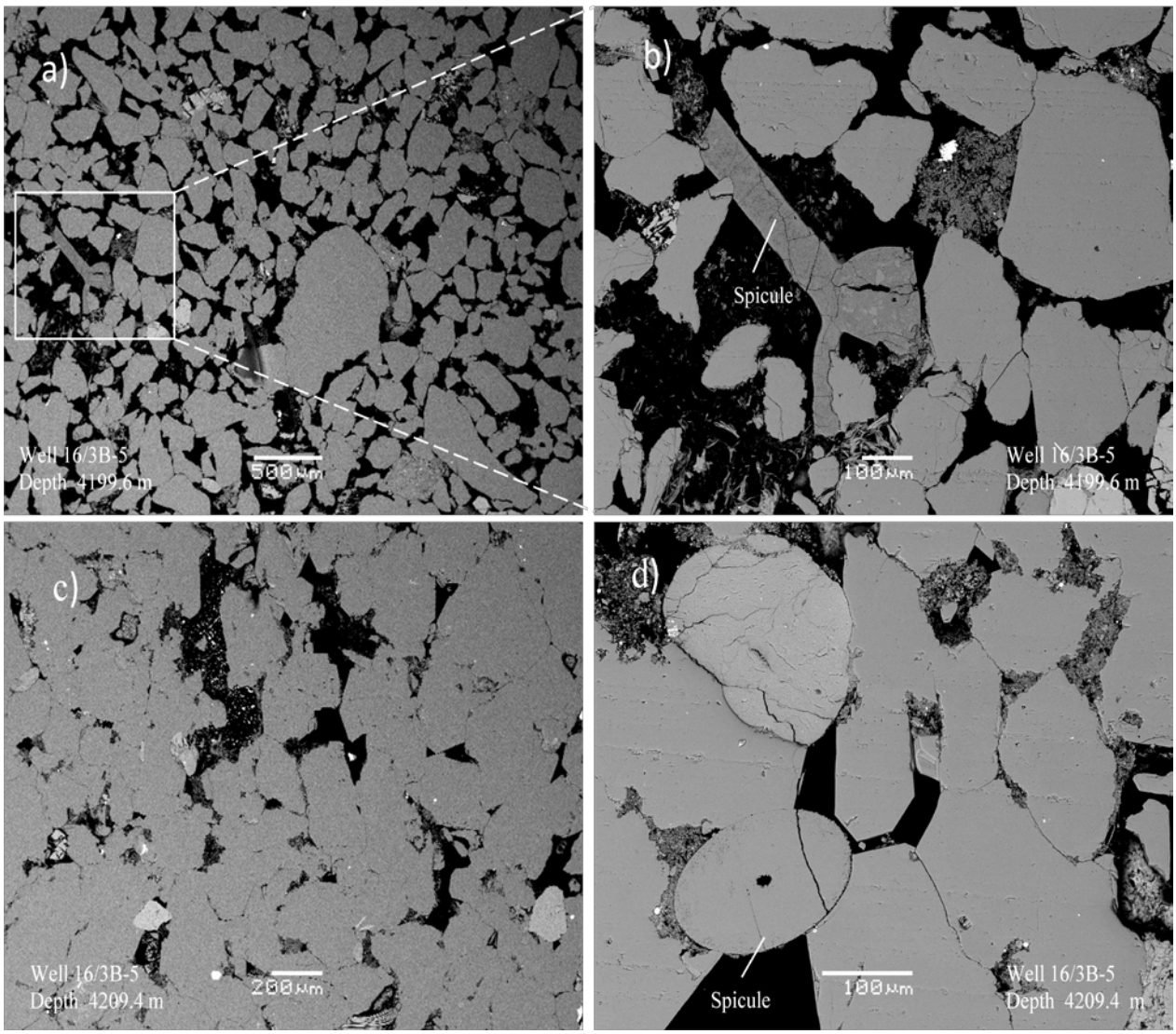

Figure 6.29: (a) Overview of Brae Formation, sample is highly porous also Sponge spicule observed (b) Close-up of cross sectional view of sponge spicule (c) Mechanically compacted sample with less porosity (d) Sponge spicule from the sample as c.

During the analysis of stub mounted samples from Brae Formation, from the depth of 4230.8m both illite and microquartz coatings were observed(Figure 6.30).

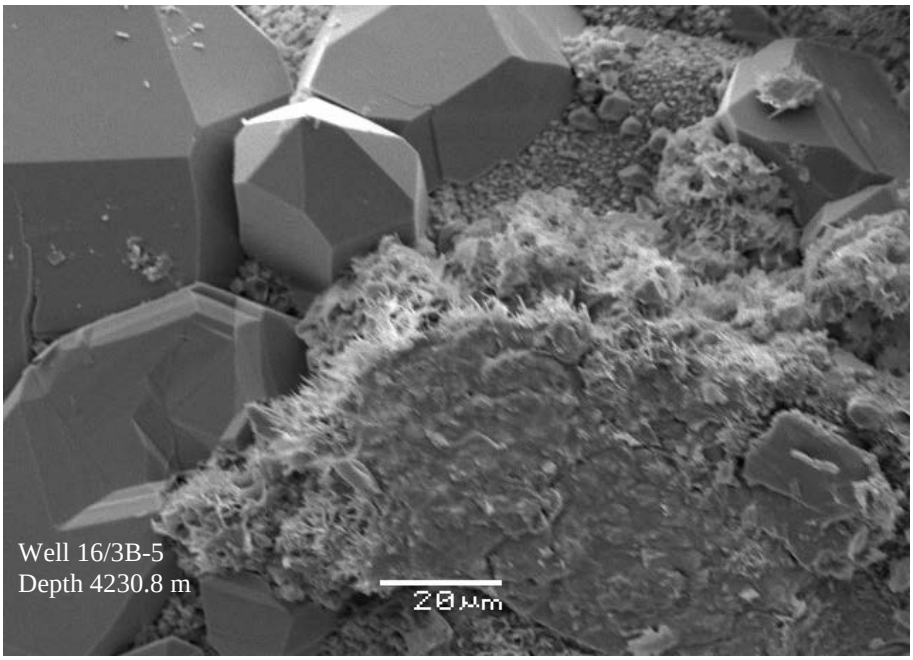

Figure 6.30: Both micro quartz coating (upper middle) and illite coating (middle) hindring quartz overgrowth, Brae Formation, Well 16/3B-5, Gudrun Field.

Visual estimation of microquartz coating coverage of the stub mounted samples for the Intra-Draupne Formation Sandstone and Brae Formation (Table 6.2) depicts the different percentages for samples. A variation was found in the observed grain coatings coverage. Some samples have most of the quartz grains covered with extensive microquartz coatings upto 75%. On the other hand some samples were devoid of coatings. Most of the samples have microquartz coating coverage upto 25%.

Quartz cementation and porosity values from the point count analysis and approximate microquartz coatings percentages from SEM have been integrated (Table 6.3). A strong relationship exists between the occurrence of microquartz coatings and preserved porosity in both formations. Samples covered with approximately 75% microquartz grain coatings have quartz cementation between 2.3-3.9% and preserved porosities of 18.6-23%. While where coatings are between 0-25%, extensive quartz cementation occurred with corresponding lower porosity value of 6%. These results strongly support the porosity preserving phenomenon by microquartz coatings.

Well	Formation	Sample	Depth(m)	Microquartz Coating Degree (approximately)				
				0	<25 %	<50%	<75%	>75%
Well 15/3-8	Intra-Draupne Formation Sandstone	BB7	4174.1		✓			
		BB5	4179.5		✓			
		BB4	4199.7			✓		
		BB14	4218.9		✓			
		BB3	4237.4			✓		
		BB12	4264.9		✓			
		BB6	4273.2				✓	
		BB11	4274.9				✓	
		BB8	4296.0		✓			
		BB1	4499.6			✓		
		BB13	4503.4					✓
Well 16/3B-5	Brae Formation	EB6	4125.2		✓			
		EB16	4128.3	✓				
		EB4	4148.4		✓			
		EB7	4157.2	✓				
		EB3	4162.0			✓		
		EB12	4166.3				✓	
		EB19	4168.7		✓			
		EB8	4178.8					✓
		EB13	4197.6					✓
		EB14	4199.6					✓
		EB9	4202.9	✓				

Table 6.2: Summary of the Occurrence of Grain-Coating Microquartz from SEM Analysis based on visual estimation of stub mounted samples.

Well	Formation	Sample	Depth	Point Count % Quartz Cement	Porosity	SEM Microquartz Coating %(approx.)
Well 15/3-8	Intra-Draupne Formation SST	BB4	4199.7	3.6	12.8	<50 %
		BB12	4264.9	3.0	12.3	<25%
		BB6	4273.2	3.6	18	<75%
		BB11	4274.9	2.6	16.2	<75%
		BB8	4296.0	2.3	10	<25%
		BB13	4503.4	3.9	18.6	>75%
Well 16/3B-5	Brae Formation	EB6	4125.2	7.3	17	<25%
		EB4	4148.4	12.6	11.6	<25%
		EB7	4157.2	7.6	12.2	0%
		EB3	4162.0	11	18	<50%
		EB12	4166.3	6.3	22.3	<75%
		EB13	4197.6	2.6	23	>75%
		EB14	4199.6	2.3	20.6	>75%
		EB9	4202.9	11	6	0%

Table 6.3: Integrated results from point count analysis and SEM showing relationship between Microquartz coating, quartz cement and Primary Porosity.

6.3.3 Authigenic clays

Authigenic clays precipitate in situ by the leaching of minerals like feldspar and mica as meteoric water flow through the rocks (Bjørlykke and Jahren, 2010). Authigenic Kaolinite is observed mainly in samples from the Brae Formation, well 16/3B-5 and Illite is present in almost all of the samples from Intra-Draupne Formation Sandstone.

Brae Formation

Porefilling kaolinite and Illite were observed in Brae formation in well 16/3B-5. Clay minerals can be identified from their characteristic morphology as authigenic. Kaolinite is observed in SEM photomicrographs as stacked booklet shape structures (Figure 6.31). Kaolinite preserves its booklet morphology at greater depths up to 4200m.

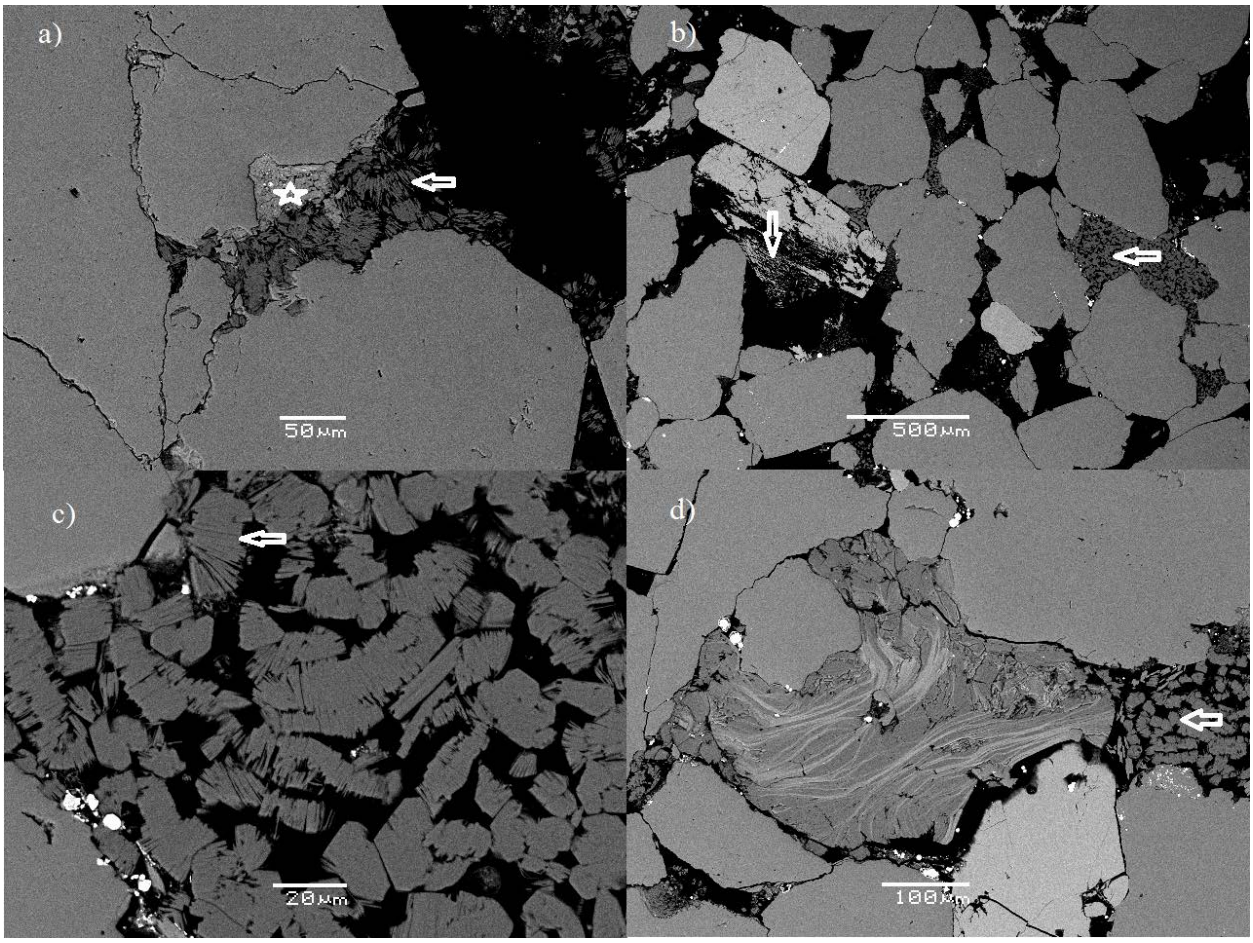

Figure 6.31: SEM photomicrograph from Brae formation well 16/3B-5, depth 4202.5m (a) Arrow indicating authigenic kaolin and star illite (b) Partially dissolved feldspar grain indicated by arrow pointing vertically down. Horizontal arrow pointing pore filling kaolinite(c) Closer view of booklet pattern of kaolin (d) Pore filling kaolin.

Kaolinite is observed in stub mounted samples with typical booklet form and vermicular pattern exhibiting its authigenic origin (figure 6.32). Overall it is observed from thin section samples that there is greater amount of Kaolinite than Illite in the Brae formation. According to Aggett, 1997, reservoir quality is affected by small amount of Kaolinite and Illite in the East Brae reservoir.

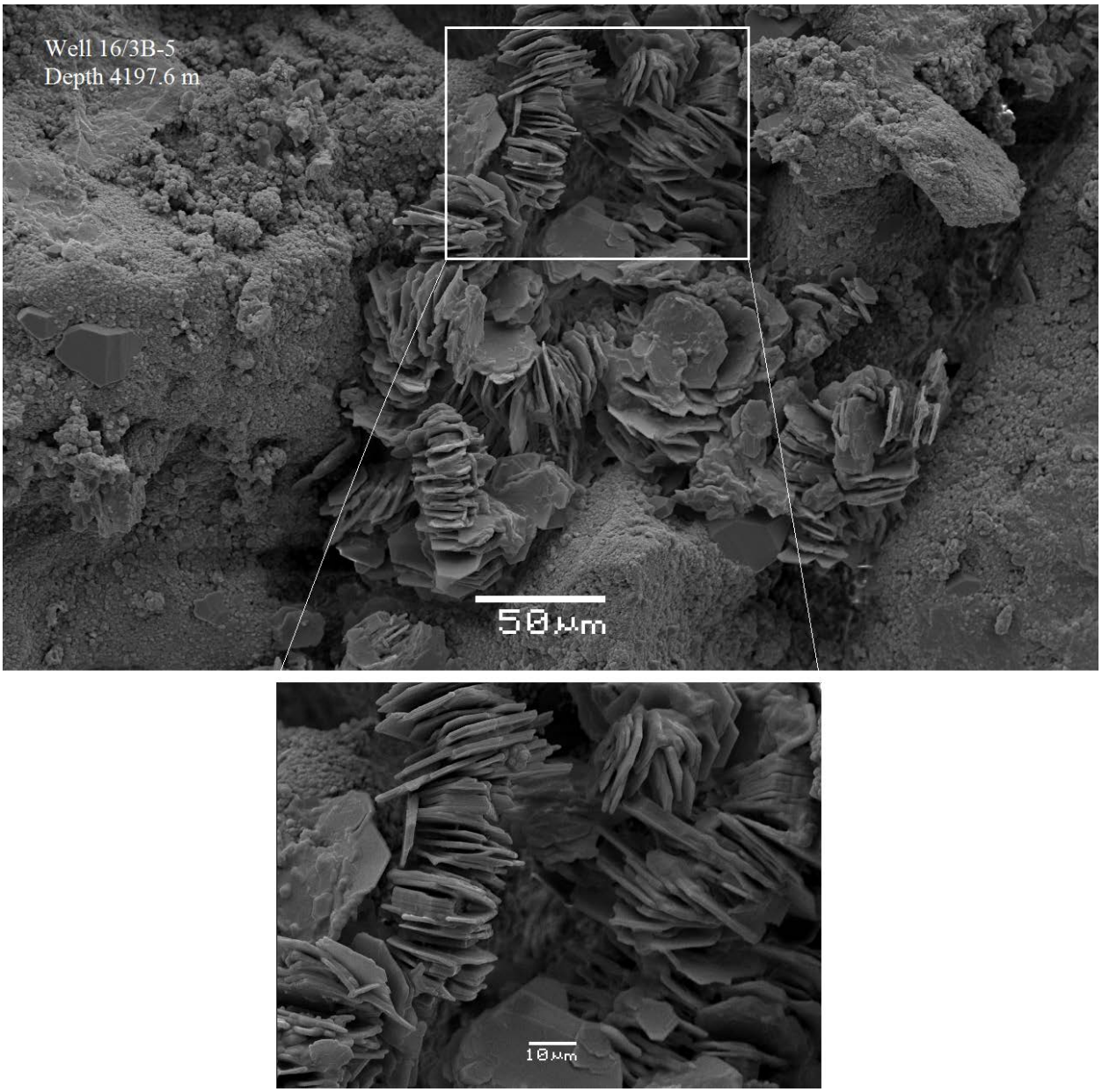

Figure 6.32: Authigenic Kaolinite precipitated between the pores, sample from Brae Formation, exhibiting typical booklet structure and specific vermicular pattern describing its authigenic origin, also the sample has extensive grain coating micro quartz, well 16/3B-5, East Brae Field South Viking Graben.

Intra-Draupne Formation Sandstone

Authigenic illite is observed from most of the samples from the Intra-Draupne Formation Sandstone, in the form of thin hair or plate like structure. Here it also seemed to be filled in

between the pores as rock wool (Bjørlykke and Jahren, 2010). Because it precipitated between the pores, it seemed to be reducing the permeability (Figure 6.33).

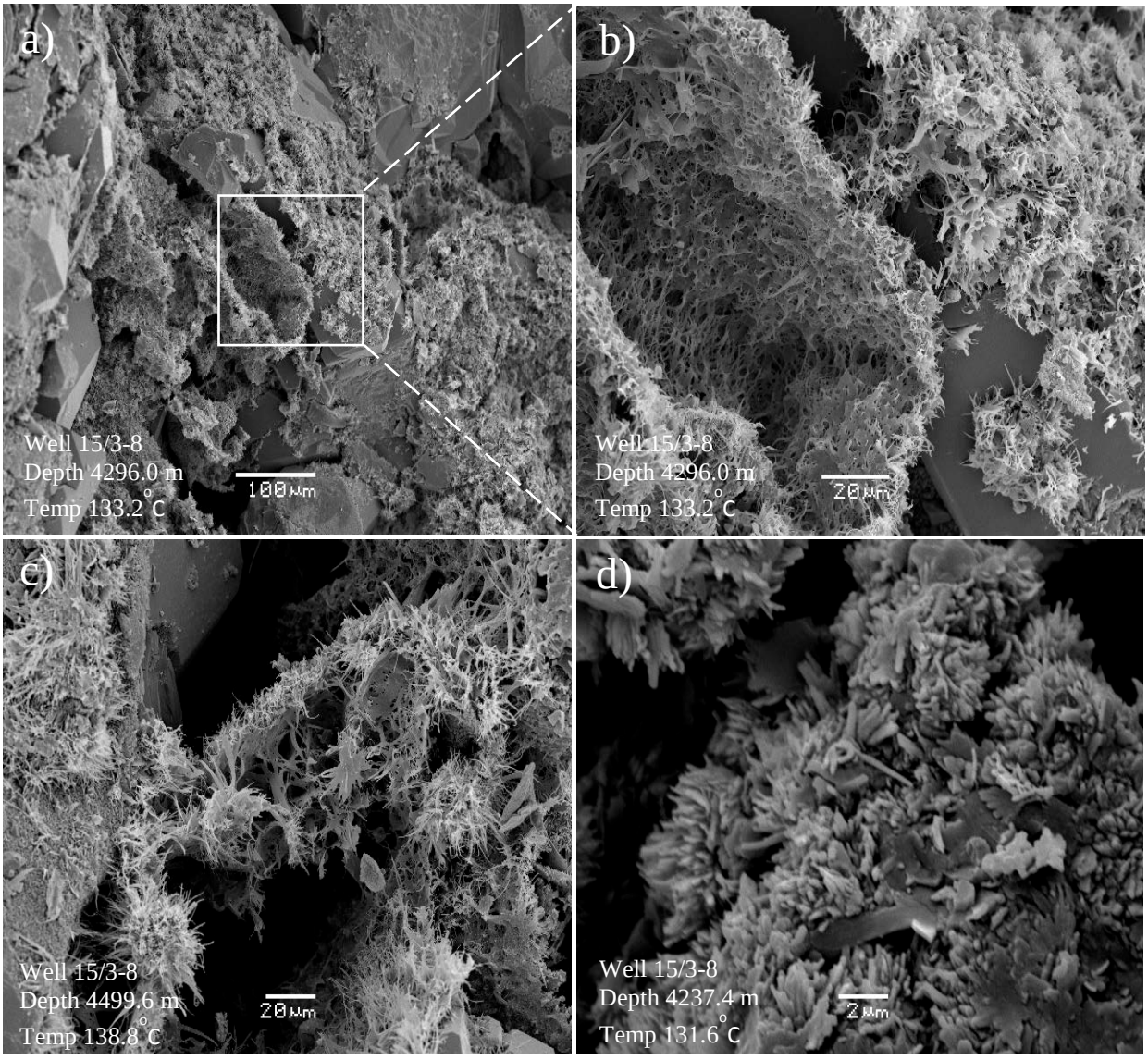

Figure 6.33: Pore filling illite observed in different samples from Intra-Draupne Formation Sandstone (a) Forming hair like and plate like pattern, Well 15/3-8, Gudrun Field (b) Detailed closer view showing its typical structure (c) Authigenic illite precipitation between pores seemed to reduce the porosity, 4499.6 m depth, Gudrun Field. (d) Illite seemed to be present as coating on grains. Kaolinite observed only in one stub mounted sample (Figure 6.34).

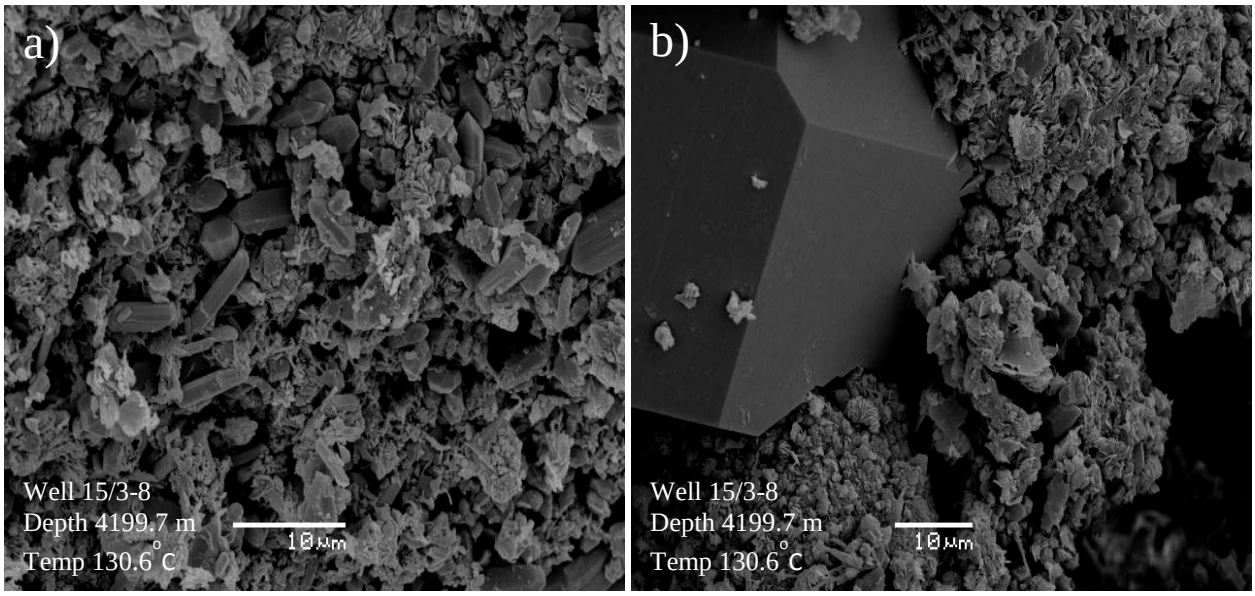

Figure 6.34: kaolinite mixed with micro quartz crystals Intra-Draupne Formation Sandstone, Well 15/3-8, Gudrun Field.

6.3.4 Feldspar Dissolution and Secondary Porosity

We can compare the amount of feldspar present with the clay minerals to establish a relationship between feldspar dissolution and precipitation of clays. Leached feldspar and authigenic clays are observed which precipitated as pore-filling mineral (6.35). Undissolved feldspar grains are found along with dissolved feldspars during the analysis of thin section slides (Figure 6.31b).

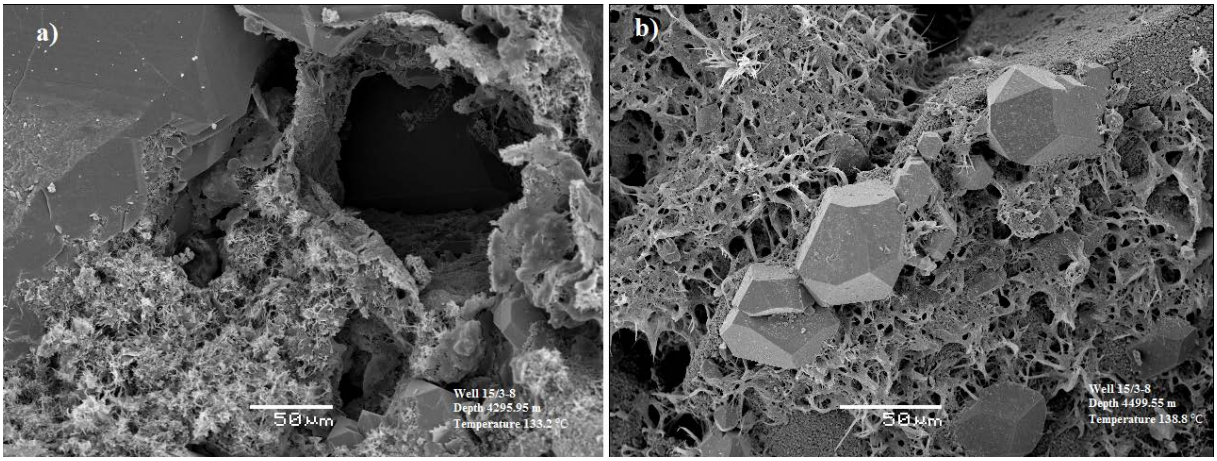

Figure 6.35: (a) Leached feldspar grain leaving behind the clay rim, Draupne Formation, well 15/3-8, Gudrun Field. (b) Illite forming network over quartz grain surface, where micro quartz coating is present it hinders the overgrowth Draupne Formation, well 15/3-8.

6.3.5 Carbonate Cementation

Carbonate observed during the SEM analysis of Intra-Draupne formation extensively (Figure 6.36). Also the point count analysis results depict more carbonate content in the Intra-Draupne Formation Sandstone than Brae Formation.

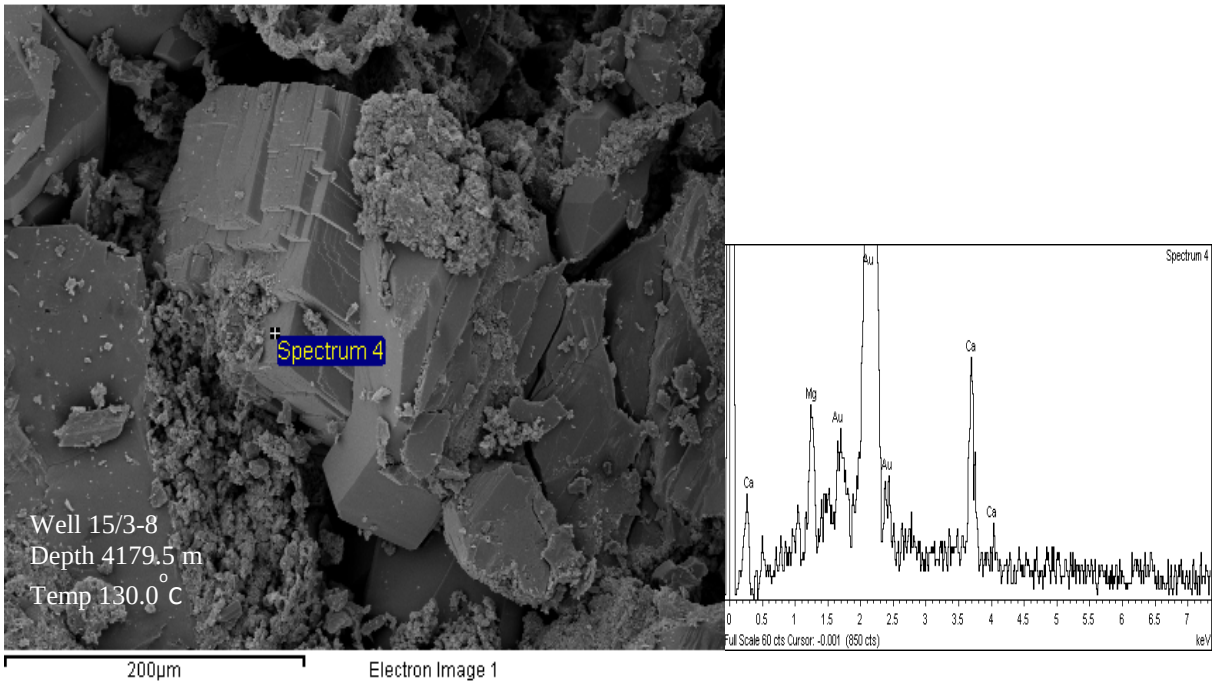

Figure 6.36: Dolomite observed from Intra-Draupne Formation, well 15/3-8.

6.3.6 Other Minerals

Pyrite observed from the stub mounted samples depict typical small framboidal crystals in the Brae Formation (Figure 6.37a), they have shape of balls. In the backscatter electron image pyrite and Sphalerite can be identified easily as bright spots (Figure 6.37b). Both of the minerals are found in the Brae Formation along with extensive porefilling illite.

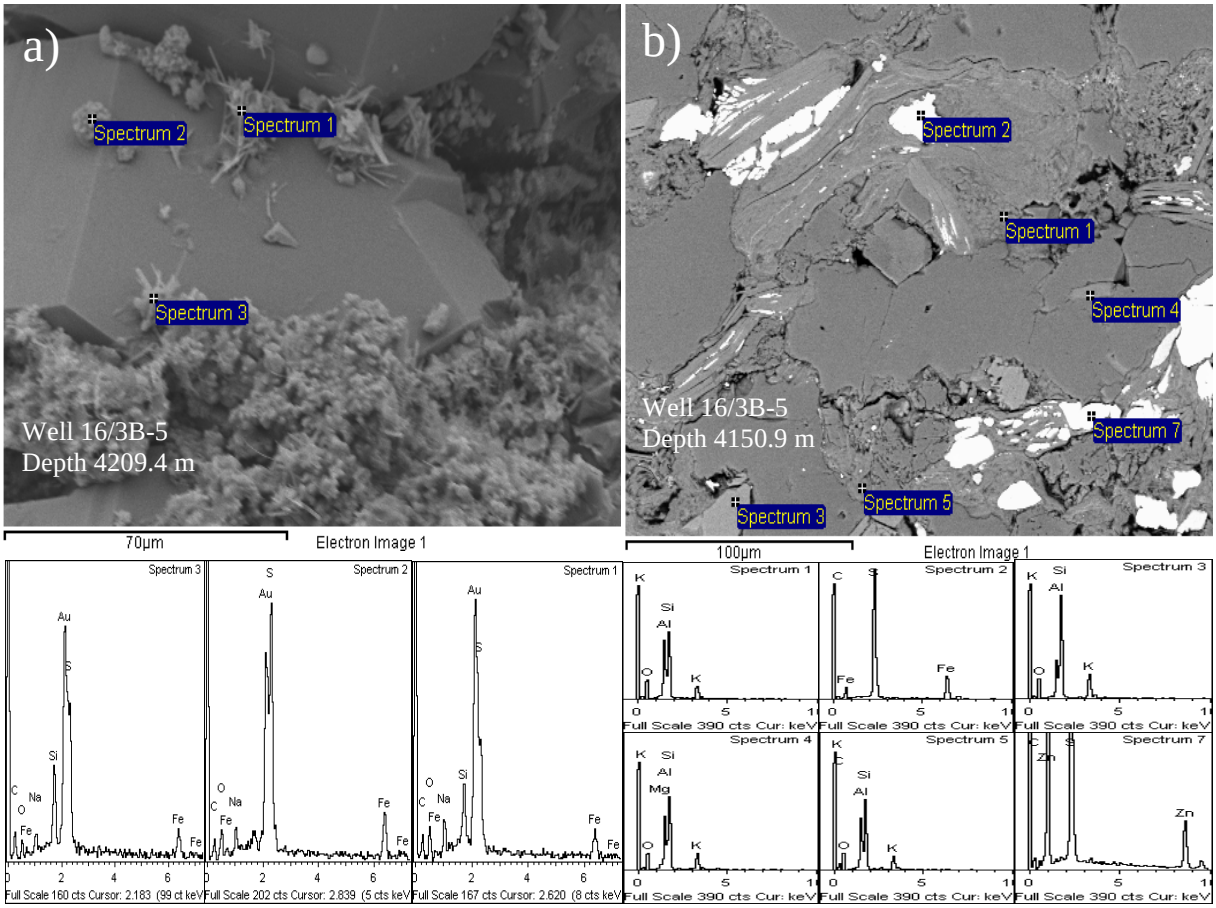

Figure 6.37: SEM images from Brae Formation, Gudrun Field (a) Small framboidal pyrite crystals (b) SEM image with spectrums of different constituents of sample, Spectrum1,3,4,5(Illite), 2(Pyrite), 7(Sphalerite).

7. KINETIC MODELING OF QUARTZ CEMENTATION

7.1 Introduction

Quartz cementation is the main factor in reduction of porosity in many deeply buried sandstone reservoirs in basins around the world (Bjørlykke and Jahren, 2010). The approach presented by Walderhaug (1996) is used in modeling quartz cementation, where the source of quartz cement is from stylolites and thick zones of clay. Quartz cementation and porosity loss are shown as a function of time.

This approach is very good at handling factors like grain size, detrital quartz percentage, clay coatings and different temperature histories. The simulation of quartz cementation in this model is performed for those situations where grain interpenetration is negligible and the source of quartz is from stylolites which are present in the sandstones which are under the process of cementation but these stylolites are not included in the model. This approach is very effective because we don't need to model the effect of vertical shortening and volume loss due to quartz dissolution. The volume of precipitated quartz cement is equal to the loss in porosity. And quartz cementation is a continuous process. The quartz cementation process is controlled by the precipitation rate and temperature is the main control on the quartz cementation because the rate of precipitation of quartz relies exponentially on temperature (Walderhaug, 1994a).

Provided constant temperature, the volume of quartz cement, Vq (in cm^3), precipitated in a 1-cm^3 volume of sandstone with quartz surface area A (in cm^2) during time t (in seconds) can be calculated as

$$Vq = MrAt/\rho \qquad (1)$$

Where M is the molar mass of quartz (60.09 g/mole), r is the rate of quartz precipitation in moles/cm^2 s, and ρ is the density of quartz (2.65 g /cm^3). The studies of quartz cemented sandstones (Walderhaug, 1994a) indicate that the quartz precipitation rate can be expressed as a logarithmic function of temperature:

$$r = a10^{bT} \qquad (2)$$

where, T is the temperature (^oC) and a and b are constants with units moles/cm^2s and $1/^oC$, respectively. When the temperature history of the sandstone is given as time-temperature points linked by linear functions, as in the current situation, T can be replaced by a linear function of time and we can rewrite the equation (2) in this way

$$r = a10^{b(C_n t + d_n)} \qquad (3)$$

where C_n is describing the heating rate ($^oC/s$), d_n is the initial temperature (^oC) and index n refers to the relevent section of temperature history curve.

From equations (1) and (3) we can calculate the amount of quartz cement Vq precipitated in a volume of sandstone from time t_0 to t_m as the sum of series of integrals, where each integral describes the volume of quartz precipitated during each time step is given by the equation

$$Vq = M/rho\ A_0\ a\int^{t1}\int$$

7.2 Effects of different parameters on Modelling

7.2.1 Grain size Effect

According to Walderhaug, 1996, when interbedded sandstones are of different grain sizes, the fine grained intervals will experience more quartz cementation and porosity loss than coarse grain sandstones. In fine grained sandstone intervals the greater amount of quartz cement is due to the availability of the increased quartz surface area for quartz precipitation. This idea is reinforced by the experiments on quartz cementation where fine grained quartz sand become cemented very quickly than coarse grain sand (Heald and Ranton., 1966). According to observations of Walderhaug (1996), the quartz cementation is enhanced in finer grained sandstones.

7.2.2 Effect of Mineralogy

The amount of nonquartz frame work grains effect the surface area available for quartz precipitation, quartz cementation is expected to occur faster in a pure quartz arenite then in arkoses with the same grain size. During experimental studies of quartz cementation it is observed that pure quartz sand undergo a more rapid quartz cementation than arkosic sand (Heald and Ranton., 1966). And also the tendency of porosity preservation around feldspar grains in quartz cemented sandstones has been observed (Bjørlykke et al., 1986).

7.2.3 Effect of Clay Coatings

A number of authors reported the phenomenon of inhabitation of growth of quartz cement due to the clay coatings present on the grains (Ehrenberg, 1993 and Bjørlykke and Jahren, 2010). So when modelling quartz cementation the factor of clay coatings should also be taken into account. Model of Walderhaug, 1996 introduces the clay coating factor, C, and it represent the fraction of qurtz grains coated by clay into equation as:

$$A = (1\text{-}C)A_0 (\phi_0 - Vq)/ \phi_0 \qquad (9)$$

When the quartz grains are coated by clay or other coatings, the value of C becomes 1, quartz surface area A is 0, and no quartz cementation occur. Other coatings like carbonate cements on quartz grains can reduce surface area for quartz cementation in the same way but in this way less porosity is preserved due to filling of most or all of the pore system by the cementing minerals.

7.2.4 Effect of Prequartz Cementation Porosity

The amount of porosity present at the onset of quartz cementation effects the precipitation of quartz cement and porosity loss in two ways. Firstly, if there is greater amount of porosity present more quartz cement is needed to fill the pores. So it takes longer time to fill the porosity in highly porous sandstones in order to be totally quartz cemented but at the same time there would be greater amount of quartz cement present at the end of the cementation process than in less porous sandstones. Secondly, the tighter grain packing is present in less

porous sandstones, in this situation more quartz grains and greater surface area is available per unit volume. This situation lead to rapid quartz cementation and porosity loss in the initially less porous sandstone during the early stage of quartz cement and surface area available for quartz cementation is less due to greater grain contacts.

7.2.5 Effect of Temperature History

Thermal maturity is considered to be the effect on sandstone porosity by several workers (Schmoker and Gautier , 1988; Schmoker and Higley, 1991).

7.3 Procedures

The temperature variations with depth were calculated for both wells by taking values from well reports (Figure 7.1).

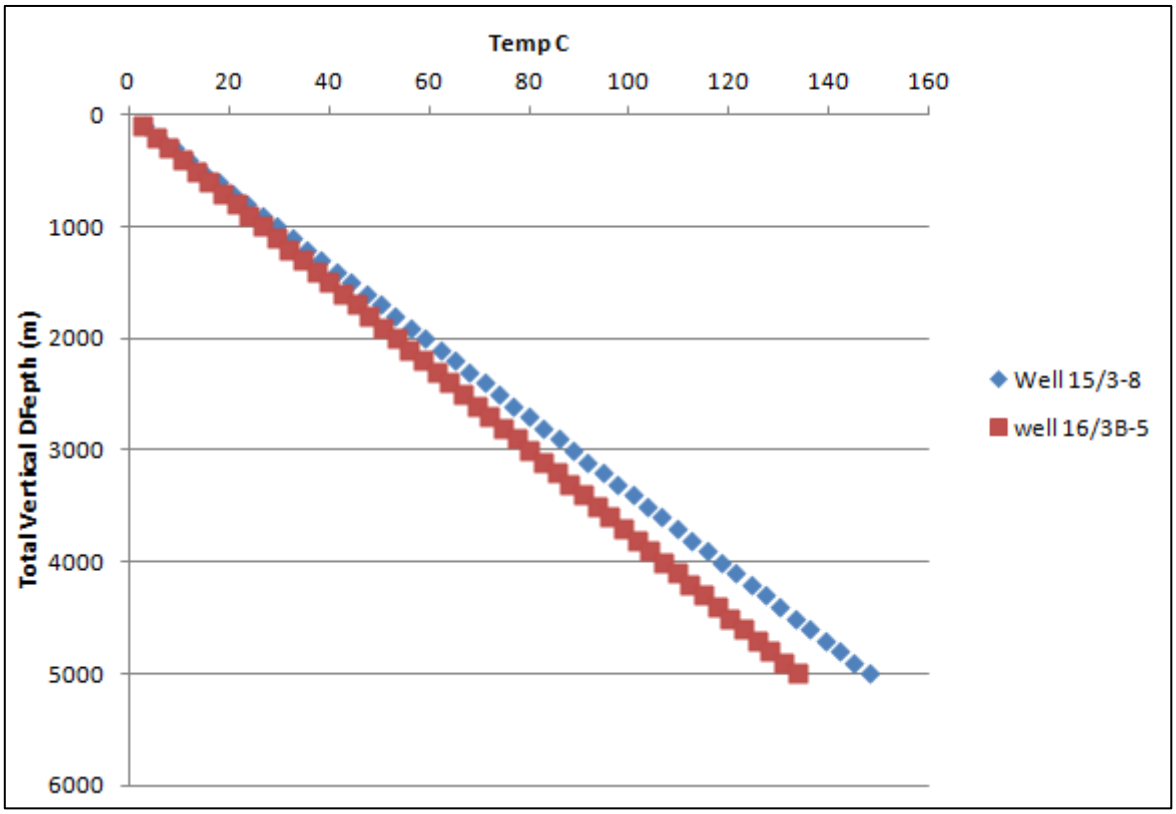

Figure 7.1: Temperature variation with depth for wells.

To calculate burial history, here data from Maast et al., 2011(Figure 8c, page 1950) is used.

There values were random, we take points and make the line by joining points then calculate the gradient by using the formula

Gradient of a line = (Y2-Y1)/X2-X1 …….. Equation 7.2

Where,

Y2 and Y1 are depth in meters.

X2 and X1 are time in million years.

Wells	Y2	Y1	X2	X1	Y=Y2-Y1	X=X2-X1	Gradient(Y/X)
15/3-1s	4500	900	6	153	3600	-147	-24,4898
15/3-2R	4100	300	3	158	3800	-155	-24,5161
15/2-1	4100	200	0	157	3900	-157	-24,8408
15/3-3	4000	200	17	156	3800	-139	-27,3381
Average	4175	400	6,5	156	3775	-149,5	-25,2508

Table 7.1 Data taken from Maast et al., 2011 to calculate burial history.

Using the equation of a straight line

Y=mx+c equation …….7.3

Where,

m=slope or gradient of line

C=Y intercept of line

Using the calculated values from table 7.1 and putting in equation 7.3, we got

Y= (-25.25(time) +4500)

Burial history curve is generated and presented in figure 7.2.

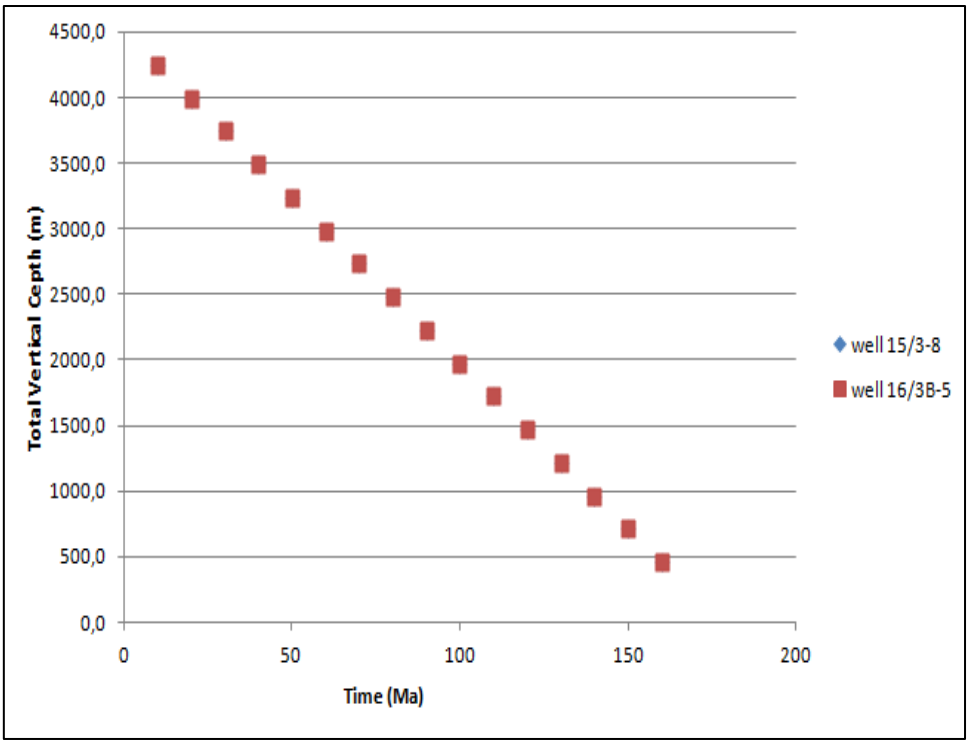

Figure 7.2 Burial histories calculated from Maast et al., 2011. Values from both wells overlap because input data used for both wells were same.

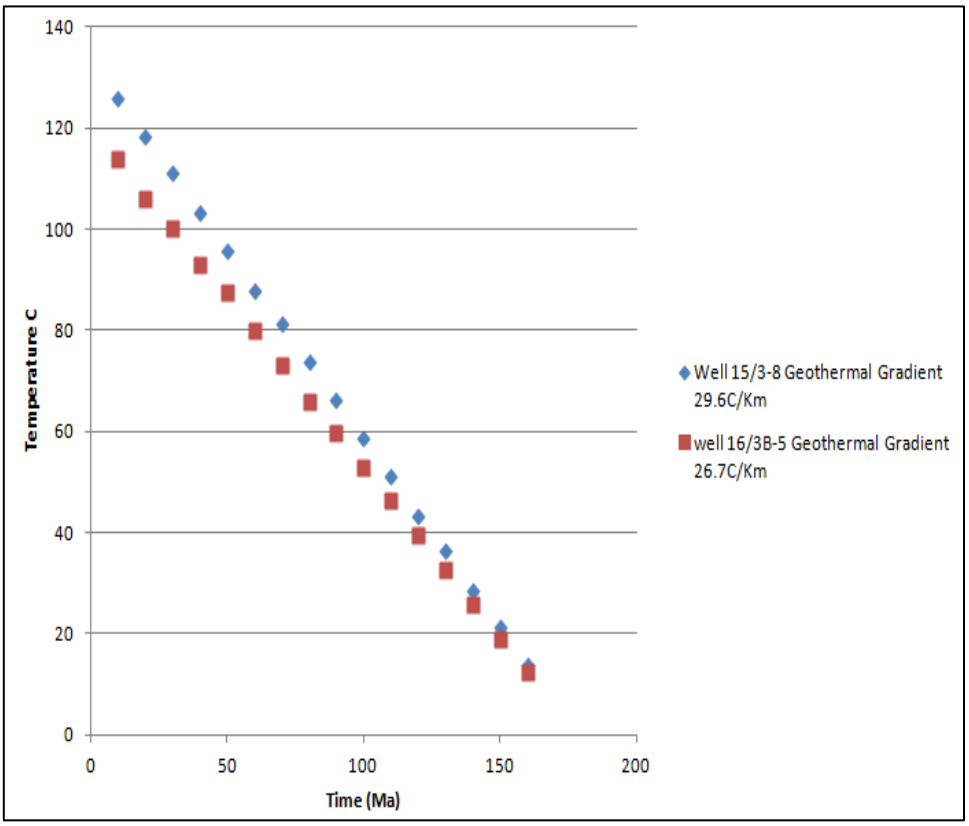

Figure 7.3 Temperature histories for wells calculated from Maast et. al., 2011.

According to Bjørlykke and Jahren, (2010), once the Quartz cementation has been started, it does not stop until the whole porosity is lost or temperature drop below 70-80^{o}C. A strong reduction in porosity and permeability has been found in deeply buried sandstone reservoirs from 3-3.5km to 4-4.5km corresponding to a temperature range between 120-160^{o}C. The main factors behind this phenomenon were found to be quartz cement. According to Walderhaug, (1996), the quartz cementation rate increases as an exponential function of temperature (Figure 7.4). This exponential increase is close to a factor of 1.7 for every 10^{o}C temperature increase. Between the temperature range of 100-140^{o}C, the quartz precipitation rate double four times, i.e., increases 16 fold. In contrast the increase in effective stress is linear with depth and increase only 30 to 40% within the corresponding depth interval of 3-4km. During this interval temperature is found to be the main controlling factor for the quartz precipitation rate.

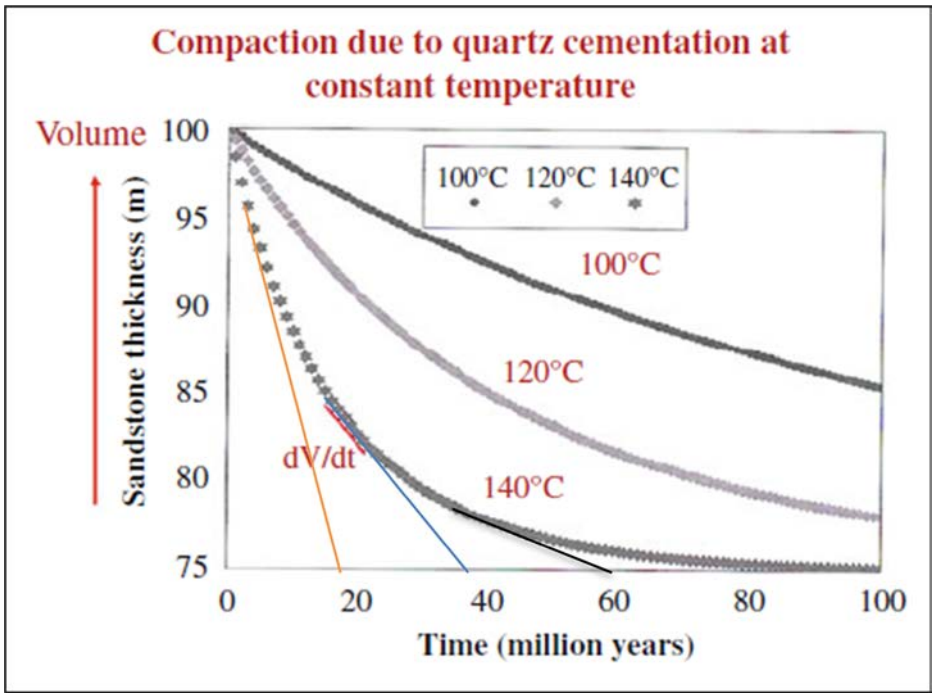

Figure 7.4: Modelling of quartz cementation and chemical compaction due to quartz dissolution and cementation as a function of time and temperature (from Walderhaug et al., 2001). The rate of porosity loss (compaction, *dv/dt*) is highest at higher temperatures.

Temperature history values generated in figure8.3 were used and quartz cement percentages were calculated for the modeled data (Table 7.2) by employing the following formula:

Modeled Quartz Cement = 1/2*(Time m.y)*(Quartz precipitation rate)

For modelling purpose, the quartz cement precipitation rate is taken 2, for every 10^{o}C. The total modeled quartz cementation has been found to be 8.5%.

Temperature(^{o}C)	Time(M.Y)	Factor	Quartz Precipitation Rate	Modelled Quartz Cement %
70-80	75	1/2	1/64	0.5
80-90	60	1/2	1/32	1.0
90-100	46	1/2	1/16	1.5
100-110	30	1/2	1/8	2.0
110-120	17	1/2	1/4	2.5
120-130	2	1/2	1/2	0.5
130-140	1	1/2	1	0.5
Total				8.5

Table 7.2: Modeled quartz cementation from temperature history curve.

In this study the time constrains prevented a full modelling of quartz cement. The calculations presented are therefore a crude approximation of expected quartz cementation in the studied reservoirs based on the Walderhaug (1996) approach.

8. DISCUSSIONS

Introduction

From the analysis of results generated in the previous chapters, several factors are found which affect the reservoir quality of sandstones starting from deposition to the deep burial during diagenesis of the sandstone. They are discussed here accordingly.

8.1 Mechanical Compaction

The Intergranular volume (IGV) is the sum of intergranular primary porosity, cement and matrix and it is calculated from the point counting of petrographic thin sections. The IGV ranges between 20-37% which demonstrates that different digenetic processes lead to the formation of sandstones. Samples analyzed during this study were taken from Intra-Draupne Formation sandstone and Brae Formation with depth range 4125m to 4500m. Some samples have higher IGV values up to 35 % (Figure 6.11). Quartz cement and porosity are found to be the major constituent of IGV. Most of the samples in the Brae Formation have higher quartz cement content. IGV values lower than 26% (considered lower limit for IGV) could be the result of (as described by Chuhan et al., 2002) initially formed microquartz grain coatings delayed the quartz cementation up to the 4-5Km burial depth and corresponding 40-50 MPa effective stress, caused the pervasive grain crushing (Figure 6.22c). Grain plucking during the thin section preparation causes the higher counts in the porosity that could result in the higher IGV values (Figure 6.21).

In granular rocks, the IGV is a very good indicator of compaction. IGV can also be described as minus cement porosity and precement porosity (Paxton et al., 2002). The process of cementation, whether it is early carbonate cement or late stage quartz cement, stabilizes the grain frame work of the sandstone and prevents/hinders further mechanical compaction. Therefore, mechanical compaction occurs in the sandstone reservoirs down to the depth of about 2-2.5km and 80^0C temperature according to Bjørlykke and Jahren, 2010, because at this temperature the quartz precipitation process is effective.

Presence of higher amount of carbonate cement and also clay content lead to the higher IGV values (Figure 6.10) as in the Intra-Draupne Formation sandstone with average value of 30.71%. The Brae Formation has lower amount of carbonate cement and clay content, thus IGV average is lower (27.35%). Secondary porosity generated from the dissolution of feldspar and mica can affect the IGV. The meteoric water flushing starts dissolution of feldspars and unstable minerals when sands are deposited. This process precipitates the pore

filling kaolinite at the same time and counter fills the porosity generated from dissolution. So only possibility of secondary porosity enhancing the IGV could be higher influx of meteoric water causing dissolution and dissolved components transported away from the subjected sandstone, leading to increase in porosity. A plot between calculated IGV and secondary porosity (Figure 6.12) displayed a linear relationship between secondary porosity and IGV.

IGV decreases up to the burial depth related to mechanical compaction limit and stabilizes at a certain value in most of the cases (Figure 6.13). According to Marcussen et al., (2009), IGV values do not decrease after the burial depth of 2260m. For the same burial depth, IGV values can vary. For example, at around 4200m the value of IGV show a difference of about 9% (Figure 6.13). This might be helpful in the prediction of porosity and reservoir quality based on the modeling of quartz cementation. According to Maast et al., (2011), if grain to grain pressure solution has occurred, it would decrease the IGV with depth and increase the quartz cementation. But during the study it is noted that the range of IGV remained the same regardless of the burial depth and the percentage of quartz cement. There is no relationship found between IGV and quartz cement (Figure 6.14) and also between IGV and burial depth (Figure 6.13). Similar observations were made by Maast et al., (2011), while incorporating data of Brae Formation/Intra-Draupne Formation Sandstone and Hugin Formation from 15 wells in the vicinity of the South Viking Graben. This study confirms that there is no effect of increase in quartz cementation on IGV.

Influence on Reservoir quality

In most of the samples, significant amount of intergranular volume is preserved, described by a high IGV value. This indicates that mechanical compaction was less effective in these formations with some exceptions where pervasive grain crushing is observed. When the quartz cementation starts, the effect of mechanical compaction hinders/stops at a depth of 2.5km and compaction occurs only due to quartz cementation.

8.2 Chemical Diagenesis (Compaction)

8.2.1 Carbonate Cementation

Carbonate cement have been observed from all the samples of the Intra-Draupne Formation sandstone during the point count analysis and also during the SEM analysis (Figure 6.36). The

Brae Formation has less amount of carbonate cement. The carbonate cement seems to be recrystallized from carbonate clasts. According to Bjørlykke and Jahren (2010) both sandstones and mudstones contain biogenic material from calcareous organisms which becomes the source of carbonate cement at later stage during the greater burial depths. Also the marine organisms of aragonite composition dissolve at an early stage during shallow burial and precipitation of calcite cement occurs in the pore spaces between the grains. Upper Jurassic and younger sandstones may be heavily cemented by calcite due to the rain of calcareous algae and foraminifera on the seafloor (Bjørlykke and Jahren, 2010).

Influence on Reservoir quality

Early carbonate cementation in sandstones can compact the sandstones at early stages ending with lower porosity in sandstones. Carbonate cementation can cause the higher IGV values if later stage dissolution is not active. The carbonate cement occurred randomly in Intra-Draupne Formation sandstones so its prediction potential seems to be low.

8.2.2 Authigenic Clays

Authigenic clays like illite and kaolin are observed from the samples. Illite is found extensively in most of the stub mounted samples from the Intra-Draupne sandstone Formation (Figure 6.33). Kaolin and illite have been observed in the Brae Formation (Figure 6.31and 6.32) as pore filling clay minerals. According to Ehrenberg et al., 1993, authigenic kaolinite will be altered to dickite at burial depth of about 3km. So, during the discussion the term kaolin is used which is referring to the kaolin group minerals. In only one sample from the Brae Formation illite was found to occur as grain coatings (Figure 6.30). Most of the illite from the Intra-Draupne Formation occurred in the form of thin hairs or plates and filled in the pores as rock wool (Figure 6.33). Its pore filling occurrence could reduce the permeability. Detailed description of processes responsible for the precipitation of clays and their alteration from one form to another at different conditions of temperature and respective depths are given below.

Shallow Diagenesis

From the observations based on SEM analysis it is obvious that the Intra-Draupne Formation Sandstone contains illite as a pore filling clay mineral. It seems that all the kaolinite converted

to illite during deep burial. Thin section observations from Brae Formation confirmed the presence of both kaolin and illite (Figure 6.31). Presence of partly leached feldspar grains along with occurrence of kaolin in the adjacent pores confirmed the authigenic origin of kaolin from the feldspar dissolution in this Formation.

According to Bjørlykke and Jahren (2010), formation of kaolinite occurred at the early stages of diagenesis during the shallow burial by the flushing of meteoric water. This reaction can be written as:

$$2K\,(Na)AlSi3O8 + 2H^{+} + 9H_2O = Al_2Si_2O_5(OH)_4 + 4H_4SiO_4 + 2K^{+}(2Na^{+})$$

Feldspar = Kaolinite dissolved silica dissolved cations.

The dissolution of mica also generates kaolinite by the action of meteoric water

$$2KAl_3Si_3O_{10}(OH)_2 + 2H^{+} + 3H_2O = 3Al_2Si_2O_5(OH)_4 + 2K^{+}$$

Muscovite = Kaolinite

Deep Diagenesis

All the samples of Intra-Draupne Formation Sandstone are taken from depth greater than 4km and the bore hole temperature is found to be $145^{o}C$ in the well 15/3-8(Table 5.1). The SEM analysis of stub mounted samples also revealed that the pore filling clay mineral is illite (Figure 7.14).

The kaolin formed at the shallow depths reacted with the remaining k-Feldspar at temperature of about $130^{0}C$ and precipitate the illite and release silica which is precipitated as quartz (Bjørlykke and Jahren, 2010).

$$KAlSi_3O_8 + Al_2Si_2O_5(OH)_4 = KAl_3Si_3O_{10}(OH)_2 + 2SiO_2 + H_2O$$

K-Feldspar + Kaolinite = Illite + Quartz + Water

Kaolin is observed in the Brae Formation from the well 16/3B-5 and with bottom hole temperature $123.72^{o}C$. So the critical temperature of $130^{0}C$ required for illitization (Bjørlykke and Jahren, 2010) has not been attained at this particular level of the reservoir and this is the reason for the presence of kaolin. Also presence of less amount of feldspar (Table 6.1) in the

Brae Formation lead to the deficiency of K^+ for the illite precipitation and the occurrence of unaltered kaolin at deeper burial.

The Intra-Draupne Formation Sandstone contains higher amount of K-feldspar (Table 6.1) and also higher amount of secondary porosity. Also, it has extensive illite (Figure 7.14) present in the pores. According to Bjørlykke (1984), the secondary porosity generated by the dissolution of k-feldspar is filled by the precipitation of clays. So the higher amount of both secondary porosity and authigenic illite precipitated from kaolin is supported. Secondary pores generated by the feldspar dissolution along with extensive illite observed during the SEM analysis (Figure 6.35).

Influence on Reservoir Quality

Abundance of illite in the pore spaces of Intra-Draupne Formation Sandstone in the SEM analysis seems to be of authigenic origin. The fibrous appearance and rock wool like character of illite in most of the samples can have a negative impact on the permeability of the sandstone reservoir. While kaolin observed in the Intra-Draupne Formation Sandstone give impression of its detrital origin (Figure 6.34) and observed only in one sample, displaying its lesser effect on the reservoir quality. Occurrence of authigenic kaolin in the Brae Formation both in the thin section slides (Figure 6.31) and stub mounted samples (Figure 6.32) can reduce the sandstone porosity.

The presence of illite in the Intra-Draupne Formation Sandstone implies that kaolin reacted with remaining k-feldspar and transformed to illite.

8.2.3 Authigenic Quartz Cementation

Quartz cementation is observed to be the main control on the porosity in both the Intra-Draupne Formation Sandstone and Brae Formation (Figure 6.4). The amount of quartz cement varies between 2.3-12.6% of the total rock volume. The higher content of quartz cement with corresponding lower porosity values are found in the Brae Formation during the point count analysis and this result is also supported in the SEM analysis in CLI images where samples are found to be extensively quartz cemented (Figure 6.22). While higher porosity values with corresponding lower amount of quartz cement were present in both formations. The higher porosities can be the consequence of some mineral coatings which were formed on the detrital quartz grains which hinder or retard the quartz cementation. Porosity variation in the Upper

Jurassic deeply buried sandstones of the Gudrun and East Brae Field is found to be the function of quartz cement content (Maast et al., 2011). During the point count analysis, quartz is the main mineral present in the samples with quartz cement as extensive authigenic mineral phase and has strong effect on porosity (Figure 6.5). The high porosity sandstones contain about 3% quartz cement while low porosity sandstones contain 11% quartz cement. Some samples do not follow this relationship. The reason for their low porosity in spite of lower quartz cement content is found to be carbonate cementation.

It is observed that quartz cementation does not affect the IGV (Figure 6.14). If the phenomenon of grain-to-grain pressure solution occurs, it would cause the IGV to decrease with depth as the quartz cementation increases. But also the IGV values do not decrease by increasing depth (Figure 6.13). From these observations it can be concluded that the source for quartz cementation is not grain to grain pressure solution but along the stylolites and clay laminae.

Modeled quartz cement percentage is about 8.5 (Table 7.2). While the point counted quartz cement values are around 2.3 to 11%. This variation can be better explained with the understanding of microquartz coatings which controls the quartz overgrowth. According to the modeling results, at the bore hole temperature of 140^0C the quartz cement values should be around 10%. But less amount of quartz cement present in more than half of the samples is the result of microquartz coatings hindering the quartz cementation.

8.3 Porosity Preserving Mechanism in the study area

During the point count analysis the quartz cement is found to be the main control on the porosity (Figure6.4). Some samples have very high quartz cementation with corresponding low porosity values. But in most of the samples high porosity values were counted despite of great burial depth (>4km). Also the porosity values derived from Petrophysical analysis (Figures 5.5&5.7) show variation but anomalous high porosity values were also observed there. In the subsequent section mechanisms responsible for preserving the higher porosity will be discussed.

8.3.1 Highly porous sandstones and presence of micro quartz grain coating

Micro quartz grain coatings are extensively observed in the SEM analysis of the stub mounted samples from both Intra-Draupne Formation Sandstone and Brae Formation (Figure 6.24 and 6.28). Visual estimation of percentage of grain coatings microquartz is made from both formations (Table 6.2). Spicules of silica sponge Rhaxella Perforata are also present in both samples. Also Maast et al., (2011), mentioned the presence of microquartz coating in the Vilje Subbasin area. This implies that there exists a strong relationship between the sponge spicules, microquartz grain coating and anomalous high porosity values.

According to Bjørlykke and Jahren, (2010) amorphous silica formed by the dissolution of Rhaxella sponges generates high super saturation of silica relative to quartz. This dissolved silica precipitate as a coating of minute quartz crystals (micro-quartz coating) on the surfaces of detrital quartz grains. Formation of this micro-quartz coating helps in preventing the precipitation of later stage quartz cementation (over-growth) and is found to be the main cause for higher porosities and good reservoir quality at depths up to 5km. The precipitation of minute micro-quartz crystals in sandstones can occur at 60-65^{o}C because at this temperature, the pore water is highly supersaturated with dissolved silica through the dissolution of Opal A and Opal CT and the quartz growth rate is slow. In several publications, these observations are mentioned (Jahren and Ramm, 2000; Taylor et al., 2010). According to Aase et al., (1996), at higher temperatures unstable silicates like Opal A, Opal CT and smectite have already dissolved at lower temperature and the pore water is saturated with respect to quartz. This saturation is insufficient to precipitate quartz on the micro-quartz surfaces. Micro-quartz coats consist of a layer of about 1-15µm, prismatic quartz crystals with c-axis orientation in a haphazard direction. The c-axis orientations of micro-quartz crystals (Haddad et al., 2006) can prevent their change into bigger syntaxial quartz overgrowths. Hence this prevents quartz cementation and is responsible for the preservation of porosity.

From the comparison of results of quartz cement and primary porosity from point count data and grain coating microquartz estimation from SEM analysis of stub mounted samples (Table 6.3), it is obvious that the samples with anomalous high porosity have higher surface area covered with microquartz coating. While samples with higher amount of quartz cement have low porosity and corresponding lesser surface area covered with microquartz coating. Samples with quartz cement around 3% have microquartz grain coating coverage up to 75%, while around 50% grain coating coverage observed in samples with corresponding 5% quartz

cement. Gradual decrease in coatings caused the enhanced quartz cementation and if the coatings are less than 30%, the quartz cementation increased up to 11% (Table 6.3). So this observation leads to the conclusion that presence of microquartz grain coating hinders/retards the quartz cementation and helps in preserving the higher porosity values in the deeply buried sandstone in the South Viking Graben.

8.3.2 Illite coating

Illite coating is observed only in one sample from the Brae Formation (Figure 6.30). To develop coating, it is necessary that there exists a precursor coating on the grains before the onset of quartz cementation at 2.5-3Km depth (70-80^{o}C). Possible precursor mineral forming the illite coating is smectite (Storvoll et al., 2002a).

Influence on Reservoir Quality

The observed porosity values are found to be anomalously high in both Intra-Draupne Formation Sandstone and Brae Formation, although the burial depth is greater than 4km with temperature above 120^{o}C. Microquartz grain coatings are found extensively in both of the wells 15/3-8 and 16-3B-5.

Microquartz grain coatings are found to cover more than 75% of the grain surface area in SEM analysis. Due to this extensive coverage anomalous high porosity is preserved in both formations. Illite coating has been observed in only one sample with minor grain coverage in Brae Formation, contributing not much in preservation of porosity.

9. CONCLUSION

- Different amount of mechanical compaction seems to have occurred in Intra-Draupne Formation Sandstone and Brae Formation based on the variable IGV values. The mechanical compaction occurred more in coarse grained samples. Greater mechanical compaction generates pervasive grain crushing supported by lower IGV values.

- The quartz cement precipitation is attributed to be sourced from dissolution at stylolites indicated from the stabilization of IGV at around 25%.

- Early carbonate cementation is observed only in Intra-Draupne Formation Sandstone but it does not affect the reservoir quality because its presence is local and it originates from the dissolution of carbonate bioclasts.

- The Intra-Draupne Formation sandstone contains more illite than Brae Formation. Higher K-feldspars content in the Intra-Draupne Formation Sandstone helps in precipitation of illite during deep burial.

- Porefilling kaolin is present extensively in Brae Formation and indicates favorable conditions for its authigenic precipitation and flushing of meteoric water in the Formation. But due to low temperature not much illitization occurs.

- Quartz cementation is the main process which controls the reservoir quality in the deeply buried Upper Jurassic sandstone reservoirs of the South Viking Graben.

- Grain coating microquartz is very common in the Upper Jurassic of the Vilje subbasin in the South Viking Graben and is preserving the anomalous high porosities in the study area. Its occurrence correlates with the dissolution of sponge spicules in the Intra-Draupne Formation Sandstone and the Brae Formation.

- The modelling results indicate that quartz cementation expected to be around 10% in the study area. But grain coatings microquartz hinders the quartz cementation with half of the samples having less than 5% cement with corresponding porosities up to 20%. The maximum quartz cement is counted to be around 11%.

REFERENCES

Aase, N. E. Bjorkum, P. A. and Nadeau, P.H. 1996. The effect of grain-coating microquartz on preservation of reservoir porosity. AAPG Bulletin, v. 80, p. 1654-1673.

Aase, N. E. and Walderhaug, O. 2005. The effect of hydrocarbons on quartz cementation: Diagenesis in the Upper Jurassic sandstones of the Miller Field, North Sea, revisited: Petroleum Geoscience, v. 11, p. 215–223, doi: 10.1144/1354-079304-648.

Adams, A.E. MacKenzie, W. S. and Guilford, C. 1986. Atlas of sedimentary rocks in thin section.: Ferdinand Enke Stuttgart Federal Republic of Germany, p. 103.

Aggett, J. 1997. Reservoir quality evaluation of the East Brae reservoir, Unpublished Badley Ashton Report **95061.**

Bishop, A.N. Kearsley, A.T. and Patience, R.L. 1992. Analysis of sedimentary organic materials by scanning electron microscopy; the application of backscattered electron imagery and light element X-ray microanalysis. Organic Geochemistry, v. 18, p. 431-446.

Bjørkum, P. A. 1996. How important is pressure in causing dissolution of quartz in sandstones?: Journal of Sedimentary Research, v. 66, p. 147–154.

Bjørlykke, K. O. 1984. Formation of secondary porosity in sandstones: how important is it? *in* D. A. McDonald and R. C. Surdam, eds., Clastic diagenesis: AAPG Memoir 37, p. 277–286.

Bjørlykke, K. Nedkvitne, T. Ramm, M. and Saigal, G. 1992. Diagenetic processes in the Brent Group (Middle Jurassic) reservoirs of the North Sea – An overview. In: Morton, A.C., Haszeldine, R.S., Giles, M.R. and Brown, S. (eds.), Geological Society Special Publication 61, Geology of the Brent Group, p. 263–287.

Bjørlykke, K. 2003. Compaction (consolidation) of sediments, in G. V. Middleton, ed., Encyclopedia of sediments and sedimentary rocks: Dordrecht, Netherlands, Kluwer Academic Publishers, p. 161–168.

Bjørlykke, K. and Jahren, J. 2010. Sandstones and Sandstone reservoirs, *in* K. Bjørlykke, ed., Petroleum Geoscience: From Sedimentary Environments to Rock Physics, Springer Verlag, p. 113-140.

Bjørlykke, K. and Aagaard, P. 1992. Clay minerals in North Sea sandstones. Special Publication Society of Economic Paleontologists and Mineralogists v. 47, p. 65-80.

Bjørlykke, K. 2010. Well Logs: A Brief Introduction, *in* K. Bjørlykke, ed., Petroleum Geoscience: From Sedimentary Environments to Rock Physics, Springer Verlag, p. 361-373.

Bloch, S. 1994. Secondary porosity in sandstones: significance, origin, relationship to sub aerial unconformities, and effect on predrill reservoir quality prediction, *in* M. D. Wilson, ed., Reservoir quality assessment and prediction in clastic rocks: SEPM Short Course 30, p. 137–160.

Bloch, S. 1994a. Importance of reservoir prediction in exploration, in M. D. Wilson, ed., Reservoir quality assessment and prediction in clastic rocks: SEPM Short Course v. 30, p. 5–8.

Bloch, S. Lander, R. H. and Bonnell, L. M. 2002. Anomalously high porosity and permeability in deeply buried sandstone reservoirs: Origin and predictability: AAPG Bulletin, v. 86, p. 301–328.

Boldy, S.A.R. and Fraser, S.I. 1999. Jurassic subtle traps; Introduction and review. p. 825-826 in Petroleum Geology of Northwest Europe: Proceedings of the 5th Conference. Fleet , A J, and Boldy, S A R (editors). (London: The Geological Society of London.)

Champel, B. 2006. Discrepancies in brine density databases at geothermal conditions. Geothermics, v.35, p. 600-606.

Chuhan, F.A. Kjeldstad, A. Bjorlykke, K. and Hoeg, K. 2002. Porosity loss in sand by grain

crushing; experimental evidence and relevance to reservoir quality. Marine and Petroleum Geology, v. 19, p. 39-53.

Cornford, C. 1998. Source rock and hydrocarbons of the North Sea. p. 376- 462 in Petroleum geology of the North Sea, basic concepts and recent advances (fourth edition). Glennie, K. W. (editor). (Oxford: Blackwell Scientific Publications.)

Doré, A. G. and five others. 1999. Principal tectonic events in the evolution of the northwest European margin. p. 41-62 in Petroleum Geology of Northwest Europe: Proceedings of the 5th Conference, Fleet, A. J, and Boldy, S. A. R. (editors). (London: The Geological Society of London.)

Dott, R. H. (1964). Wacke, Graywacke and matrix-what approach to immature sandstone classification: Journal of Sedimentary Petrology, v.34, p. 625-632.

Ehrenberg, S.N. 1993. Preservation of anomalously high porosity in deeply buried sandstones by grain-coating chlorite; examples from the Norwegian continental shelf. AAPG Bulletin 77, p. 1260-1286.

Emery, D. Smalley, P. C. and Oxtoby, N. H. 1993. Synchronous oil migration and cementation in sandstone reservoirs demonstrated by quantitative description of diagenesis: Philosophical Transactions of the Royal Society of London, v. 344, p. 115–125.

Emery, D. and K. J. Myres, 1996. Sequence Stratigraphy, Oxford:Blackwell Science.

Erratt, D. Thomas G. M. and Wall G. R. T. 1999. The evolution of the Central North Sea Rift. p. 63-82 in Petroleum Geology of Northwest Europe: Proceedings of the 5th Conference. Fleet, A J, and Boldy, S A R (editors). (London: The Geological Society of London.)

Fraser, S.I. Robinson, A. M. Johson, H. D. Underhill, J. R. Kadolsky, D. G. A. Connel, R. Johannessen, P. and Ravnas, R. 2002. Upper Jurassic, in D. Evnas, A. Armour, and P. Bathurst, eds., Millenium Atlas: Petroleum Geology of the central and northern North Sea: London, The Geological Society of London, p. 157-189.

Fraser, S. Robinson, A. Johnson, H. Underhill, J. Kadolsky, D. Connell, R. Johannessen, P. Ravnas, R. Evans, D. Graham, C. Armour, A. and Bathurst, P. 2003. Upper Jurassic: Geological Society of London, United Kingdom.

Folk, R. L. 1951. Stages of textural maturity in sedimentary rocks: Jour. Sedimentary Petrology, v. 21, p. 127-130.

Gardner, G. H. F. Gardner, L. W. and Gregory, A. R. 1974, Formation velocity and density: The diagnostic basics for stratigraphic traps: Geophysics, v. 39, p. 770–780, doi:10 .1190/1.1440465.

Gluyas, J. G. Robinson, A. G. Emery. D. Grant, S. M. and Oxtoby, N. H. 1993. The link between petroleum emplacement and sandstone cementation, in J. R. Parker, ed., Petroleum geology of northwest Europe: Proceedings of the 4th Conference: London, Geological Society, p. 1395–1402.

Haddad, S. C. Worden. R. H Prior, D. J. and Smalley, P. C. 2006. Quartz cement in the Fontainebleau sandstone, Paris Basin, France: Crystallography and implication for mechanisms of cement growth: Journal of Sedimentary Research, v. 76, p. 244–256, doi:10.2110/jsr.2006.024.

Harms, J.C. Tackenberg, P. Pollock, R. E. Pickles, E. and Anonymous. 1980. The Brae Field area. 5.

Heald, M. T. and Larese, R. E. 1974. Influence of coatings on quartz cementation: Journal of Sedimentary Petrology, v. 44, p. 1269–1274.

Hendry, J. P. and Trewin, N. H. 1995. Authigenic quartz micro fabrics in Cretaceous turbidities: Evidence for silica transformation processes in sandstones: Journal of Sedimentary Research, v. 65, p. 380–392.

Hinde, G. J. 1890. On a new genus of siliceous sponges from the Lower Calcareous Grit of Yorkshire: Quarterly Journal of the Geological Society, v. 46, p. 54–61.

Jackson, J. A. and McKenzie, D. P. 1983. The geometrical evolution of normal fault systems. Journal of Structural Geology, Vol. 5, p. 471-482.

Jahren, J. S. 1993. Microcrystalline quartz coatings in sandstones: A scanning electron microscope study (abs.): Extended abstracts of the 45th Annual Meeting of the Scandinavian Society for Electron Microscopy: Sweden, Scandinavian Society for Electron Microscopy, p.111–112.

Jahren, J. S. And Ramm, M. 2000. The porosity-preserving effects of microcrystalline quartz coatings in arenitic sandstones: Examples from the Norwegian continental shelf, in R. H. Worden and S. Morad, eds., Quartz cementation in sandstones: Oxford, Blackwell Science, International Association of Sedimentologists Special Publication 29, p. 271–280.

Johnson, H. D. and Fisher, M J. 1998. North Sea plays: geological controls on hydrocarbon distribution. p. 463-547 in Petroleum geology of the North Sea, basic concepts and recent advances (fourth edition). Glennie, K W(editor). (Oxford: Blackwell Scientific Publications.)

Karlsen, D.A. Nedkvitne, T. Larter, S.R. and Bjørlykke, K. 1993. Hydrocarbon composition of authigenic inclusions – application to elucidation of petroleum reservoir filling history. Geochemica et Cosmochemica Acta, v. 57, p. 3641–3659.

Knott, S.D. Burchell, M. T. Jolley, E J. and Fraser, A. J. 1993. Mesozoic to Cenozoic plate reconstructions of the North Atlantic and hydrocarbon plays of the Atlantic margins. p. 953-974 in Petroleum Geology of Northwest Europe: Proceedings of the 4th Conference. Parker, J R (editor). (London: The Geological Society of London.)

Lander, R.H. and Walderhaug, O. 1999. Reservoir quality prediction through simulation of sandstone compaction and quartz cementation: AAPG Bulletin, v. 83, p. 433-499.

Leishman, P. M. 1994. Sedimentology, reservoir geometry and reservoir quality of the East Brae Field, United Kingdom North Sea: Ph.D. thesis, University of Aberdeen, Aberdeen, United Kingdom, p. 80.

Maast, T. E. Jahren, J. Bjørlykke, K. 2011. Diagenetic controls on reservoir quality in middle to upper Jurassic sandstones in the South Viking Graben, North Sea AAPG Bulletin, 95 (11), p. 1937-1958.

McBride, E. F. 1989. Quartz cement in sandstones: a review: Earth Science Reviews, v. 26, p. 69–112.

Marchand, A. M. E. Haszeldine, R. S. Macaulay, C. I. Swennen, R. and Fallick, A. E. 2000. Quartz cementation inhibited by crestal oil charge:Miller deep water sandstone, U.K. North Sea: Clay Minerals, v. 35, p. 210–210.

Marchand, A. M. E. Haszeldine, R. S. Smalley, P. C. Macaulay, C. I. and Fallick, A. E. 2001. Evidence for reduced quartz cementation rates in oil-filled sandstones: Geology, v. 29, p. 915–918, doi:10.1130/0091-7613(2001) 029<0915:EFRQCR>2.0.CO;2.

Marcussen, Ø. Maast, T. E. Mondol, N. H. Jahren, J. and Bjørlykke, K. 2010. Changes in physical properties of a reservoir sandstone as a function of burial depth: The Etive Formation, northern North Sea: Marine and Petroleum Geology, v. 27, p. 1725–1735, doi:10.1016/j.marpetgeo .2009.11.007.

Martin, M. A. and Pollard, J E. 1996. The role of trace fossil (ichnofabric) analysis in the development of depositional models for the Upper Jurassic Fulmar Formation of the Kittiwake Field (Quadrant 21, UKCS). p. 163-183 in Geology of the Humber Group: Central Graben and Moray Firth, UKCS. Hurst, A, Johnson, H D, Burley, S D, Canham, A C, and Mackertich, D S (editors). Special Publication of the Geological Society of London, No. 114.

Michelsen, O. Nielsen, L H. Johannessen, P N. Andsbjerg, J. and Surlyk, F. 2003. Jurassic lithostratigraphy and depositional development onshore and offshore Denmark. In The Jurassic of Denmark and Greenland. Surlyk, F, and Ineson, J R (editors). Bulletin of the Geological Society of Denmark.

Milton, N J. 1993. Evolving depositional geometries in the North Sea Jurassic rift. p. 425-442 in Petroleum Geology of Northwest Europe: Proceedings of the 4th Conference. Parker, J R (editor). (London: The Geological Society of London.)

Mitchener, B.C. Lawrence, D. A. Partington, M. A. Bowman, M. B. J. and Gluyas, J. 1992. Brent Group: Sequence stratigraphy and regional implications. p. 45-80 in Geology of the Brent Group. Morton, A C, Haszeldene, R S, Giles, M R, and Brown, S (editors). Special Publication of the Geological Society of London, No. 61.

Paxton, S.T. Szabo, J.O. Ajdukiewicz, J.M. and Klimentidis, R.E. 2002. Construction of an intergranular volume compaction curve for evaluating and predicting compaction and porosity loss in rigid-grain sandstone reservoirs. AAPG Bulletin 86, p. 2047-2067.

Pemberton, S. G. Maceachern, J. A. and Frey, R.W. 1992. Trace fossil models: environmental and allostratigraphic significance. p. 47-73 in Facies Models - Response to Sea-Level Change. Walker, R. G, and James, N P (editors). (St. John's, NFD: Geological Association of Canada.)

Ramm, M. and Bjørlykke, K. 1994. Porosity/depth trends in reservoir sandstones; assessing the quantitative effects of varying pore-pressure, temperature history and mineralogy, Norwegian Shelf data. Clay Minerals v. 29, p. 475-490.

Rattey, R. P. and Hayward, A. P. 1993. Sequence stratigraphy of a failed rift system: the Middle Jurassic to Early Cretaceous basin evolution of the Central and Northern North Sea. p. 215-249 in Petroleum Geology of Northwest Europe: Proceedings of the 4th Conference. Parker, J. R. (editor). (London: The Geological Society of London.)

Raymer, L. L. Hunt, E. R. and Gardner, J. S. 1980. An improved sonic transit time-to-porosity transform: 21st Annual Logging Symposium Transactions: Louisiana, Society of Professional Well-Log Analysts, p. 1–13.

Richards, P. C. Lott, G.K. Johnson, H.D. Knox, R.W. O.B. and Riding, J. B. 1993. Jurassic of the Central and Northern North Sea. Lithostratigraphic Nomenclature of the U.K. North Sea, v. 3. Knox, R WO'B, and Cordey W.G. (editors). (Nottingham: British Geological Survey.)

Roberts, D. G. and five others. 1999. Paleozoic to Tertiary rift and basin dynamics: mid-Norway to the Bay of Biscay - a new concept for hydrocarbon prospectivity in the deep water frontier. p. 7-40 in Petroleum Geology of Northwest Europe: Proceedings of the 5th

Conference. Fleet A. J., and Boldy S.A. R., (editors). (London: The Geological Society of London.)

Schmoker, J. W. and Gautier, D. L. 1988. Sandstone porosity as a function of thermal maturity: Geology, v. 16, p. 1007–1010.

Schmoker, J. W. and Higley, D. K. 1991. Porosity trends of the Lower Cretaceous J sandstone, Denver basin, Colorado: Journal of Sedimentary Petrology, v. 61, p. 909–920.

Sheldon, H. A. Wheeler, J. Worden, R. H. and Cheadle, M. J. 2003. An analysis of the roles of stress, temperature, and pH in chemical compaction of sandstones: Journal of Sedimentary Research, v. 73, p. 64–71, doi:10.1306 /070802730064.

Stephen, R. Branter, F. 2003. The East Brae Field, Blocks 16/03a, 16/03b, UK North Sea. p. 191-197 in United Kingdom Oil and Gas Fields, Commemorative Millenium Volume. Gluyas, J. G. & Hichens, H. M. (eds)2003. (London: The Geological Society of London, Memoir, 20).

Storvoll, V. Bjorlykke, K., Karlsen, D. and Saigal, G. 2002a. Porosity preservation in reservoir sandstones due to grain-coating illite; a study of the Jurassic Garn Formation from the Kristin and Lavrans fields, offshore mid-Norway. Marine and Petroleum Geology v. 19, p. 767-781.

Stow, D. A.V. Bishop, C. D. and Mills, S. J. 1982. Sedimentology of the Brae oilfield, North Sea: fan models and controls. Journal of Petroleum Geology, v. 5, p. 129-148.

Stow, D. A. V. 1983. Sedimentology of the Brae oilfield, North Sea: a reply. Journal of Petroleum Geology, v. 6, p. 103-104.

Stow, D. A. V. and Atkin, B. P. 1987. Sediment facies and geochemistry of Upper Jurassic mudrocks in the Central North Sea area. p. 797-808 in Petroleum geology of North West Europe. Brooks J., and Glennie, K. W. (editors). (London: Graham & Trotman.)

Taylor, A. M. and Gawthorpe, R. L. 1993. Application of sequence stratigraphy and trace fossil analysis to reservoir description: examples from the Jurassic of the North Sea. p. 317-335 in Petroleum Geology of Northwest Europe: Proceedings of the 4th Conference. Parker, J R (editor). (London: The Geological Society of London.)

Thyberg, B. Jahren, J. Winje, T. Bjørlykke, K. Faleide, J.I. and Marcussen, Ø. 2009. Quartz cementation in Late Cretaceous mudstones, northern North Sea: Changes in rock properties due to dissolution of smectite and precipitation of microquartz crystals. Marine and Petroleum Geology, p. 1–13.

Ramm, M. and Bjørlykke, K. 1994. Porosity/depth trends in reservoir sandstones: Assessing the quantitative effects of varying pore pressure, temperature history and mineralogy, Norwegian shelf area: Clay Minerals, v. 29, p. 475– 490, doi:10.1180/claymin.1994.029.4.07

Taylor, T.R. Giles, M. R. Hathon, L. A. Diggs, T. N. Braunsdorf, N. R. Birbiglia, G. V. Kittridge, M. G. Macaulay, C. I. and Espejo, I. S. 2010. Sandstone diagenesis and reservoir quality prediction: myths, and reality: AAPG Bulletin, v. 94, p. 1093-1132.

Turner, C.C. Cohen, J. M. Connell, E .R. and Cooper, D. M. 1987. A depositional model for the South Brae Oilfield. p. 853-864 in Petroleum geology of North West Europe. Brooks, J, and Glennie, K W (editors). (London: Graham & Trotman.)

Underhill, J. R. 1991a. Implications of Mesozoic-Recent basin development in the Inner Moray Firth, UK. Marine and Petroleum Geology, v. 8, p. 359-369.

Underhill, J. R. 1991b. Controls on Late Jurassic seismic sequences, Inner Moray Firth: a critical test of Exxon's original sea-level chart. Basin Research, v. 3, p. 79-98.

Underhill, J. R. and Partington, M. A. 1993. Jurassic thermal doming and deflation in the North Sea: Implication of the sequence stratigraphic evidence. p. 337-346 in Petroleum Geology of Northwest Europe: Proceedings of the 4th Conference. Parker, J. R. (editor). (London: The Geological Society of London.)

Underhill, J. R. Sawyer, M. J. Hodgson, P. Shallcross, M. D. and Gawthorpe, R. L. 1997. Implications of fault scarp degradation for Brent Group prospectivity, Ninian Field, Northern North Sea. Bulletin of the American Association of Petroleum Geologists, v. 81, p. 999-1022.

Vollset, J. and Doré, A. G. (editors). 1984. A revised Triassic and Jurassic lithostratigraphic nomenclature for the Norwegian North Sea. Bulletin of the Norwegian Petroleum Directorate, No. 3.

Walderhaug, O. 1990. A fluid inclusion study of quartz-cemented sandstones from offshore mid-Norway; possible evidence for continued quartz cementation during oil emplacement. Journal of Sedimentary Research v. 60, p. 203-210.

Walderhaug, O. 1996, Kinetic modeling of quartz cementation and porosity loss in deeply buried sandstone reservoirs: AAPG Bulletin, v. 80, p. 731–745.

Walderhaug, O. 1994a. Precipitation rates for quartz cement in sandstones determined by fluid-inclusion microthermometry and temperature-history modeling: Journal of Sedimentary research, v. A64, p. 324-333.

Walderhaug, O. 1994b. Temperatures of quartz cementation in Jurassic sandstones from the Norwegian continental shelf -evidence from fluid inclusions: Journal of Sedimentary research, v. A64, p. 311-323.

Walderhaug, O. 1996. Kinetic modelling of quartz cementation and porosity loss in deeply buried sandstone reservoirs.: AAPG Bulletin, v. 80, p. 731-745.

Walderhaug, O. and Bjørkum, P.A. 1998. Calcite cement in shallow marine sandstones: Growth mechanisms and geometry. International Association of Sedimentologists, Special Publication 26, p. 179–192.

Warren, E.A. & Smalley, P.C. (1994) North Sea formation Water Atlas. Geol. Soc. London Memoir 15.

Wentworth, C.K. 1922. A scale of grade and class terms of clastic sediments. J. Geol., v. 30, p.377-392.

Williams, L. A. Parks, G. A. and Crerar, D. A. 1985. Silica diagenesis: I. Solubility controls: Journal of Sedimentary Petrology, v. 55, p. 301–311.

Wilson, M. D. 1994. Introduction, in M. D. Wilson, ed., Reservoir quality assessment and prediction in clastic rocks: SEPM Short Course 30, p. 1–4.

Wyllie, M. R. J. Gregory, A. R. and Gardner, L. W. 1956. Elastic wave velocities in heterogeneous and porous media: Geophysics, v. 21, p. 41–70, doi:10.1190/1.1438217.

Yielding, G. 1990. Footwall uplift associated with Late Jurassic normal faulting in the northern North Sea. Journal of the Geological Society of London, v. 147, p. 219-222.

Zanella, E. Coward Mike, P. Spencer, A. Vejbaek, O. Kubala, M. Goldsmith Philip, J. Husmo, T. Robinson, A. Sorensen, K. Thomas, D. Lorange, E. Evans, D. Graham, C. Armour, A. and Bathurst, P. 2003. Structural framework: Geological Society of London London United Kingdom.

Ziegler, P. A. 1982. Geological Atlas of Western and Central Europe. (Amsterdam: Shell International Petroleum Maatschappij, B.V.)

Ziegler, P. A. 1990a. Geological Atlas of Western and Central Europe (second edition). (Bath: Geological Society for Shell Internationale Petroleum Maatschappij B.V., The Hague.)

http://npdmap1.npd.no/website/npdgis/viewer.htm. Last accessed 23rd May, 2012.

http://factpages.npd.no/factpages/Default.aspx?culture=en. Last accessed 30th May, 2012.

References

APPENDIX

Table of textural analysis

Well	Sample	Depth(m)	Lithology	Grain Shape	Sorting	Remarks
15/3-8	BB4	4199,7	HD Turbiditic Sandstone	Sub-angular	Poor	Carbonate Cement, sponge spicules, quartz overgrowth, pyrite
15/3-8	BB18	4225,7	HD Turbiditic Sandstone	Sub-angular	Poor	Carbonate cement, highly porous
15/3-8	BB16	4253.8	HD Turbiditic Sandstone	Sub-rounded	Moderate	Quartz overgrowth, secondary porosity, illitized
15/3-8	BB12	4264.9	HD Turbiditic Sandstone	Sub-angular	Poor	Quartz overgrowth, secondary porosity, illitized
15/3-8	BB6	4273.2	HD Turbiditic Sandstone	Angular	Poor	
15/3-8	BB11	4274.9	HD Turbiditic Sandstone	Angular	Poor	
15/3-8	BB8	4296.0	HD Turbiditic Sandstone	Sub-angular	Poor	Abundance of carbonate cement, mechanically compacted
15/3-8	BB17	4479.6	HD Turbiditic Sandstone	Sub-angular	Poor	
15/3-8	BB13	4503.4	HD Turbiditic Sandstone	Angular	Poor	Sponge Spicules, secondary porosity
16/3B-5	EB6	4125.2	HD Turbiditic Sandstone	Sub-rounded	Well	Much mechanical compaction, sheared quartz observed
16/3B-5	EB16	4128.3	HD Turbiditic Sandstone	Sub-rounded	Moderate	
16/3B-5	EB4	4148.3	HD Turbiditic Sandstone	Sub-rounded	Moderate	
16/3B-5	EB5	4150.9	HD Turbiditic Sandstone	Sub-rounded	Moderate	
16/3B-5	EB7	4157.2	HD Turbiditic Sandstone	Sub-rounded	Moderate	Very illitized, porous, micaceous, pyrite
16/3B-5	EB3	4162.0	HD Turbiditic Sandstone	Sub-rounded	Moderate	Secondary porosity, sponge spicules
16/3B-5	EB12	4166.3	HD Turbiditic Sandstone	Sub-rounded	Moderate	
16/3B-5	EB13	4197.6	HD Turbiditic Sandstone	Angular	Poor	
16/3B-5	EB14	4199.6	HD Turbiditic Sandstone	Sub-angular	Poor	Sponge Spicules, highly porous
16/3B-5	EB15	4202.2	HD Turbiditic Sandstone	Sub-rounded	Moderate	Mechanically compacted(pervasive crushing), kaolin observed
16/3B-5	EB9	4209.4	HD Turbiditic Sandstone	Sub-angular	Moderate	Sutured contacts between grains due to mechanical compaction
16/3B-5	EB10	4230.8	HD Turbiditic Sandstone	Sub-angular	Poor	Secondary porosity, very illitized, Secondary porosity